To the Graduate Council:

I am submitting herewith a thesis written by Courtney D. Eleazer entitled "Age-related Histomorphometric Changes in Human Fetal Long Bones." I have examined the final electronic copy of this thesis for form and content and recommend that it be accepted in partial fulfillment of the requirements for the degree of Master of Arts, with a major in Anthropology.

___Dr._Murray K. Marks_____

Murray K. Marks, Major Professor

We have read this thesis
and recommend its acceptance:

___Dr. Walter Klippel_____

___Dr. Joanne Devlin_____

Accepted for the Council:

___Carolyn R. Hodges_____

Carolyn R. Hodges, Vice Provost and
Dean of the Graduate School

(Original signatures are on file with official student records.)

AGE-RELATED HISTOMORPHOMETRIC CHANGES IN HUMAN FETAL LONG BONES

A thesis
Presented for the
Master of Arts
Degree
The University of Tennessee, Knoxville

Courtney D. Eleazer
December 2007

Copyright © 2007 by Courtney D. Eleazer
All rights reserved.

Dedication

To my parents, Ed and Nancy Eleazer,
for teaching me that anything is possible.

Acknowledgements

I would like to thank Dr. Darinka Mileusnic of the Medical Examiner's Office of the University of Tennessee, Knoxville for assisting with the donation of the fetal specimens for this study. Thank you also to Dr. Murray K. Marks of the Mineralized Tissue Histology lab here at the University of Tennessee for access to the myriad materials necessary for histological research and help with procuring fetal specimens. I would like to express my appreciation for the other members of my committee, Dr. Walter Klippel and Dr. Joanne Devlin, for their editing suggestions and expertise in this field. And last, but not least, Dr. Sam Stout and Dr. Margaret Streeter for their crucial advice without which this research would be quite unsuccessful.

Abstract

The goal of this study is to investigate the age-related changes in histomorphometry among the six long bones of the human fetus. Histological studies have become increasingly important in distinguishing fragmentary human remains from non-human remains as well as estimating age at death in forensic cases. However, little work has been done with subadult material due to its distinct growth patterns and unique microscopic composition. This study attempts to provide a preliminary investigation into the potential of utilizing histomorphometry in the estimation of age at death of fetal remains. Microscopic methods may prove invaluable to the task of aging fragmentary remains that lack the characteristic features necessary for conventional metric methods that require the preservation of entire skeletal elements.

Seven stillborn cadavers of known sex and gestational age (17-35 weeks) were the subjects of study. Thin sections were taken from the midshafts of the six long bones and examined under a light microscope. For each slide, a maximum of 111 measurements were taken: maximum sagittal medullary diameter (anterior-posterior), maximum transverse medullary diameter (medial-lateral), medullary area, maximum cortical thickness (taken at each quadrant), minimum cortical thickness (taken at each quadrant), and a maximum of 25 separate trabecular diameters per quadrant.

The results of this research indicate that several histological measurements possess potential for predicting fetal age. Statistically significant correlations between both maximum and minimum cortical thicknesses and age were present for all six long bones. The humerus and tibia have the strongest correlations between cortical thickness

and age, while the radius possesses the weakest correlation with age. The results of an ANCOVA employing age as a covariate indicate that fetal age is a significant linear predictor of trabecular thickness in all long bones except the radius. The values for trabecular thickness are significantly different among quadrants within the femur, tibia, humerus, and ulna. However, only in the humerus and radius does the *rate* of linear change in trabecular thickness with age differ by quadrant location. Future research conducted on a larger sample size is expected to determine the accuracy with which this method can be applied to fetal age estimation.

Table of Contents

Section Page

Chapter 1: Introduction ..... *- 1 -*

Chapter 2: Bone Biology and Histology ..... *- 5 -*

Chemical Composition of Bone ..... **- 5 -**

Embryology of Bone ..... **- 6 -**

Macroscopic Structure of Bone Tissue ..... **- 8 -**

Microscopic Structure of Bone Tissue ..... **- 9 -**

Bone Cells ..... **- 18 -**

Bone Formation ..... **- 19 -**

Bone Growth and Modeling ..... **- 21 -**

Bone Remodeling ..... **- 25 -**

Chapter 3: Previous Research in Fetal Long Bone Histology ..... *- 30 -*

Chapter 4: Materials and Methods ..... *- 34 -*

Chapter 5: Results ..... *- 44 -*

Medullary Diameters and Medullary Area ..... **- 45 -**

Maximum and Minimum Cortical Thickness ..... **- 53 -**

Trabecular Thickness ..... **- 64 -**

Chapter 6: Discussion ..... *- 74 -*

Chapter 7: Conclusions ..... *- 86 -*

References Cited ..... *- 88 -*

Appendix ..... *- 93 -*

Vita ..... *-144-*

List of Tables

Table	Page
Table 1: Actual and developmental ages of fetal specimens	- 34 -
Table 2: Pearson's Correlation Coefficients for Maximum Cortical Thickness	- 63 -
Table 3: Pearson's Correlation Coefficients for Minimum Cortical Thickness	- 63 -
Table 4: ANCOVA Summary for Age Effect of Trabecular	- 70 -
Table 5: ANCOVA Summary for Quadrant Effect of	- 70 -
Table 6: ANCOVA Post Hoc Summary for Trabecular Thickness by Bone	- 71 -
Table 7: ANCOVA Summary for Quadrant/Age Interaction of	- 72 -
Table A1: Osteometric Measurements of the Long Bones of Fetal Specimens	- 72 -
Table A2: Medullary Diameters and Medullary Area by Bone	- 72 -
Table A3: Maximum and Minimum Cortical Thickness by Quadrant	- 72 -
Table A4: Mean Maximum and Minimum Cortical Thickness Across All Quadrants by Bone	- 72 -
Table A5: Mean Trabecular Thickness of the Femur by Quadrant	- 72 -
Table A6: Mean Trabecular Thickness of the Tibia by Quadrant	- 72 -
Table A7: Mean Trabecular Thickness of the Fibula by Quadrant	- 72 -
Table A8: Mean Trabecular Thickness of the Humerus by Quadrant	- 72 -
Table A9: Mean Trabecular Thickness of the Radius by Quadrant	- 72 -
Table A10: Mean Trabecular Thickness of the Ulna by Quadrant	- 72 -
Table A11: Mean Trabecular Thickness Across Quadrants by Bone	- 72 -
Table A12: Raw Data for Trabecular Thickness (nm)	- 72 -

List of Figures

Figure — Page

Figure 1: Human and nonhuman cortical bone ..... - 3 -
Figure 2: Linear osteon banding ..... - 3 -
Figure 3: Limb bud formation in the human embryo ..... - 7 -
Figure 4: Compact bone and cancellous bone ..... - 20 -
Figure 5: The periosteal and endosteal surfaces ..... - 22 -
Figure 6: Woven bone trabeculae ..... - 24 -
Figure 7: Classical and twisted plywood models of lamellar bone structure ..... - 26 -
Figure 8: Microscopic structure of human cortical bone ..... - 27 -
Figure 9: Lamellar bone apposition within woven bone trabeculae ..... - 27 -
Figure 10: Formation of a non-Haversian canal ..... - 28 -
Figure 11: Primary osteons and non-Haversian canals ..... - 8 -
Figure 12: Endochondral ossification of the diaphysis of a long bone ..... - 10 -
Figure 13: The four zones of ossification of the growth plate ..... - 10 -
Figure 14: Long bone modeling ..... - 13 -
Figure 15: The three life cycles of the BMU ..... - 13 -
Figure 16: BMU remodeling of the surface of a cancellous trabecula ..... - 15 -
Figure 17: Resorption space ..... - 16 -
Figure 18: Cement line ..... - 17 -
Figure 19: Skeletal elements of each specimen ..... - 36 -
Figure 20: Seven cuts scored on the bones for sectioning ..... - 37 -
Figure 21: Epoxy resin embedding of bone segments ..... - 37 -
Figure 22: Buehler Isomet low speed diamond saw ..... - 39 -
Figure 23: Petrographic slide of the humeral midshaft of Fetus 5 ..... - 39 -
Figure 24: Woven bone trabecular thickness ..... - 41 -
Figure 25: Medullary Diameters of the Femur Across Fetal Specimens ..... - 46 -
Figure 26: Medullary Diameters of the Tibia Across Fetal Specimens ..... - 46 -
Figure 27: Medullary Diameters of the Fibula Across Fetal Specimens ..... - 47 -

List of Figures (cont.)

Figure — Page

Figure 28: Medullary Diameters of the Humerus Across Fetal Specimens ..... - 47 -
Figure 29: Medullary Diameters of the Radius Across Fetal Specimens ..... - 48 -
Figure 30: Medullary Diameters of the Ulna Across Fetal Specimens ..... - 48 -
Figure 31: Sagittal Medullary Diameter by Bone ..... - 51 -
Figure 32: Transverse Medullary Diameter by Bone ..... - 51 -
Figure 33: Medullary Area by Bone ..... - 54 -
Figure 34: Maximum Cortical Thickness of the Femur by Quadrant ..... - 55 -
Figure 35: Maximum Cortical Thickness of the Tibia by Quadrant ..... - 55 -
Figure 36: Maximum Cortical Thickness of the Fibula by Quadrant ..... - 56 -
Figure 37: Maximum Cortical Thickness of the Humerus by Quadrant ..... - 56 -
Figure 38: Maximum Cortical Thickness of the Radius by Quadrant ..... - 57 -
Figure 39: Maximum Cortical Thickness of the Ulna by Quadrant ..... - 57 -
Figure 40: Maximum Cortical Thickness of the Anterior Quadrant by Bone ..... - 60 -
Figure 41: Maximum Cortical Thickness of the Medial Quadrant by Bone ..... - 60 -
Figure 42: Maximum Cortical Thickness of the Posterior Quadrant by Bone ..... - 61 -
Figure 43: Maximum Cortical Thickness of the Lateral Quadrant by Bone ..... - 61 -
Figure 44: Average Trabecular Thickness in the Femur by Quadrant ..... - 65 -
Figure 45: Average Trabecular Thickness in the Tibia by Quadrant ..... - 65 -
Figure 46: Average Trabecular Thickness in the Fibula by Quadrant ..... - 66 -
Figure 47: Average Trabecular Thickness in the Humerus by Quadrant ..... - 66 -
Figure 48: Average Trabecular Thickness in the Radius by Quadrant ..... - 67 -
Figure 49: Average Trabecular Thickness in the Ulna by Quadrant ..... - 67 -
Figure 50: Average Trabecular Thickness Across All Quadrants by Bone ..... - 68 -

Chapter 1: Introduction

As research into human bone histology expands, it becomes increasingly difficult to obtain specimens with which to conduct destructive analysis. This is especially true within American anthropology departments, ingrained with the desire to curate biological and cultural artifacts for indefinite periods of time lest information be lost to future generations of researchers. However, with the rising appeal of geomorphometric data collection, histological methods may soon become more palatable within anthropology. Furthermore, the steady increase in fragmentary and commingled remains associated with mass disasters and mass grave production has spurred a need for improved histological techniques that has not yet been fully appreciated or acknowledged in the anthropological community. Fragmentary remains, by their very nature are especially challenging to the development of a biological profile as the diagnostic portions of the bone that would typically be utilized in such analysis are often absent. In such situations, destructive histological examination may prove the most useful course of action given the condition of the remains and their relative utility to forensic investigation.

Most researchers, however, are not merely as concerned with the application of histological methods to forensic cases as they are with the destruction of skeletal material that could potentially be utilized in myriad other research studies that do not require destructive measures. Yet it is exactly these types of studies that are required in order to assess the applicability of human bone histology to forensic anthropology. As the popularity of body donation expands with the recent surge of interest in forensics among

popular culture, the current dearth of skeletal material available for anthropological study may become a thing of the past. It is crucial, as scientists, that forensic anthropologists remain open-minded to the constant redefinition and improvement of this discipline's methodology. In histology lies the ability to classify skeletal remains that have formerly been of little diagnostic value. By adopting a holistic approach to anthropology, researchers ought to utilize and expand upon the techniques and foundation of knowledge produced by the biomedical field which has a long history of destructive yet informative studies.

In an anthropological context, histological methods are most useful in (1) estimating age and (2) distinguishing between human and nonhuman remains. Determining the species classification of a bone fragment is a relevant endeavor in both forensic and archaeological settings, as commingling of human and nonhuman remains can occur in disturbed contexts. Human bone exhibits a distinct histomorphology compared to other animals, because human beings are the only species that possesses Haversian bone throughout the entire cortical layer (Figure 1). Although many other species within the mammalian class possess Haversian bone, this type of tissue is usually limited to the very center of the cortex and is surrounded by a more primitive bone type, called plexiform bone, at the periosteal and endosteal surfaces (Jowsey, 1966). The Haversian bone present in nonhuman animals also differs from that of humans in its microscopic structure. In nonhuman animals, the osteons tend to cluster into linear bands of four to six (Figure 2) while those of the human are much more numerous and randomly scattered throughout the cortex. Thus, in the investigation of whether a bone fragment is human or nonhuman, the presence of plexiform bone tissue ensures a

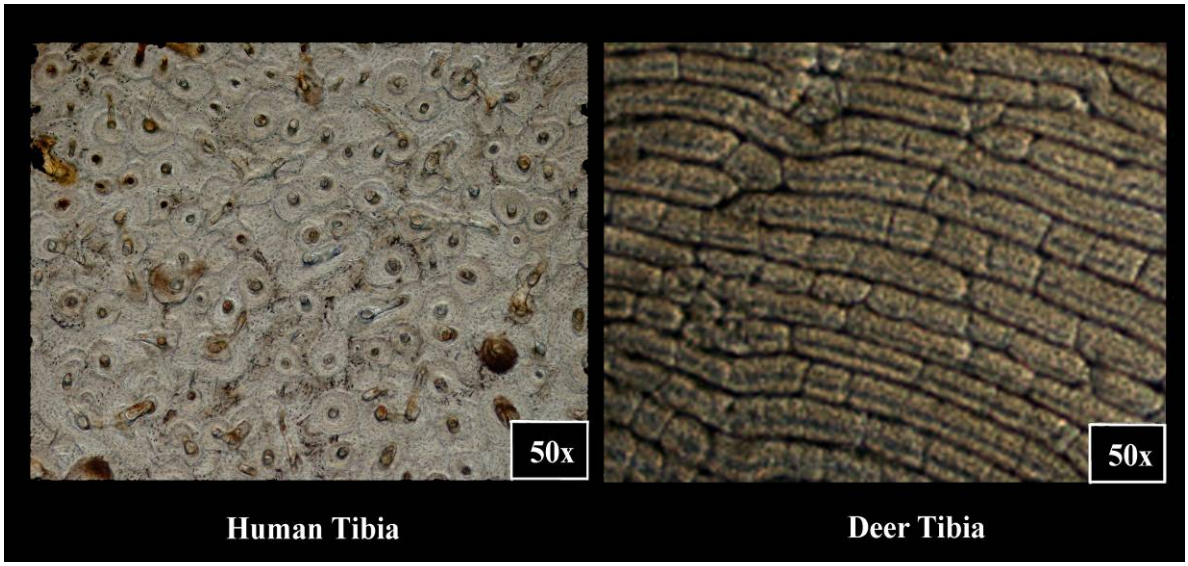


Figure 1: Human and nonhuman cortical bone
A digital image of two light micrographs (50x) demonstrating the difference between lamellar and plexiform cortical bone microstructure.

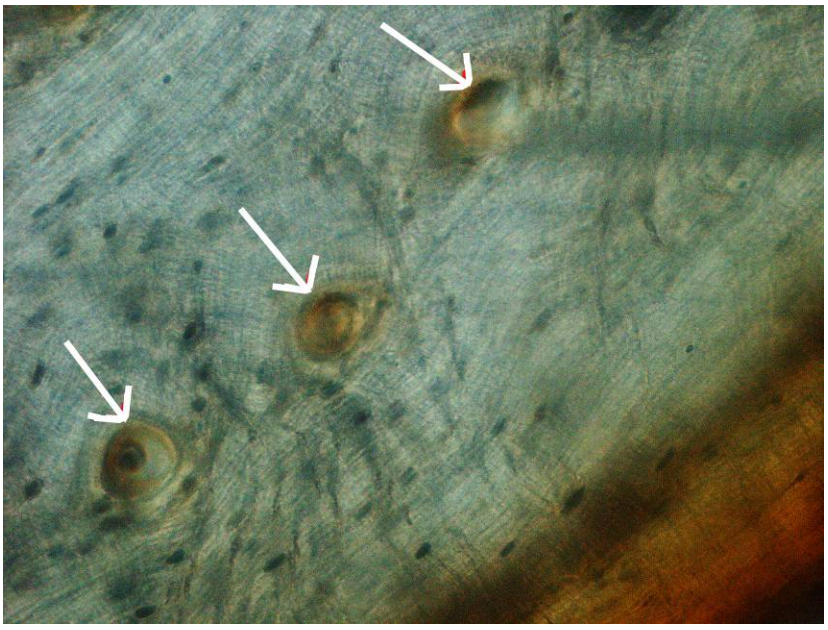


Figure 2: Linear osteon banding
A digital image (200x) of a light micrograph indicating osteons (arrows) arranged in a linear band. Cross section taken from the humerus of a juvenile macaque (*Macaca mulatta*).

nonhuman classification, while the presence of Haversian bone does not necessarily denote a human classification. Further assessment of the type of Haversian bone and arrangement of osteons is necessary to distinguish between human and nonhuman remains.

The assessment of age from relatively complete adult skeletal material is quite complicated in the absence of particularly diagnostic elements, such as the os coxae and ribs. The situation becomes even more problematic with fragmentary remains, which are often missing the more delicate joint surfaces upon which most aging techniques rely. Even if one is lucky enough to find a portion of the os coxae or ribs, the surfaces of interest are not likely to have survived most taphonomic processes. The same can be said of fetal and infant skeletal remains whose age assessment usually involves the dimensions of the entire bone. For long bones, the full length of the bone is required to determine age; yet in cases of fragmentation, the true anatomical length is not preserved. In all of these situations, histological examination is the most appropriate course of action for age estimation. Unfortunately, while methods of histological age estimation have been developed for multiple adult long bones and axial bones, there has not yet been a complete examination of subadult histology. This thesis attempts to investigate whether age-related changes in histomorphometry are present in fetal skeletal remains and, if present, whether these changes may be utilized in estimating age at death.

Chapter 2: Bone Biology and Histology

Chemical Composition of Bone

Bone is unlike any other tissue in the body because its extracellular components are calcified, a characteristic that allows it to provide internal support for muscle attachment and protection of vital organs. Although bone is close in tensile strength to cast iron, it is less than one-third as heavy, maximizing its hardness while maintaining mobility. Despite its rigidity, bone is a dynamic living tissue that is in a constant state of reconstruction throughout the course of an individual's lifetime in response to external mechanical stimuli (Bloom and Fawcett, 1968).

Bone is composed of five basic substances: collagen, water, hydroxyapatite mineral, proteoglycans, and noncollagenous proteins. Approximately 95% of the organic component of bone is collagen, a structural protein that gives bone its flexibility and tensile strength. These collagenous fibers are embedded in a ground substance of polysaccharides, called proteoglycans, which help control the rate of bone mineralization through their ability to bind minerals to water and regulate the movement of molecules through the extracellular matrix. The remainder of the organic component consists of noncollagenous proteins which have multiple functions that help maintain bone health, including: facilitating the mineralization of osteoid, accelerating bone remodeling, and promoting hydroxyapatite crystal formation. The inorganic component of bone consists almost entirely of hydroxyapatite crystals [$Ca_{10}(PO_4)_6(OH)_2$] which give bone its rigidity and compression strength. These hexagonally symmetric crystals form through assisted

nucleation at specific loci on collagen fibrils. The rest of the inorganic component includes common minerals (e.g.., calcium, magnesium, sodium, potassium) that are stored in bone for future use in basic cellular functions (Martin et al., 1998).

Embryology of Bone

All connective tissues, including bone, form from the differentiation of various mesenchyme tissue cells into osteoprogenitor cells during the early embryonic period. The craniofacial skeleton is formed from an ectomesenchyme tissue produced by the neural crest cells of the ectoderm. The rest of the axial skeleton forms through the process of somitogenesis, or segmentation of the paraxial mesoderm. During the third week of gestation when the neural plate folds to form the neural groove, the paraxial mesoderm becomes segmented into somites, or paired blocks of mesoderm located along either side of the neural tube. Segmentation of the paraxial mesoderm into somites begins in the region of the future neck and commences caudally at a rate of one somite per 90 minutes. These somites will eventually form the dermis, skeletal muscle, and cartilage models of the future vertebrae and ribs of the developing embryo (Larsen et al., 2001).

The appendicular skeleton originates from lateral plate mesoderm. Limb formation occurs between 26 and 28 days after fertilization when ectoderm, somites, and lateral plate mesoderm proliferate to form extensions called limb buds (Figure 3). These limb buds consist of rapidly dividing mesenchyme cells that are covered by ectoderm. Once the limb bud has formed, its mesenchyme begins to differentiate into osteoprogenitor cells that will produce the osteoblastic cells of the future proximal and

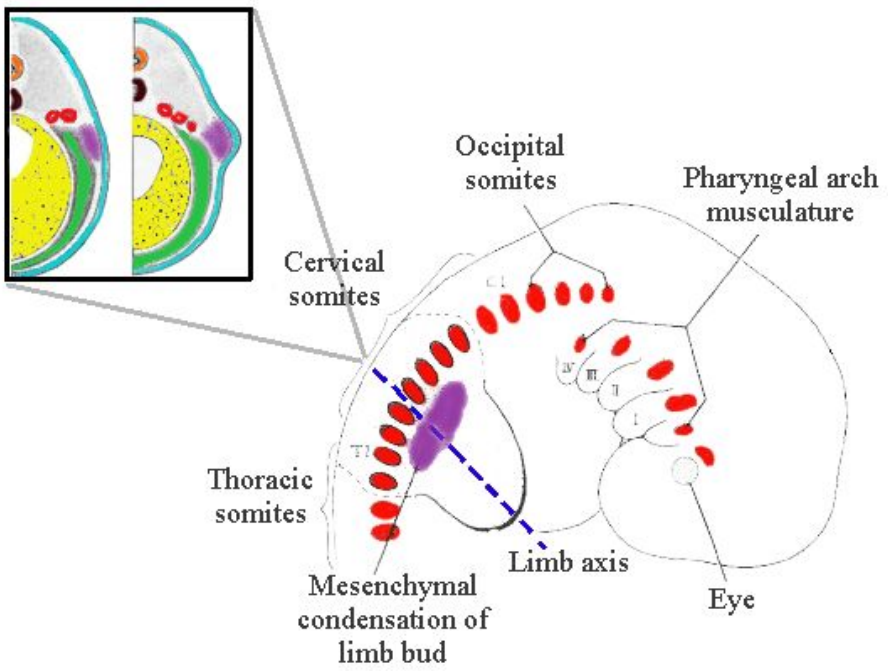


Figure 3: Limb bud formation in the human embryo
Dotted blue line represents a cross section through the embryo at the level of the developing limb bud. Internal structures include: (yellow) endoderm; (green) lateral plate mesoderm; (red) somites; (orange) spinal cord; (brown) notochord; (blue) ectoderm; (purple) mesenchymal condensation of developing limb bud. Adapted from Sadler (2006).

distal limb segments. The differentiation of mesenchymal cells into particular skeletal structures is directed by Hox genes (Larsen et al., 2001). The upper limb buds develop by about 26 days gestation; however, the mesenchymal condensations of the humerus, radius, and ulna do not form until about 37 days gestation. The lower limb is slightly behind the upper limb in development, with budding commencing by stage 13 (28 days) and mesenchymal condensations of the long bones by stage 17 (41 days) (Hall, 2005).

Macroscopic Structure of Bone Tissue

On a macroscopic level, two types of bone are distinguishable, cancellous (or spongy) bone and compact (or cortical) bone (Figure 4). Cancellous bone is concentrated at the epiphyses of the long bones and consists of bony spicules called trabeculae that are arranged in a three dimensional labyrinthine latticework separated by spaces containing bone marrow. Compact bone, on the other hand, is a solid mass that does not contain any open spaces visible to the naked eye. In long bones, the diaphysis is made up mostly of compact bone with a central opening, the medullary cavity, which contains yellow bone marrow in the adult. A thin layer of compact bone also covers the cancellous bone of the epiphyses, making the entire periosteal (or outer) surface of the long bone cortical in structure. The majority of the long bone, excluding the articular surfaces of the epiphyses

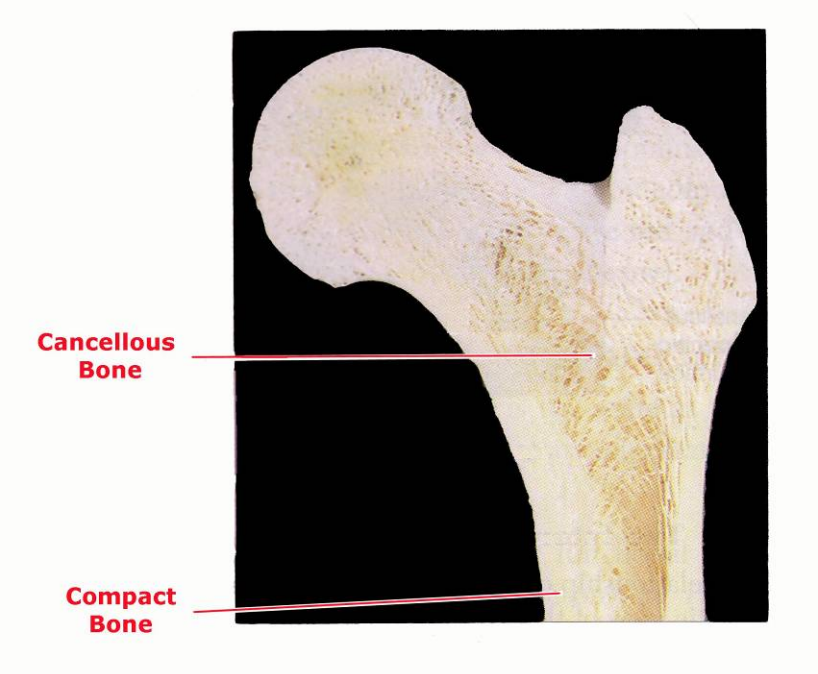


Figure 4: Compact bone and cancellous bone
A digital image of a longitudinal section of the proximal femoral epiphysis

identifying compact and cancellous bone types. Adapted from Martini et al. (2006).

and the attachment sites of tendons and ligaments, is covered with a thin layer of osteogenic connective tissue, or periosteum. Internally (or endosteally), the medullary cavity, bone marrow cavities of the cancellous bone, and osteons are lined with a second osteogenic layer called the endosteum. Both the periosteum and endosteum are osteogenic and are responsible for the deposition of bone during modeling and fracture repair (Netter, 2002). Thus, the bone lying directly under the periosteum is termed "periosteal," while that directly under the endosteum is called "endosteal" (Figure 5).

Microscopic Structure of Bone Tissue

There are two principal types of bone present in the human body, woven bone and lamellar bone. Woven bone is a structurally immature tissue type that is laid down very quickly (more than 4 μm a day) and acts as a temporary scaffold upon which more organized lamellar bone is later deposited. Unlike lamellar bone, it does not contain any osteonal or plexiform structures (Figure 6). Woven bone tissue is the only type of bone tissue which can be formed *de novo*, meaning that existing bone or cartilage tissue is not required for woven bone to be laid down. This type of bone tissue is prevalent in the early mammalian embryo, but it is gradually replaced overtime by lamellar bone until the adult skeleton is almost entirely composed of lamellar bone. In the adult skeleton, some woven bone persists near the cranial sutures, in the osseous labyrinth of the temporal bone, in tooth sockets, and near tendon and ligament attachment sites. At these sites, however, the woven bone is usually mixed with mature bone. Woven bone is also found in postnatal

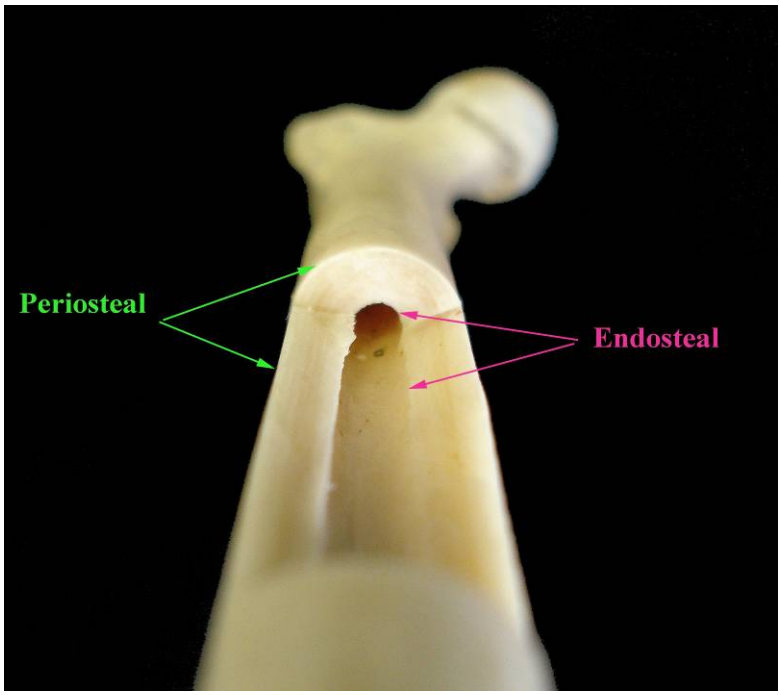


Figure 5: The periosteal and endosteal surfaces of the bony diaphysis
A digital image of a dissected femoral diaphysis of a dog (*Canis familiaris*) showing the outer (periosteal) and inner (endosteal) cortical surfaces.

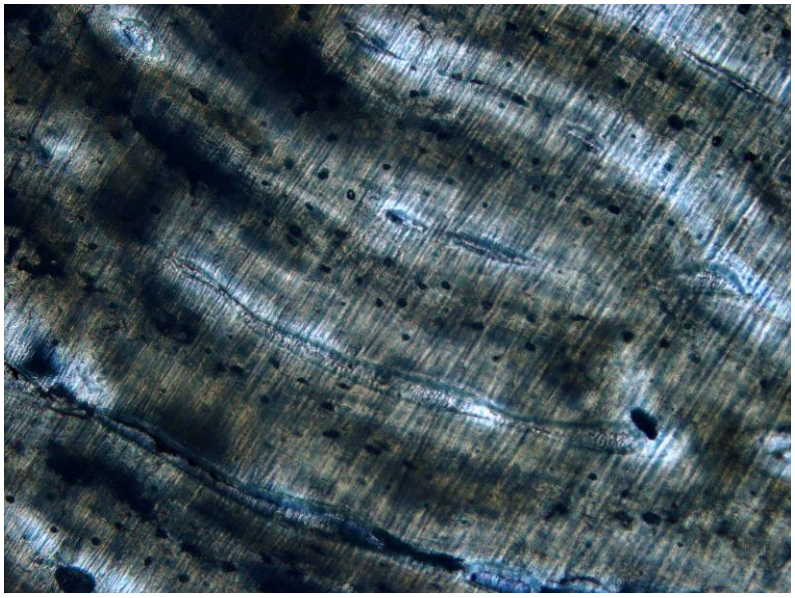


Figure 6: Woven bone trabeculae
A digital image (200x) of a light micrograph showing woven bone trabeculae in a midshaft cross section of the femur of a human fetus (33 weeks gestation).

life during fracture repair in the form of a temporary fracture callus that bridges the gap between bone segments (Currey, 2002).

Woven bone is highly flexible and easily deformed due to its haphazard arrangement of collagen fibrils and mineral crystals. It is considered to be less dense than lamellar bone because the collagen fibrils are more loosely packed; however, woven bone can oftentimes become more mineralized than lamellar bone, making it much more brittle (Christel et al., 1981). The bundles of collagen fibers present in woven bone are said to be "coarse" due to their larger size (30 μm in diameter compared to 2-4 μm in lamellar bone) and are oriented almost randomly throughout the ground substance (Currey, 2002). This morphology is the reason that this type of bone was previously termed coarse-fibered bone, or coarse bundled bone, in the literature (Su, 2003). The osteocytes tend to be larger, more irregular in shape, and more densely packed than those of lamellar bone (Bourne, 1956; Currey, 1984). In addition, the lacunae appear more rounded than those of adult bone (Vaughn, 1970).

Lamellar bone, on the other hand, is much more organized than its predecessor, and thus it develops much more slowly (less than 1 μm a day). The collagen fiber bundles of lamellar bone are considered "fine" and are arranged parallel to one another in sheets (lamellae) that vary in thickness from 3 to 7 μm. Older sources refer to this type of bone as "fine-fibered." Each successive sheet of lamellar bone has a preferred direction of collagen fiber orientation that differs from adjacent lamellae (Currey, 2002). It was once thought that the collagen fibers of each successive lamella lay at 90 degree angles to one another (Ascenzi et al. 1967); however, recent studies have discovered that some lamellar collagen fibers have a "twisted plywood" structure (Giraud-Guille, 1988). In this

structure (Figure 7), the collagen fibers continuously change direction so that in a sense there really are no individual lamellae, yet the lamellar structure of the bone tissue is maintained because the fiber orientation repeats itself as the fibers rotate through each 180 degree cycle. Both the classical and twisted plywood schemes of lamellar structure have been proven to exist in human compact bone, however, their relative distribution has not yet been determined (Martin et al., 1998).

There are three common forms of lamellar bone present in human compact bone: concentric, interstitial, and circumferential (Figure 8). Concentric lamellae are rings of lamellar bone arranged in concentric circles within primary and secondary osteons. These lamellae vary in size and number between and within osteons; yet, there are generally between 4 and 20 lamellae per secondary osteon. Secondary osteons are usually surrounded by irregular fragments of lamellar bone called interstitial lamellae. This particular type of lamellar bone is a by-product of remodeling caused by the invasion of the circumferential and concentric lamellae of preexisting bone by BMUs during the production secondary osteons. The more Haversian systems present in a particular cross section, the more fragmented the surrounding bone tissue becomes. This fragmentary appearance is due to the fact that newly-created Haversian systems cannot only break up the monotony of circumferential lamellae (to be discussed next) but also invade older Haversian systems and primary osteons, leaving behind fragments of concentric lamellae from both. Thus, interstitial lamellae can consist of both of the other types of lamellar bone, concentric and circumferential lamellae. The third type of lamellar bone,

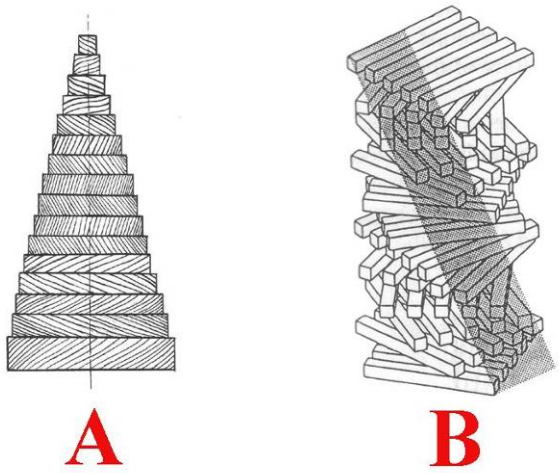


Figure 7: Classical and twisted plywood models of lamellar bone structure
(A) Classical view of the collagen fiber orientation of lamellar bone. Adapted from Bloom and Fawcett (1968). (B) Twisted plywood model of the collagen fiber orientation of lamellar bone. Adapted from Martin and Burr (1998).

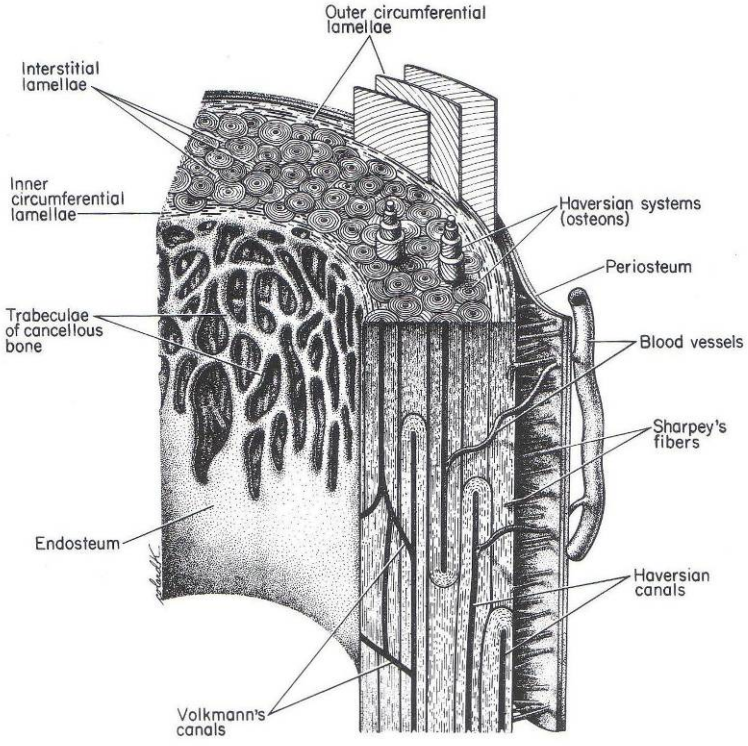


Figure 8: Microscopic structure of human cortical bone
A diagram exhibiting the microscopic structures present in a longitudinal section of a human long bone. Adapted from Martin et al. (1998).

circumferential lamellae, encircles much to all of the circumference of the shaft at both the periosteal (outer circumferential lamellae) and endosteal surfaces (inner circumferential lamellae). During slower periods of growth, sheets of circumferential lamellae are laid down progressively until the desired cortical thickness is reached (Bloom and Fawcett, 1968). Cancellous bone is also composed of lamellae; however these lamellae are usually not penetrated by vascular channels. Thus, Haversian systems are not present, and the osteocytes are nourished directly from the surface of the trabeculae via canaliculi.

There has been much confusion in the literature concerning the difference between primary and secondary osteons, mostly due to issues with terminology and a lack in consensus concerning the mechanisms of their formation. A secondary osteon, (also referred to as a Haversian system, secondary Haversian canal, replacement osteon, and secondary Haversian system) is a set of concentric lamellae that is deposited after the resorption of preexisting bone tissue. These structures can be distinguished from primary osteons in cross section due to their cementing lines that delineate the outer border of the secondary osteon from the surrounding bone matrix. This cementing line is the result of the tunneling of the BMU into the cortical layer. Primary osteons, (also called primary Haversian systems and primary Haversian canals), on the other hand, lack this outline because they do not require resorption in order to be formed. The lamellae of a primary osteon are deposited on a preexisting bone surface, usually the vascular spaces present between woven bone trabeculae (Figure 9). Some authors also recognize a third structure commonly referred to as a non-Haversian canal, or primary canal. During the formation of circumferential lamellae, blood vessels can sometimes become incorporated into the

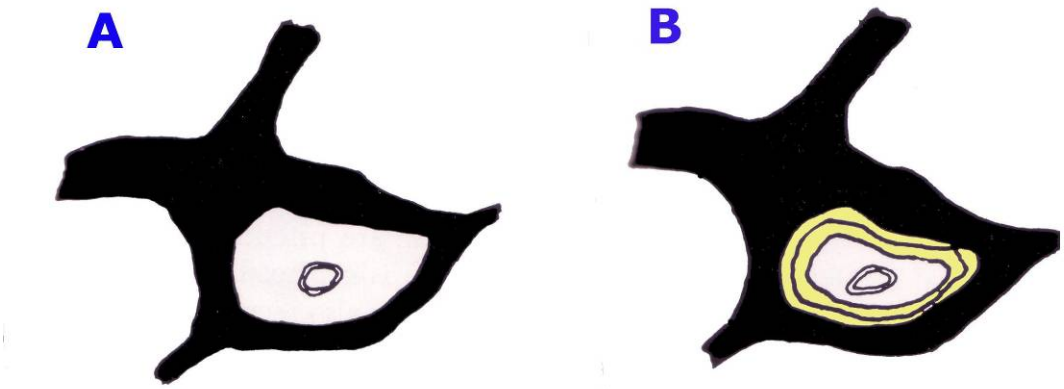


Figure 9: Lamellar bone apposition within woven bone trabeculae
(A) Woven bone trabeculae (black) with open space and a single blood vessel within its center. (B) Woven bone trabeculae with open space filled partially with lamellar bone (yellow). Adapted from Hall (1965).

growing diaphysis at the periosteal surface (Figure 10); however, these vascular canals should not be confused with primary osteons, as has frequently been done in the literature. Unlike primary osteons, these non-Haversian canals (Figure 11) are much smaller in diameter, having very few concentric lamellae, and they are surrounded by circumferential lamellae containing very few lacunae (Enlow, 1963).

All calcified bone tissue contains a certain number of osteocytes housed in spaces called lacunae. Radiating out of these lacunae are small, branching tunnels (canaliculi) that allow communication and exchange of metabolites between the cellular extensions of neighboring osteocytes. In this way, all the osteocytes of a given bone are connected to one another through a network of tunnels essential to the maintenance of the bone cells and thus the surrounding bone tissue. Lacunae often lie with their longest axis parallel

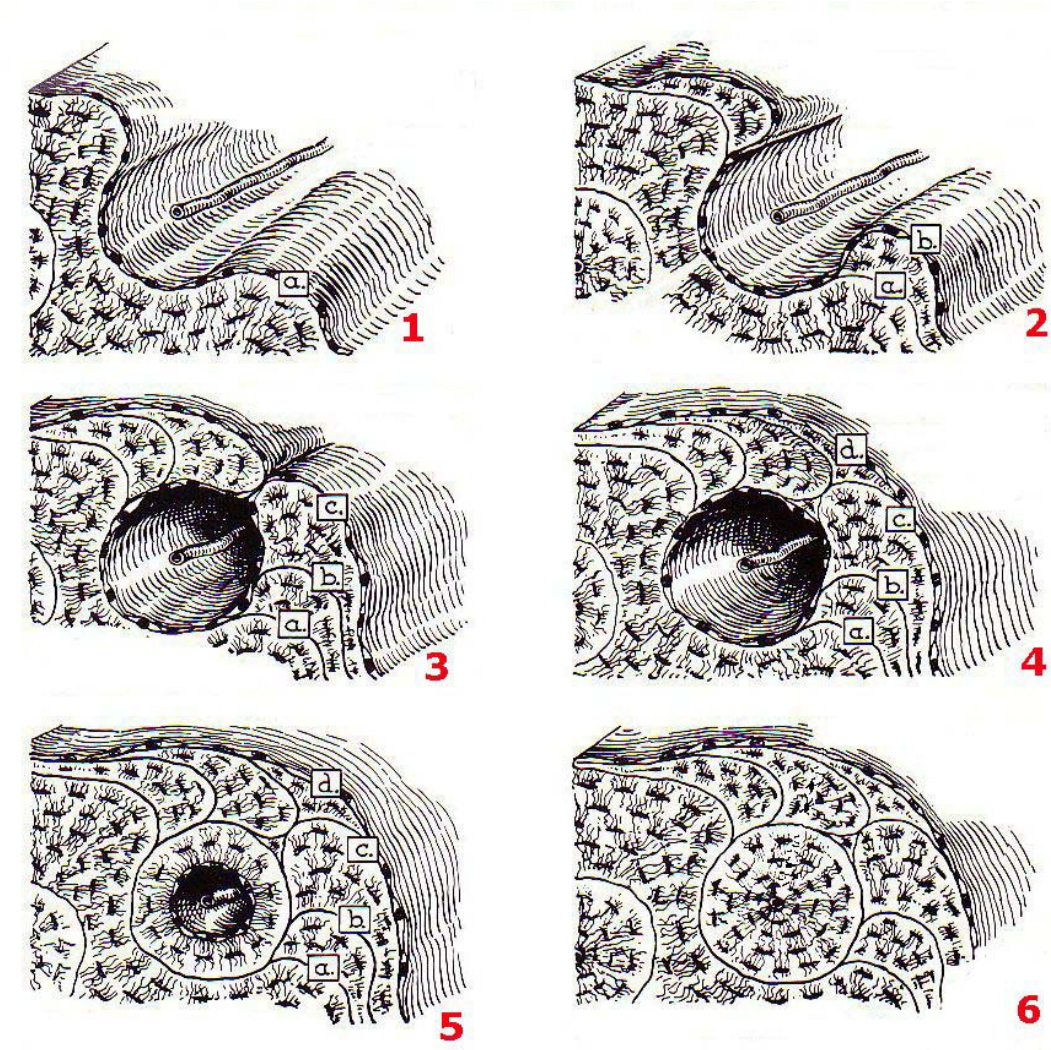


Figure 10: Formation of a non-Haversian canal

A schematic diagram showing the process by which blood vessels are incorporated into the developing periosteal surface. (1-2) circumferential lamellar bone is deposited in consecutive layers around the vessel. (2-3) lamellar bone encloses the vessel within a canal. (5-6) the non-Haversian canal is filled with concentric lamellae. Adapted from Ham and Cormack (1979).

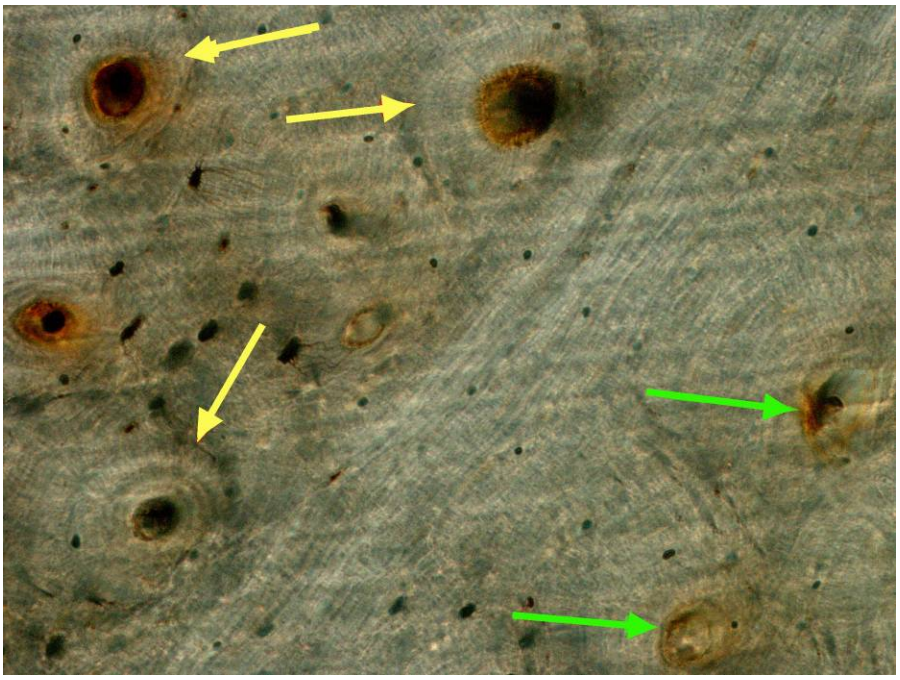


Figure 11: Primary Osteons and non-Haversian canals
A digital image (400x) of a light micrograph taken from a cross section of the humerus of a juvenile macaque (*Macacca mulatta*). Primary osteons (yellow arrows) are separated from non-Haversian canals (green arrows) by circumferential lamellae.

to the lamellar layer in which they reside; therefore, they appear as black ovals oriented into concentric rings in Haversian systems and in linear bands in circumferential lamellae (Hall, 1965).

Two types of vascular channels are present in compact bone: (1) longitudinally-oriented Haversian canals which contain one to two blood vessels each and (2) Volkmann's canals which run horizontally, the Haversian canals to one another and allowing the blood vessels from the endosteum and periosteum to communicate with those of the Haversian systems. Unlike Haversian canals, these channels are not lined by

concentric lamellae (Bloom and Fawcett, 1968).

Bone Cells

There are four basic types of bone cells: osteoprogenitor cells, osteoclasts, osteoblasts, and osteocytes. Osteoprogenitor cells are totipotent mesenchymal cells that line the innermost layer of the periosteum and endosteum, the connective tissues that line the outside and the inside of the bone. Through mitosis, they produce daughter cells that have the potential to become osteoblasts, the cells that are responsible for the production of new bone. This continued potential for differentiation is crucial to the maintenance and repair of the bone during biomechanical stress or injury. Osteoclasts are multinucleated cells that are produced by red bone marrow when serum calcium levels in the blood drop below a particular point. The ruffled border of these cells functions as an acidic bone tissue dissolver that releases enzymes through exocytosis of its lysosomes. Once an osteoclast removes bone tissue, calcium can be reintroduced into the bloodstream and a resorptive bay called a Howship's lacunae is produced in the bone layer. Osteoblasts are produced by the differentiation of osteoprogenitor cells triggered by metabolic and/or biomechanical stresses. These cells are responsible for secreting the osteoid that later becomes mineralized to form bone tissue, a process called osteogenesis (Currey, 2002). Mineralization of bone tissue increases bone density and is essential for maintaining proper bone strength (Martin et al., 1998).

During osteogenesis, some of the osteoblasts become surrounded by bone matrix and differentiate into osteocytes, their function being converted from bone formation to

bone maintenance. The spaces in which osteocytes reside, lacunae, are connected to one another by small tunnels called canaliculi. Osteocytes are able to communicate with one another through cytoplasmic projections into these small tunnels. This communication is crucial to the biochemical homeostasis of the bone (Hall, 1965).

Bone Formation

Bone formation occurs in two fundamentally different ways: intramembranous ossification and endochondral ossification. In both processes, bone is formed through the ossification of pre-existing embryonic connective tissue. Intramembranous ossification, however, is more evolutionarily primitive and continues throughout life. It also occurs in every bone in the human skeleton, as this type of ossification is responsible for subperiosteal appositional growth and bone remodeling (Scheuer and Black, 2000). During intramembranous ossification, some mesenchyme tissue cells differentiate into osteoblasts and begin to secrete osteoid within the center of a membrane. The entire membrane is eventually transformed into bone as additional bone is laid down around this primary ossification center. Bones produced through intramembranous ossification include the bones of the cranial vault, facial bones, and portions of the pelvis, sternum, clavicle, and scapula (Ham and Cormack, 1979).

All long bones form by way of the second ossification process, called endochondral ossification. Endochondral ossification involves the ossification of a hyaline cartilage model rather than a membrane, making this process much more complex than intramembranous bone formation. During endochondral ossification, some

of the mesenchyme cells differentiate into chondrocytes which secrete cartilage matrix that will eventually grow to become the cartilage model of the future bone. Invasion of this cartilage model by capillaries causes proliferation and differentiation of the outermost layer of cartilage cells into osteoblasts and osteocytes. These newly created osteogenic cells form a thin layer of subperiosteal bone matrix, called the bony collar, around the shaft of the cartilage model (Figure 12). The cartilage within the center of this bony collar begins to calcify and thin and eventually disintegrates. This process begins with the invasion of capillaries and osteogenic cells into the cartilage model at a specific location called the periosteal bud. Once the osteogenic cells and capillaries of the periosteal bud have reached the interior of the midsection of the cartilage model, a center

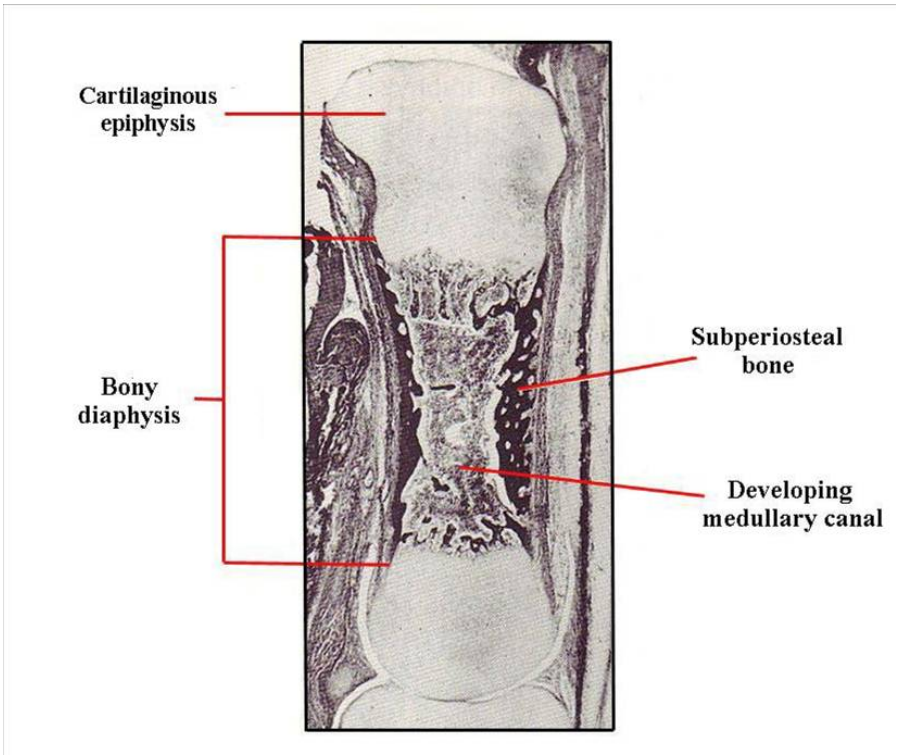


Figure 12: Endochondral ossification of the diaphysis of a long bone
A diagram identifying the relationship of the cartilaginous epiphyses to the developing bony diaphysis. Adapted from Ham and Cormack (1979).

of ossification has been officially formed. Next, the invading osteogenic cells gather around the remaining calcified cartilage spicules within the center of the bony collar and differentiate into osteoblasts which secrete bone around these cartilage remnants. Because the remaining cartilage is in the form of an irregular network filled with many spaces, this bone is cancellous bone with calcified cartilage cores, also known as primary spongiosa or woven bone. This layer of bone is rather short-lived, as osteoclasts soon resorb most of it to produce the medullary cavity and expand the length of the shaft. Once the medullary cavity has formed and the shaft is completely ossified, the first stage of endochondral ossification ceases and any subsequent changes are due to longitudinal and transverse growth (Ham and Cormack, 1979).

Bone Growth and Modeling

The bony diaphysis grows in length from the replacement of cartilage by bone secreted from osteogenic cells. Where the bony diaphysis and cartilaginous epiphyses meet (called the growth plate or metaphysis), cartilage is replaced by bone near the developing shaft, while new cartilage is simultaneously produced at the same rate on the epiphyseal side. At the metaphysis, there are four zones of ossification (Figure 13) that account for the rapid longitudinal growth of the diaphysis. The zone furthest away from the primary ossification center and closest to the epiphysis is the germinal zone. Here, the osteogenic cells closest to the epiphyseal plate actively differentiate into chondrocytes. These chondrocytes are relatively small and randomly distributed throughout the cartilage model, but begin to enlarge through the accumulation of glycogen as they approach the

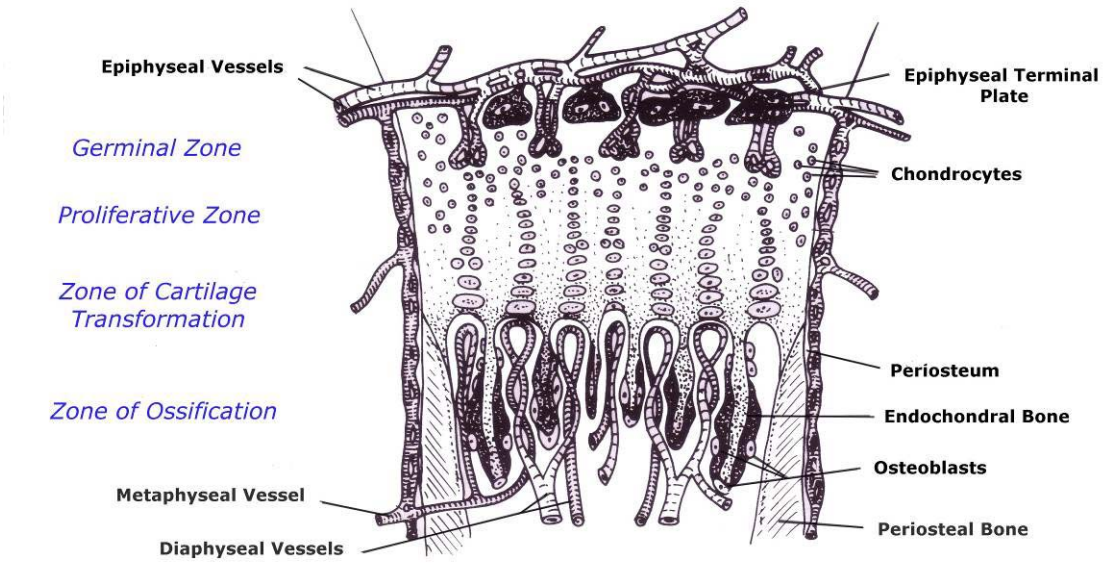


Figure 13: The four zones of ossification of the growth plate
A diagram demonstrating the conversion of the cartilage model into the growing bony diaphysis through the process of ossification.
Adapted from Scheuer and Black (2000).

adjacent proliferative zone. As the chondrocytes divide by mitosis, they become arranged in longitudinal columns within the proliferative zone. Once in the zone of cartilage transformation, the chondrocytes begin to hypertrophy in preparation for their subsequent replacement by bone. As the chondrocytes hypertrophy, they remove surrounding cartilage that produces large empty tunnels surrounded by calcified cartilage upon the death of the cell. Rather than degenerating, some of the chondrocytes differentiate into osteoblasts once they reach the zone of ossification and secrete a layer of bone on the calcified cartilage remaining from the previous zone. Like the tissue deposited within the bony collar, this newly-created bone is a type of cancellous bone that forms trabeculae with calcified cartilage cores. Later on, when the cartilaginous cores of these primary spongiosa are eventually replaced with lamellar bone tissue the bone is said to have

become secondary spongiosa. As the metaphysis is slowly incorporated into the diaphysis during the growth of the long bone, these trabeculae are resorbed by osteoclasts to maintain the dimensions of the medullary cavity (Scheuer and Black, 2000).

All bones are formed and maintained through the processes of modeling and remodeling during growth and development. Modeling refers to the change in size and shape of bone through the independent actions of osteoblasts and osteoclasts which consistently alter the architecture of the growing bone to fit the current mechanical demands of physical loading. Because normal bone tissue has essentially the same strength and mechanical properties throughout the human skeleton, changes in a particular bone's strength and rigidity must occur to its cross-sectional and longitudinal shape rather than its microscopic structure. Modeling is required to maintain the typical shape of a certain skeletal element during the course of longitudinal growth, and is thus most active during infancy, slowly subsiding shortly after skeletal maturity where remodeling activity takes over (Frost, 1990a).

Modeling commences immediately after the medullary cavity has formed and the bony collar is completely ossified. At this stage in development, the majority of the developing long bone still consists of the cartilaginous epiphyses which lie at either end of a relatively small bony collar and central spongy bone at the bone's midsection. As the bone grows in length, the metaphyses undergo periosteal resorption and endosteal expansion in order to be incorporated into the diaphysis (Figure 14). Periosteal resorption occurs when osteoclasts trim bone away from just beneath the periosteum, while endosteal expansion involves the addition of bone through osteoblastic activity beneath the endosteum. As the former metaphysis becomes part of the diaphysis, the diaphysis

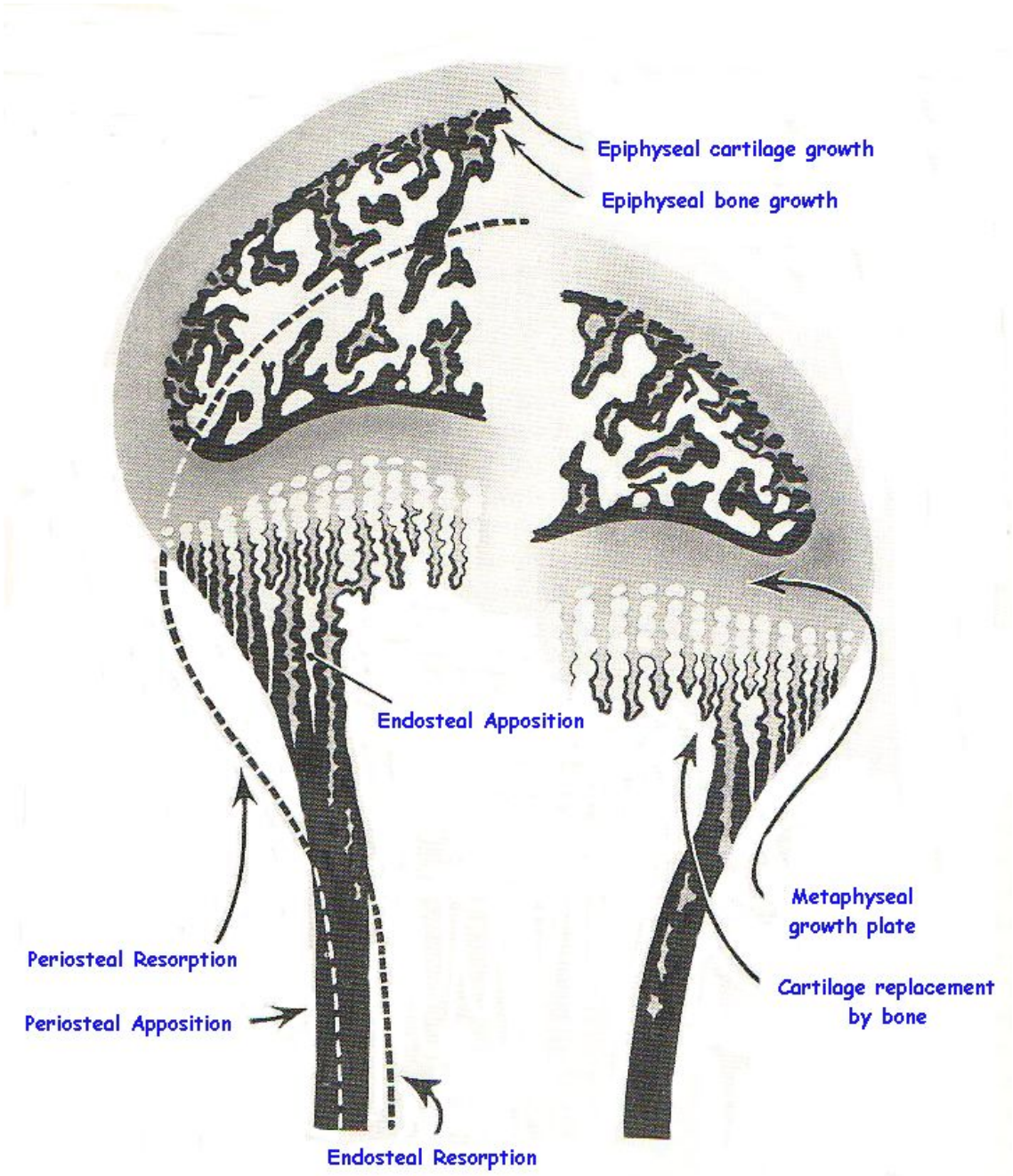


Figure 14: Long bone modeling

A diagram showing the modeling processes necessary for the maintenance of proper long bone morphology during growth. Adapted from Ham and Cormack (1979).

must continually increase in diameter during longitudinal growth in order to maintain a proper shape. This process involves the opposite conditions of periosteal expansion and endosteal resorption (Enlow, 1963). Thus, a cross section through the midshaft of a growing bone is a snapshot in time of a complex array of separately created and modified bone layers. Depending upon the conditions of growth, the cross section can contain multiple layers of bone of diverse types deposited at various times during growth and development.

Bone Remodeling

As bone tissue ages, microscopic damage in the form of stress fractures can occur through mechanical usage. In order to avoid these fatigue fractures, older bone tissue must be destroyed and replaced by new bone through remodeling, also known as bone turnover. Remodeling is not concerned with changes in size or shape of the bone, but rather the maintenance of bone tissue at the microscopic level. Unlike modeling, remodeling involves the cooperation of both osteoblasts and osteoclasts in groupings called BMUs (basic multicellular units). These groups of cells are composed of roughly 10 osteoclasts, hundreds of osteoblasts, and their associated blood vessels and nerves. BMUs can be generated at any bone surface that is lined with osteogenic connective tissue (i.e., periosteal, cortical-endosteal, trabecular, and Haversian). Each BMU undergoes three lifecycle stages (referred to collectively as ARF): activation, resorption, and formation (Figure 15). The first step in remodeling occurs with activation of osteoclast formation through the fusion of monocytes. This process occurs at the site of origin for the BMU and takes about 3 days to complete (Martin et al., 1998). These

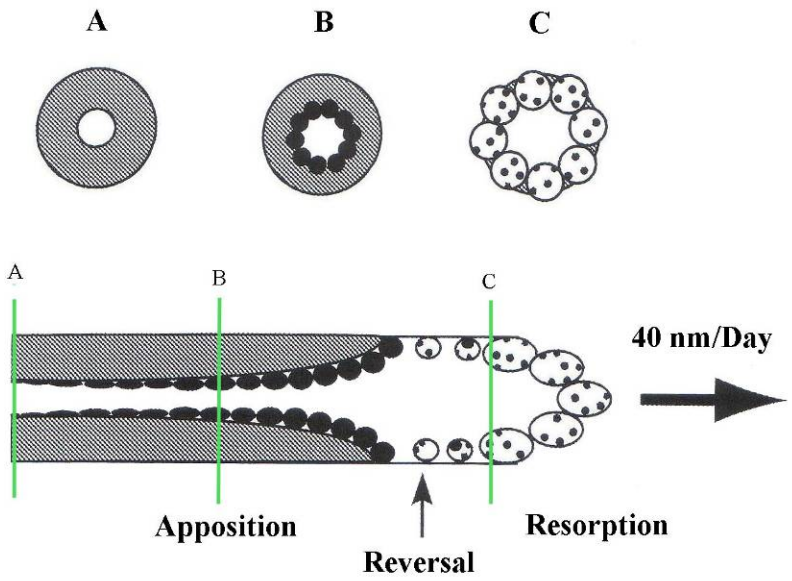


Figure 15: The three life cycles of the BMU
A diagram depicting the three active stages of the BMU (basic multicellular unit). Green lines indicate different cross sections along the length of the BMU. Solid black circles represent osteoblasts while spotted circles are osteoclasts. Adapted from Martin et al. (1998).

newly-formed osteoclasts begin to resorb bone at a rate of about 40 μm per day either across a bone surface (as in trabecular bone) (Figure 16) or else they burrow into the cortex of compact bone (Frost, 1964). The activity of the osteoclasts forms what is called a resorptive space in cross section, an empty space within the cortical layer with a rugged outline (Figure 17). Eventually, the osteoclasts experience apoptosis (or programmed cell death) which signals the initiation of osteoblast formation from precursor cells. After proliferating and lining the resorptive cavity, the osteoblasts begin to secrete osteoid onto the resorbed surface. Over the next 10 days, this organic matrix will become mineralized with the deposition of mineral crystals within and between its collagen fibers (Frost, 1963). When a BMU tunnels through compact bone, a secondary osteon is created. These osteons are said to be secondary due to the fact that they develop *after* the affected bone

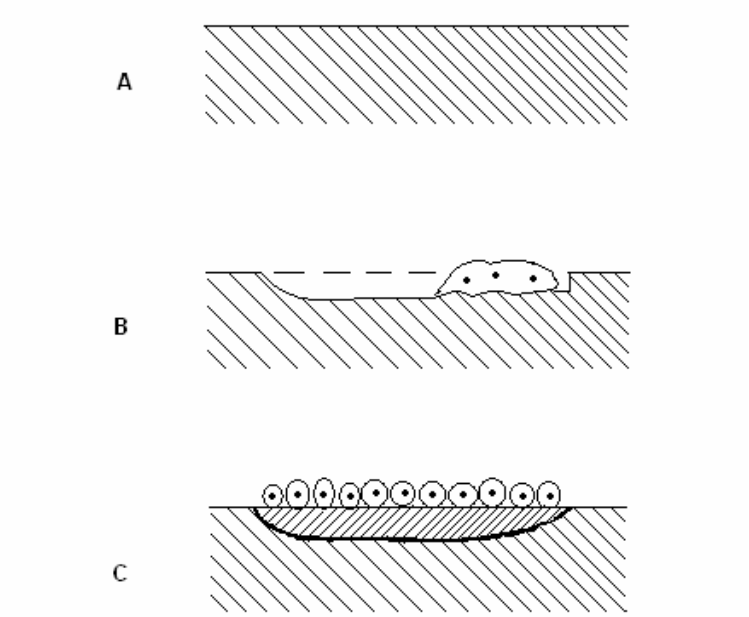


Figure 16: BMU remodeling of the surface of a cancellous trabecula
A schematic diagram showing the stages of trabecular remodeling.
(A) BMU inactivity. (B) osteoclastic activity removes old bone.
(C) osteoblastic activity deposits new bone on resorbed surface.

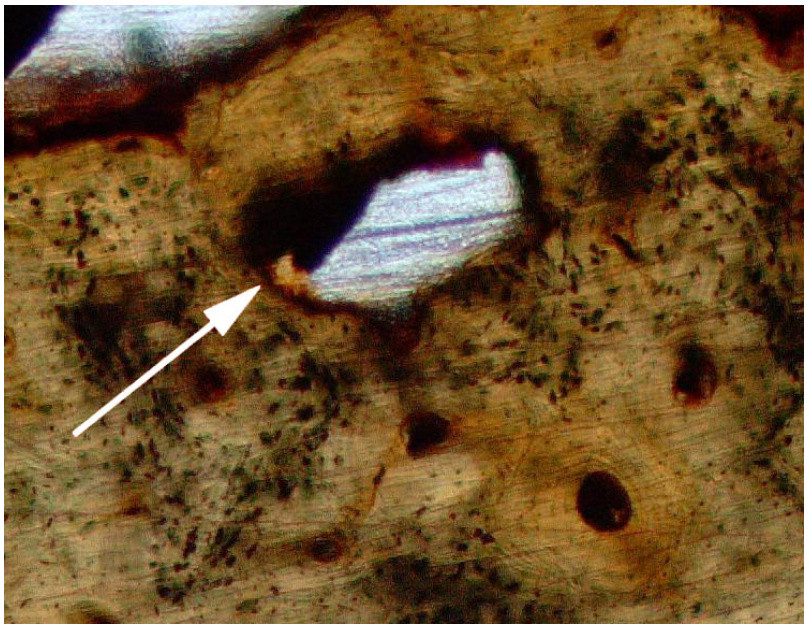


Figure 17: Resorption space
A digital image (200x) of a light micrograph taken from a cross section of the femur of a juvenile macaque (*Macacca mulatta*).
A resorption space (arrow) is indicated.

tissue has ossified and require the resorption of preexisting bone tissue. Primary osteons, on the other hand, are osteons that are created without resorption prior to osteoid deposition. In a BMU tunnel, the reversal from osteoclastic to osteoblastic activity creates an empty space between the resorptive and formative regions along the tunnel's length. This space represents the lag time present between resorption and formation that is caused by the differential activity rates of both cell types. While an osteoblast can only secrete 1 micrometer of bone per day, an osteoclast resorbs tens of micrometers per day. This reversal line coincides with the future cement line of the secondary osteon (Figure 18), as osteoblasts will soon lay down concentric lamellae within the newly-created tunnel. Once the BMU is isolated within the bone's cortex, a constant vascular supply is needed to provide nutrients to the working cells, including the osteoblasts that will be left

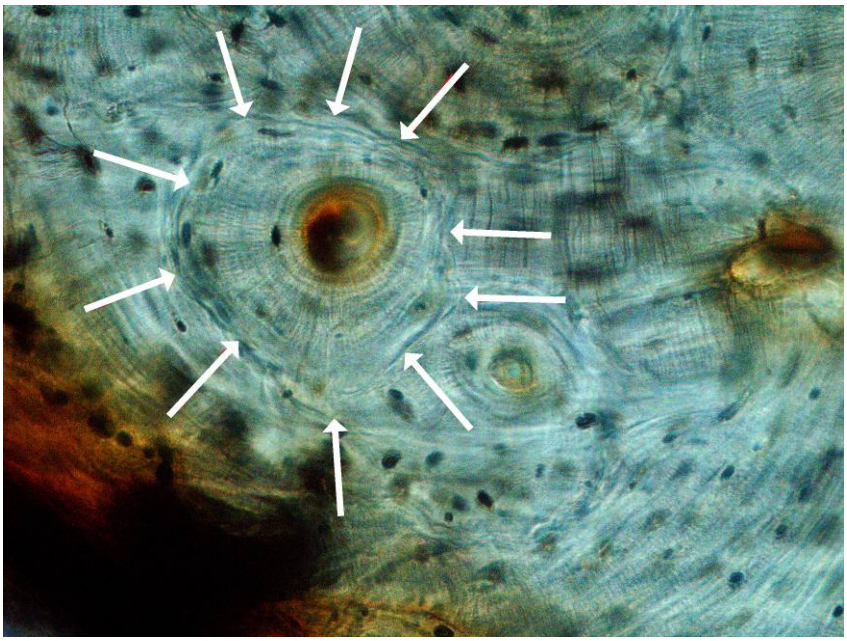


Figure 18: Cement line
Digital image (400x) of a cement line (arrows) surrounding a secondary osteon in a cross section of the humerus of a juvenile macaque (*Macacca mulatta*).

behind to become osteocytes. Thus, the tunnel can never be completely refilled with bone, and a Haversian canal is thus created containing two capillaries for nutrient supply (Martin and Burr, 1989).

The process of remodeling occurs throughout an individual's lifetime; however its rate is highest during bone growth. The apposition and resorption of bone is also a necessary process for maintaining homeostasis of blood level calcium, as the majority of the body's calcium is stored in the skeleton for future use. The presence of calcium in blood is essential for many biological processes, including intercellular communication, muscle cell contraction, and nerve signal firing. When blood calcium levels are too low, osteoclastic activity is stimulated to release calcium stored in bone tissue, while osteoblastic activity is inhibited. The opposite occurs when blood calcium levels are too high and osteoblasts must be able to store excess calcium into bone tissue.

Chapter 3: Previous Research in Fetal Long Bone Histology

Numerous studies (e.g., Balthazard and Müller, 1921; Gruenwald, 1966; Gardner, 1971; Burton et al., 1989; Dhem et al., 1990; Glorieux et al., 1991; Rodriguez et al., 1992) have attempted to describe the relationship between fetal growth and histological structures in the long bones (mostly the femur), but only recently have researchers been able to shed any light on the mechanisms responsible for these phenomena. No previous research has been performed in an attempt to determine whether the age of fetal specimens can be predicted accurately from long bone histomorphometry; rather, the majority of studies in this field have focused on clinical diagnosis of neonatal osteopenia and rickets (Su, 2003). Therefore, while the general qualitative trends in fetal histomorphology may be relatively well-known, this subject is oftentimes glossed over in the literature.

Despite recent advances in the understanding of fetal long bone growth, confusion remains regarding the exact timing of the appearance of secondary osteons in the human appendicular skeleton. These deficiencies in research over the past few decades are likely due to a combination of three compounding factors: (1) the difficulty associated with obtaining fetal specimens for histological study which leads inevitably to small sample sizes, (2) the complexities of long bone growth and resultant variation in microscopic structure of bone tissue types, and (3) the lack of a complete understanding of bone biomechanics and the mechanisms associated with remodeling and modeling events.

One of the earliest studies conducted on fetal bone histology was that of Balthazard and Müller (1921) who examined decalcified sections taken from the long bones of several fetuses up to 6 lunar months in age. Generalizations were made by these researchers as to the formation of particular microscopic bone tissue structures; however, like with most research in this field up until quite recently, their work suffers from conflation of microscopic structures (particularly primary and secondary osteons) and their modes of formation. The classic view of human bone remodeling holds that remodeling begins at birth with the advent of extensive fetal movement, and thus, secondary osteons should reveal themselves only in the newborn infant (Frost, 1987).

Demeter and Mátyás (1928) were among the first to conclude that secondary osteons were not characteristic of the early prenatal period. Their conclusions, however, were drawn from a single ground section taken from the femoral midshaft of a 5-lunar-month-old fetus. In 1956, Engfeldt and Zetterström also found no Haversian systems in ground sections of the femoral diaphysis of a newborn infant; however, they do not disclose the conditions surrounding the death of this infant or the number of days it survived after delivery. Fazekas and Kósa (1978) contend that in the mature fetus, Haversian systems can be found in the ventral and lateral quadrants of the femur. These secondary osteons are surrounded interstitially by woven bone and seem to arise first in the posterior quadrant where they spread anteriorly on either side of the medullary canal until the medullary canal is entirely encompassed by osteons by the age of 3. After the formation of this osteonal ring, the secondary osteons expand toward the periosteal surface until the majority of the femoral wall consists of these osteons in the 6-year-old.

Other authors assert that Haversian systems can form prior to extrauterine life. Burton et al. (1989) observed Haversian remodeling in the six long bones and 6th and 7th ribs of four preterm neonates, some as young as 24 weeks gestation. At the time, this research created quite a stir, because remodeling was still considered by most to be a response to increased bone loading which would theoretically create microdamage that is repaired by the remodeling process. However, since fetuses and preterm infants have a characteristic poverty of movements compared with term infants, a direct relationship between loading and remodeling in the fetal appendicular skeleton does not seem plausible.

It appears that remodeling is much more complex than was once thought. Remodeling occurs not only in response to microdamage, but is also a normal and stochastic process of bone maintenance. Remodeling is part of a regulatory feed-back system (called the mechanostat) that allows bone to respond to increased loading by increasing its strength (modeling) and to decreased loading by decreasing bone strength (remodeling) (Stout, 1982; Frost, 1987). This latter type of remodeling occurs at the same rate in all long bones, while remodeling in response to microdamage will be most active in bones that accrue the most damage (Martin and Burr, 1989; Mori and Burr, 1993). The sample utilized by Burton et al. consisted of preterm neonates that survived for several days after delivery. It has recently been shown that fetal loading in the intrauterine environment during the late gestational period is critical for normal fetal bone formation. Fetal bone loading is a unique process that involves the impact of the limbs against the uterus and substantial resistance against fetal movement provided by the amniotic fluid. Thus, preterm infants who have been robbed of a proper fetal loading environment are

prone to developing osteopenia after preterm birth and have heightened bone remodeling and suppressed bone formation (Miller, 2003).

All of these studies together provide a wealth of knowledge that can serve as the theoretical basis for fetal age estimation via histological analysis. The assumption, as with any aging method in physical anthropology, is that these characteristics will present themselves in a predictable pattern that parallels the aging process. Given the biological constraints under which long bones form and grow, it seems reasonable to assume that a direct relationship exists between their microscopic structures and macroscopic morphology from which age can be inferred.

Chapter 4: Materials and Methods

This research was conducted in the Mineralized Tissue Histology Laboratory in the Department of Anthropology at the University of Tennessee. Established by Dr. Murray K. Marks, this laboratory houses a full array of equipment for epoxy resin embedding and thin sectioning, as well as light microscopy.

Seven stillborn cadavers of known gestational age and sex were donated to the Mineralized Tissue Histology Laboratory by the Medical Examiners Office of the University of Tennessee Regional Medical Center. Permission was granted by the hospital's institutional review board for histological sampling of these fetuses before incineration. The sample consisted of fetuses ranging in age from 17 to 35 weeks gestation with no two fetuses having the same gestational age (Table 1). The six long bones (humerus, radius, ulna, femur, tibia, and fibula) of the right side were extracted

Table 1: Actual and developmental ages of fetal specimens
*estimated by long bone length via Fazekas and Kósa (1978).

	Actual Age (weeks gestation)	Developmental Age* (weeks gestation)	Sex
Fetus 1	17	17	M
Fetus 2	17.5	14	M
Fetus 3	23	24	F
Fetus 4	23.5	22	M
Fetus 5	25	25	F
Fetus 6	33	38	M
Fetus 7	35	37	M

from each fetal specimen and cleaned of superficial soft tissue with micro-dissecting tools. All skeletal elements used in this study were taken arbitrarily from the right side to control for fluctuating asymmetry (except for the left tibia and fibula of Fetus 2, which was substituted for a damaged right distal leg segment).

After extraction, the skeletal elements were soaked in a solution of distilled water and double-strength degreaser for no longer than 48 hours to remove any remaining soft tissue. The long bones were subsequently allowed to soak in distilled water for an additional 24 hours and then laid out to dry for a minimum of 12 hours. Once the skeletal elements were cleaned and dried, photographs were taken of each bone prior to histological sectioning with a centimeter scale for comparison purposes (Figure 19). Three measurements were recorded for each bone: maximum length, maximum sagittal diameter at midshaft, and maximum transverse diameter at midshaft. In order to account for potential growth retardation in these stillborn cadavers, the developmental age of each fetus was estimated via long bone length (Fazekas and Kósa, 1978) and compared with actual age to quantify the fetus's developmental progress. The developmental ages of the fetal specimens are presented in Table 1. The presence of distinct differences between actual gestational age and estimated developmental age in five of the seven fetal cadavers highlights the efficacy of analysis in terms of the latter age scheme. Considering that in the forensic setting, the actual age of a fetal specimen is unknown and that fetal death is often associated with growth retardation, all statistical analysis in this study was conducted employing developmental age. In addition to fetal growth retardation, error in reporting of last menstrual period (LMP), a very commonly documented occurrence, could also have resulted in inaccurate recording of the gestational age of the fetal



Figure 19: Skeletal elements of each fetal specimen
Digital image of the six appendicular bones from which midshaft thin sections were made for each of the seven fetal specimens (with centimeter scale). Clockwise from left: humerus, fibula, ulna, radius, tibia, femur.

specimens utilized in this study. Not only do some women give the date of their first missed period rather than their last menstrual period, but light bleeding can oftentimes occur in the first month of pregnancy and be mistaken for menstruation (Lubchenco et al., 1963; Gruenwald, 1966).

Seven marks were delineated on the bones with permanent marker, separating each bone into seven equal parts along its length (Figure 20). These seven marks represent seven separate cuts to be made per bone. Cut 4, by definition, represents the midshaft of the long bone diaphysis, as three proximal (cuts 1-3) and three distal (cuts 5-7) marks lie to either side of this demarcation. The long bones were then embedded in epoxy resin blocks to facilitate the thin sectioning of such small histological specimens (Figure 21). In instances when the long bone was too long to fit into the plastic mold, a

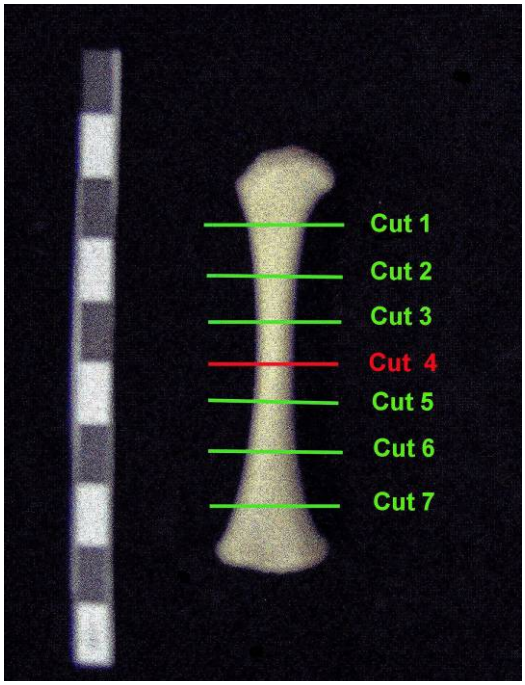


Figure 20: Seven cuts scored on the bones for sectioning
Digital image of the seven cuts delineated on each long bone for thin sectioning (with centimeter scale). Cut 4 is the midshaft of the bone used in this study.



Figure 21: Epoxy resin embedding of bone segments
A digital image of various fetal bone segments embedded in epoxy resin blocks prior to thin sectioning.

Dremel multi tool was used to cut the bone into appropriately-sized segments. Care was taken to divide the bone between cut marks so as to preserve the actual location chosen for thin sectioning. In accordance with procedures outlined in previous research (Marks et al., 1996), copper wire and superglue were used to position the sections of bone as close to anatomical position as possible within the epoxy resin blocks, with the anterior portion of the shaft facing upward. A vacuum dessicator was then used to eradicate air bubbles from the epoxy resin blocks.

Once the epoxy resin had hardened, cuts were made using a Buehler Isomet low speed diamond saw (Figure 22) and mounted to a petrographic slide (Figure 23). Each slide was labeled with an inventory number (e.g., 28T4) consisting of three parts: the fetal specimen number (07-Fetus 1, 27-Fetus 2, 18-Fetus 3, 08-Fetus 4, 28-Fetus 5, 17-Fetus 6, 02-Fetus 7), the bone (H-humerus, R-radius, U-ulna, F-femur, T-tibia, Fi-fibula), and the cut number (1-7). Fetal specimen numbers refer to the order in which the fetal remains were catalogued at the morgue, such that 18 (Fetus 3) was the eighteenth fetus to be inventoried by the author. When only a few fetal remains were elected for histological research, the inventory numbers were dropped for a more appropriate numbering system (Fetus 1, Fetus 2, etc.). The slides were subsequently ground to within 150 μm using a Metaserv 2000 Polisher machine. Each slide was cleared with xylene for no longer than 20 minutes to eliminate discoloration due to taphonomic bone staining and maximize translucency (Stout and Paine, 1992).

This thesis presents the results of measurements taken from only the midshaft of each bone, while the results of the other six cuts will be utilized in future research which



Figure 22: Buehler Isomet low speed diamond saw
A digital image of the saw used in thin sectioning of the epoxy resin blocks.

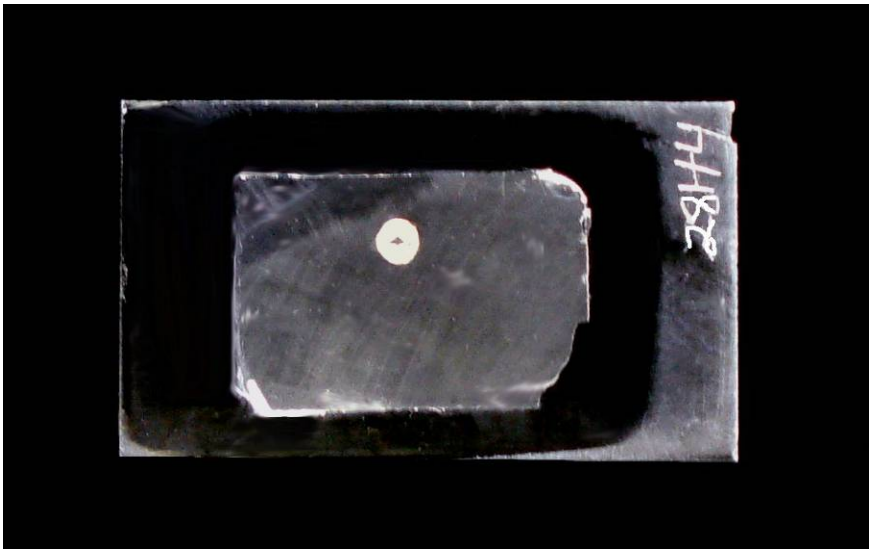


Figure 23: Petrographic slide of the humeral midshaft of Fetus 5
A digital image of the microscopic slide of the humeral midshaft cross section of Fetus 5 (25 weeks gestation). Note the inventory number (28H4) at top right.

will evaluate intra-bone variation. For each midshaft thin section, measurements were taken at each quadrant using digitally-captured images from a Leica DMRX research microscope with a Sony digital camera linked to a Sony mixer and Image-Pro Express software. Images were taken at 16x, 50x, 100x, and 200x power magnification depending on the size of the bone.

For each slide, a maximum of 111 measurements were taken: maximum sagittal medullary diameter (anterior-posterior), maximum transverse medullary diameter (medial-lateral), medullary area, maximum cortical thickness (taken at anterior, posterior, medial, and lateral quadrants), minimum cortical thickness (taken at anterior, posterior, medial, and lateral quadrants), and a maximum of 25 separate trabecular diameters per quadrant. Maximum sagittal medullary diameter was defined as the greatest distance in the anterio-posterior plane occupied by the medullary canal. Likewise, maximum transverse medullary diameter is the greatest distance present in the medio-lateral plane. Maximum and minimum cortical thicknesses were defined as the largest and smallest distances respectively between periosteal and endosteal surfaces in a particular quadrant. These two measurements were always taken parallel to the transverse plane for the medial and lateral quadrants and parallel to the sagittal plane for the anterior and posterior quadrants. If the medullary canal was not present (i.e., the fibula of Fetus 1 and the ulna of Fetus 3) the midpoint of the maximum sagittal diameter at midshaft and maximum transverse diameter at midshaft was used in place of the endosteal surface for these two measurements in each quadrant. For each quadrant, a maximum of 25 woven bone trabeculae were randomly chosen for measurement of trabecular thickness (Figure

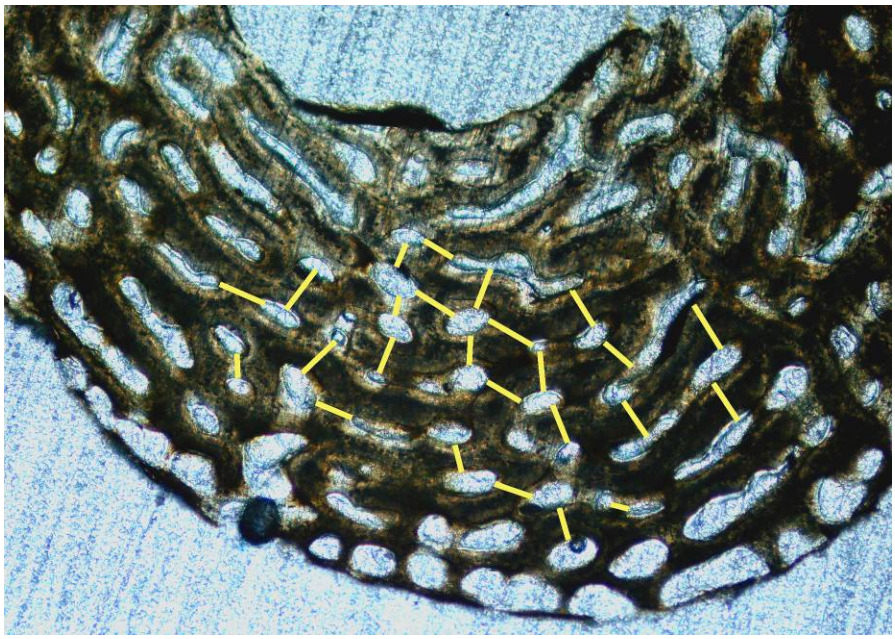


Figure 24: Woven bone trabecular thickness
A digital image (50x) of a light micrograph showing the posterior quadrant of the tibial midshaft of Fetus 5 (25 weeks gestation) The yellow lines represent 25 separate measurements of trabecular thickness taken at this quadrant.

24). In cases where fewer than 25 trabeculae were present in a particular quadrant, all trabeculae visible within the quadrant were measured. The outermost and innermost trabeculae were not included in this analysis due to the potential for variation caused by recent periosteal and/or endosteal resorption or apposition.

In order to maintain consistency between all fetal ages, a woven bone trabecula was defined as the distance between adjacent open spaces in the bone. Therefore the use of "trabecula" to describe the object being measured in this case is in reality an oversimplification, because measurements taken from older fetuses will more than likely include the concentric lamellae between woven bone trabeculae (Hall, 1965). However, current methodology used in this research did not allow for adequate visualization of

separate bone layer tissue types, and, thus, a distinction could not be made between woven and lamellar bone in this fetal collection. Future research, however, will attempt to elucidate the differences in bone layer types between the seven fetuses used as specimens in this study.

Raw data were compiled into an Excel file and analyzed in SAS. For comparative purposes, line graphs of the maximum sagittal and transverse medullary diameters were created for each individual long bone. Separate line graphs were also produced for each individual long bone of the maximum cortical thicknesses and average trabecular thicknesses separated by quadrants. Additionally, values for sagittal medullary diameter, transverse medullary diameter, medullary area, maximum cortical thickness, minimum cortical thickness, and trabecular thickness were averaged across quadrants and compared between bones.

Lack of replication for age in the medullary variables prevented statistical analysis from being conducted; therefore, generalizations concerning changes in said variables with age were constructed visually from the graphs. Pearson's rho analysis was conducted on maximum and minimum cortical thickness to determine the extent to which these measurements are correlated with age. This type of analysis was chosen due to the fact that the small sample size examined in this study limited the number of measurements per fetus for each of these variables to only four (for each quadrant). A fixed effects ANCOVA analysis was also performed with trabecular thickness as the dependent variable, quadrant as a fixed factor, and age as a covariate. Age was chosen as a covariate because of the potential this variable has for affecting the relationship between quadrant and trabecular thickness. The ANCOVA analysis was run in SAS with

two main effects (quadrant and age) and an interaction term of quadrant upon age. Once the model for each long bone was run with the interaction term included, those bones that lacked a significant interaction between age and quadrant were reanalyzed with the interaction term dropped from the model. This approach is seldom employed, yet it returns the most accurate results and is recommended by most researchers versed in proper statistical techniques (Engqvist, 2005). Differences between means were examined independently across the four quadrants for each bone using the entire fetal sample. In all statistical analyses, an alpha of 0.05 was used to determine statistical significance. When significant differences were found between quadrants of the same bone, a least significant difference (LSD) post hoc test was performed to determine which quadrants differed from one another. This test was chosen due to its ability to maintain a constant alpha (α=0.05) across all paired comparisons.

Chapter 5: Results

The osteometric measurements taken from the uncut long bones of the seven fetal specimens are listed in the appendix (Table A1) along with the raw data collected for sagittal and transverse medullary diameters and medullary area (Table A2), and maximum and minimum cortical thicknesses (Table A3). The cortical thickness means for each bone averaged across quadrants are also given (Table A4). The means for trabecular thickness for each quadrant are presented separately for each bone in Tables A5-A10. Trabecular thickness means for each bone across quadrants (Table A11) and the raw data for trabecular thicknesses (Table A12) are also provided.

The following figures illustrate the results of analysis of the raw data. The values for each fetus in these figures are presented in order of developmental age rather than actual age due to the potential for growth retardation in this fetal collection. This decision was made based on the differences present between gestational age and estimated age based on equations of Fazekas and Kósa (1978) utilizing long bone length. Because each developmental stage is represented by only one fetus, any conclusions drawn from these figures are extremely preliminary and situational in nature. In no way does the author suggest that a single fetus can represent an entire range of variation present in a stage of fetal development. All generalizations made from the following graphs refer to the relationships present between the particular fetuses sampled for this study and are not intended to be extrapolated to fetal development in general.

Medullary Diameters and Medullary Area

The three medullary variables (sagittal medullary diameter, transverse medullary diameter, and medullary area), by definition, are represented by only a single measurement for each fetus. Because replication for age is lacking in these variables, statistical significance tests cannot be performed to elucidate whether a linear relationship exists between each of these variables and age. General trends in medullary dimensions with changes in age, however, can be demonstrated using simple line graphs.

The values for maximum sagittal and transverse medullary diameters are presented for each long bone in figures 25-30. In the femur (Figure 25), the transverse and sagittal diameters of the medullary canal are extremely similar in size and trend up through fetus 5; both diameters increase in size at the third stage of development (fetus 4) and subsequently decrease in size only to increase drastically at the sixth stage of development (fetus 7). At this stage, the sagittal diameter is much wider than the transverse diameter. This difference is magnified in the last stage (fetus 6) where the transverse length drops significantly, while the sagittal length remains roughly the same width. This leaves a difference in size between the two measurements of almost 1000 nanometers.

Unlike the femur, the tibia (Figure 26) shows no tendency toward similar sagittal and transverse medullary diameters in six of the seven fetuses. The developmentally youngest fetus (fetus 2) has similar sagittal and transverse diameters, while the second youngest (fetus 1) has a much wider sagittal diameter and slightly smaller transverse diameter than the first. The relationship in size between these two diameters is reversed in the next stage (fetus 4), with transverse length exceeding sagittal length only slightly.

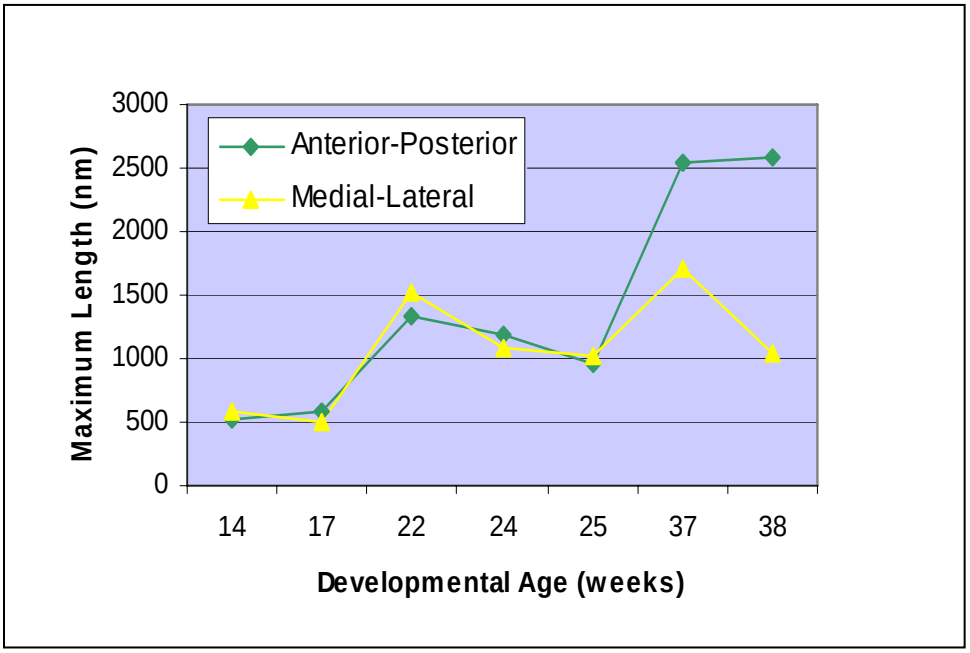


Figure 25: Medullary Diameters of the Femur Across Fetal Specimens

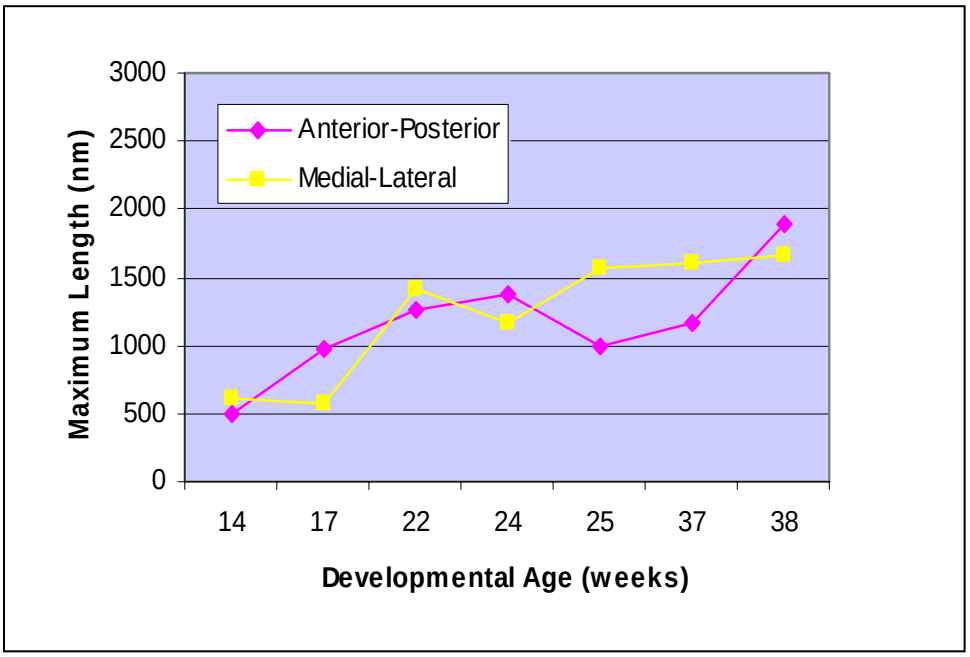


Figure 26: Medullary Diameters of the Tibia Across Fetal Specimens

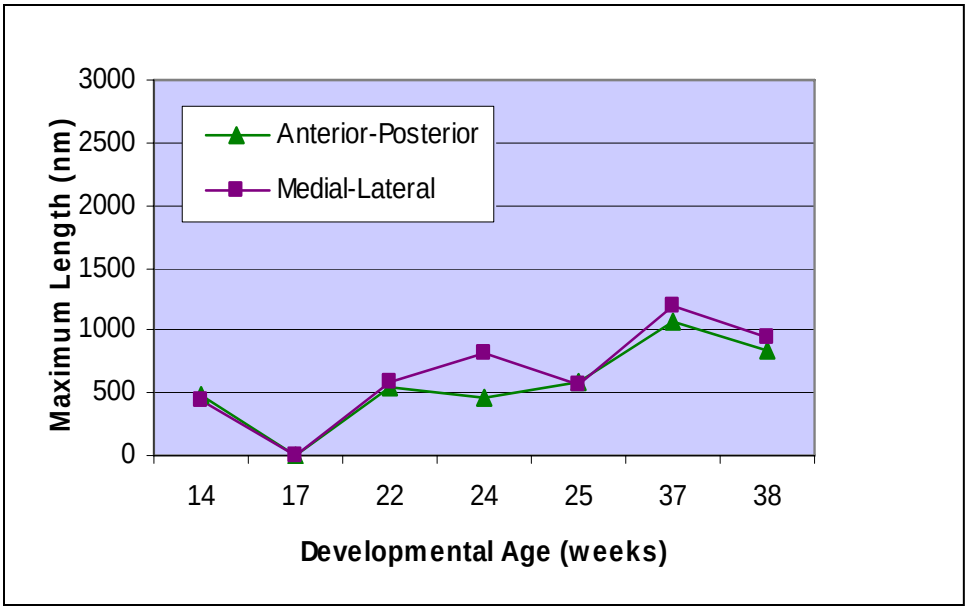


Figure 27: Medullary Diameters of the Fibula Across Fetal Specimens

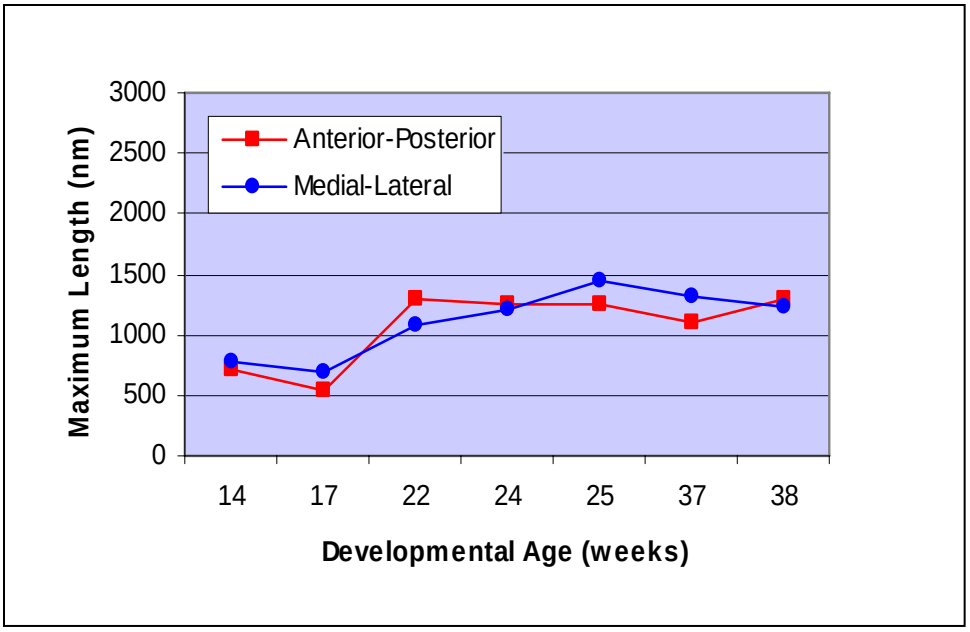


Figure 28: Medullary Diameters of the Humerus Across Fetal Specimens

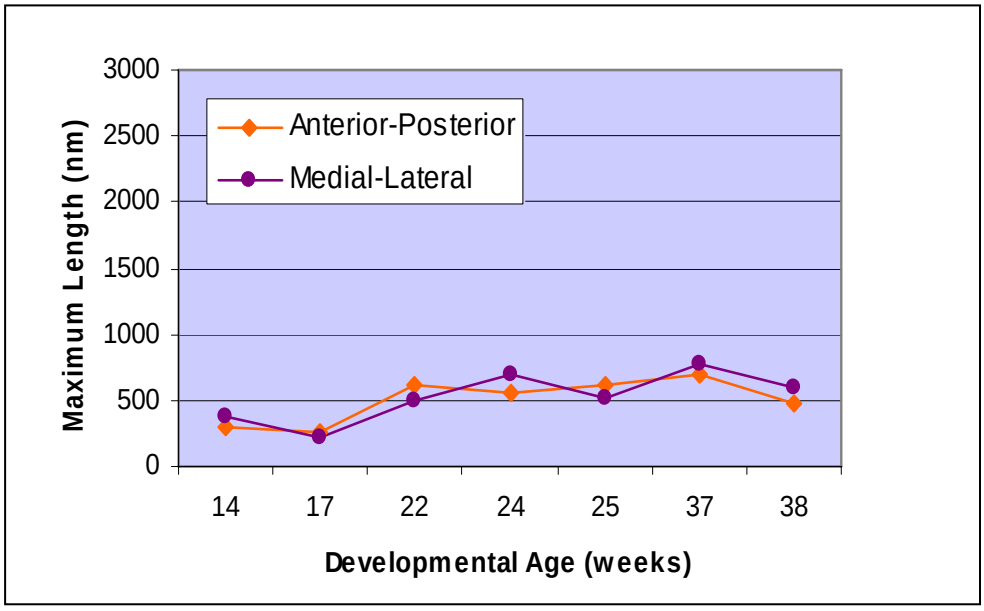


Figure 29: Medullary Diameters of the Radius Across Fetal Specimens

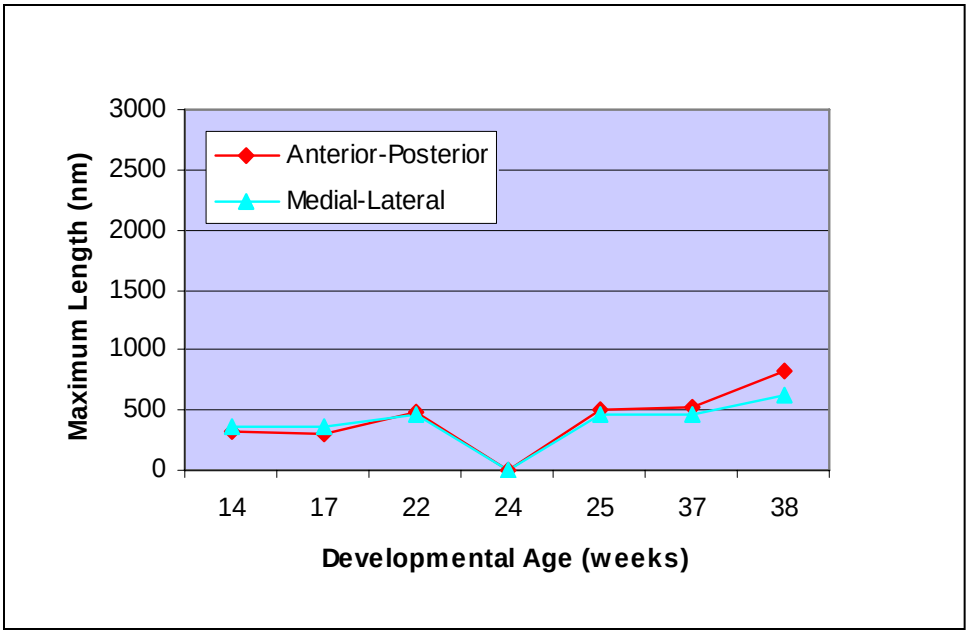


Figure 30: Medullary Diameters of the Ulna Across Fetal Specimens

Fetus 3, like fetus 1, has a much larger sagittal diameter than transverse diameter. Fetus 5 possesses the largest divergence in size between the two diameters, with transverse length a little more than 500 nanometers larger than the sagittal length. Fetus 7 is similar to fetus 5, although the difference in size between the two diameters is slightly smaller. Fetus 6, on the other hand, has a much larger sagittal length than any other fetus.

The age-related changes in medullary dimensions of the fibula (Figure 27) follow a very similar course in all fetuses except fetus 3. Because the fibula of fetus 1 lacks a medullary canal, we can only conclude that there is a similar increase in size of both the sagittal and transverse diameters between the first and third fetal stages. In the fourth stage (fetus 3), the transverse diameter increases while the sagittal diameter decreases. In the fifth stage (fetus 5), the opposite occurs, causing both diameters to converge on a value very similar to that present in fetus 4. Both diameters increase in the sixth stage (fetus 7) and subsequently decrease in fetus 6. At these last two developmental stages, the sagittal diameter is slightly smaller than that of the transverse.

In the humerus (Figure 28), the transverse diameter is slightly larger than the sagittal in the first two developmental stages, although both decrease between the first and second stage. The only other bone to possess a decrease in both diameters between the first and second stages is the radius. In the humerus' third stage, both diameters increase in size but the sagittal diameter exceeds the transverse. In the fourth stage (fetus 3), the transverse diameter continues to increase while the sagittal decreases to meet the transverse. This trend is continued in the fifth stage (fetus 5) so that the transverse dimension is wider than that of the sagittal dimension. This difference in size is maintained in the sixth stage (fetus 7) although both diameters are slightly smaller than

those of fetus 5. In the final developmental stage, the transverse diameter continues its decreasing trend while the sagittal diameter increases to a value slightly larger than the transverse.

Like the humerus, the radius (Figure 29) possesses a decrease in both medullary diameters between the first and second developmental stages. Likewise, both diameters increase in size during the third stage; however, unlike the humerus, the radius has more similarity present between the two measurements in all fetuses. The sizes of the transverse and sagittal diameters in the radius are also small compared with those of the humerus.

In the ulna (Figure 30), the medullary diameters are the most similar in size compared with the other five long bones. Like all of the other bones, the values for both medullary measurements increase during the third stage (fetus 4). Because the ulna of fetus 3 lacks a medullary canal, we can only conclude that medullary dimensions do not change much between the third and fifth stages. In the seventh stage, however there is a slight increase in size of both diameters, with the sagittal dimension exceeding the transverse by about 200 nanometers. This difference is the largest present in the ulna between the two medullary measurements.

In figures 31 and 32, the sagittal and transverse medullary diameters are presented for all long bones. One of the most obvious trends in these graphs is the apparent separation of the long bones into two groups. For both sagittal and transverse measurements, the ulna, radius, and fibula of all seven fetuses cluster together at lower values than the other three bones. Furthermore, the sagittal and transverse medullary diameters of the six long bones are the most similar in size during the first stage of

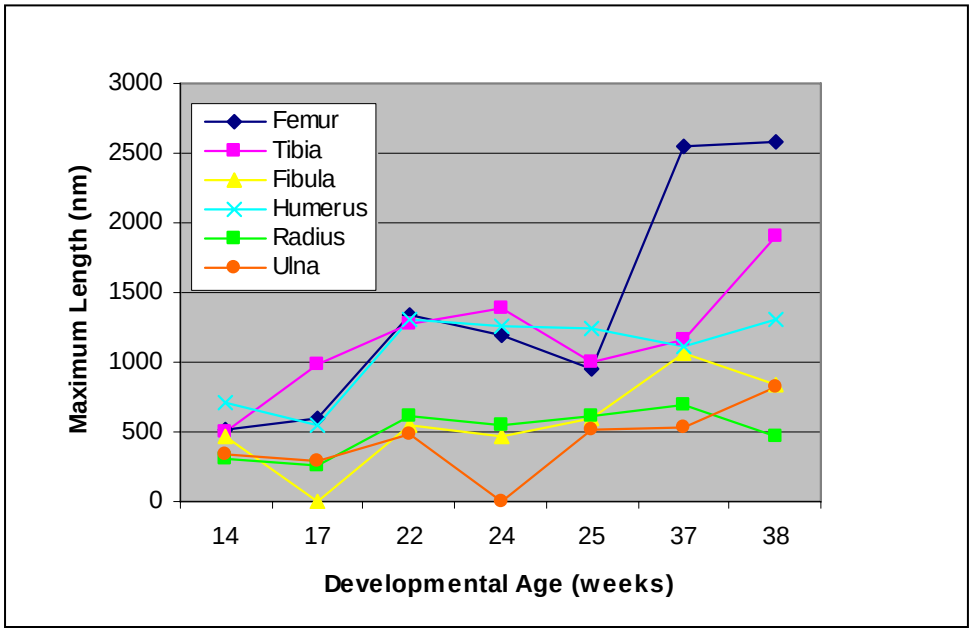


Figure 31: Sagittal Medullary Diameter by Bone

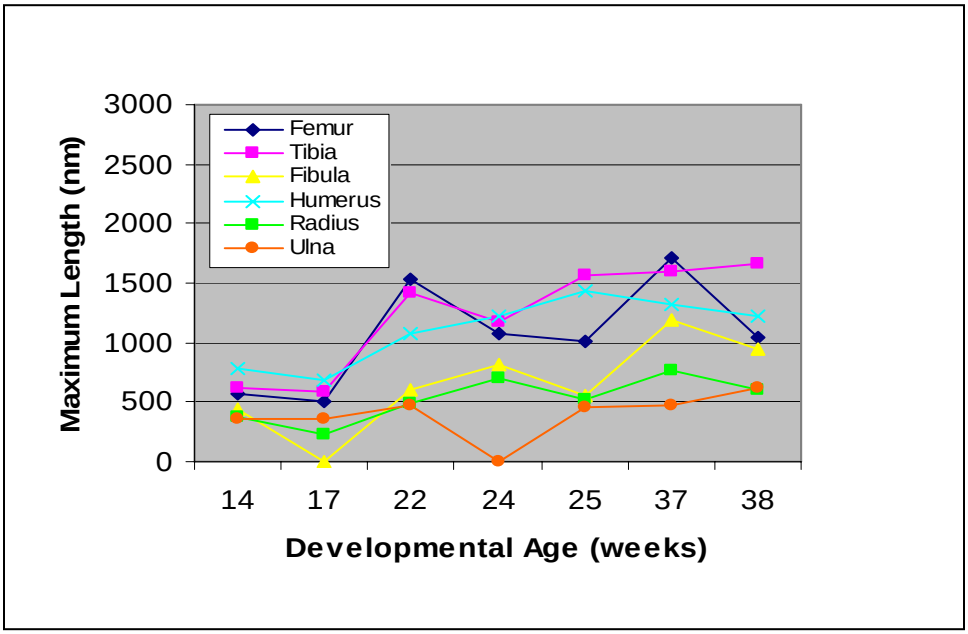


Figure 32: Transverse Medullary Diameter by Bone

development after which they diverge from one another. For the sagittal medullary diameter (Figure 31), there is a large separation in size between the humerus, femur, and tibia on the one hand and the radius, ulna, and fibula on the other during the third and fourth developmental stages. This separation, however, is reduced in fetus 5. In the last two developmental stages, the widest variation in sagittal medullary diameters is found. It is interesting to note that the femur, tibia, and humerus follow a similar trend in size change up until the fifth developmental stage (fetus 5). After the fifth developmental stage, the sagittal diameter of the femur grows tremendously in relationship to the other five long bones, while the sagittal diameters of the humerus and tibia remain relatively the same. In the seventh stage, both the humeral and tibial diameters increase but do not come close in size to the femoral diameter.

The sagittal diameters of the radius and ulna are almost identical in size and trend excluding the last developmental stage where the ulnar diameter increases while the fibular and radial diameters decrease. The trend lines of the radius, ulna, and fibula are also relatively flat compared to those of the other three long bones. It seems that the sagittal medullary diameters of these smaller long bones do not change much over the course of development; although there is a general increase in length of the sagittal diameter over time, this increase is relatively small compared with that of the other three long bones.

In figure 32, one can see that there is certainly less similarity in transverse medullary diameter between the six long bones than there is in sagittal diameter. The pattern present in size of the transverse medullary diameter among the ulna, fibula, and radius is not unlike that of the sagittal diameter for these same bones; there is relatively

little change overtime compared with the other three long bones, and the ulna, fibular, and radial diameters tend to be lower than the other three bones at each stage of development. Yet, most of the differences between the sagittal and transverse diameters lie with the tibia and femur. Unlike with the sagittal medullary diameter, the transverse diameter of the femur does not increase drastically in the last two stages of development. In fact, it actually decreases in the last stage (fetus 6) to the same size as that of fetus 5. In addition, the transverse medullary diameter of the tibia does not increase much during the last stage of development as the sagittal diameter does; rather it stays relatively the same size between the fifth and seventh stages.

The medullary area of each long bone is presented in figure 33. The trends in size changes of medullary area are not unlike those of the sagittal and transverse diameters. There are some exceptions, however, mostly in the femur. Particularly interesting is the medullary area of the femur of fetus 7, which exceeds the next largest medullary area by over 857,000 nm^2. The seventh developmental stage also exhibits a relatively drastic decrease in femoral medullary area to match that of the tibia at this stage. With a glance at the sagittal and transverse diameters of the femur (Figure 25), one can see that the drastic increase in size at stage 6 is largely due to increase in sagittal diameter while the decrease at stage 7 is due to decrease in transverse diameter.

Maximum and Minimum Cortical Thickness

Although both maximum and minimum cortical thicknesses were measured for each quadrant in all six of the long bones, results of only the maximum cortical

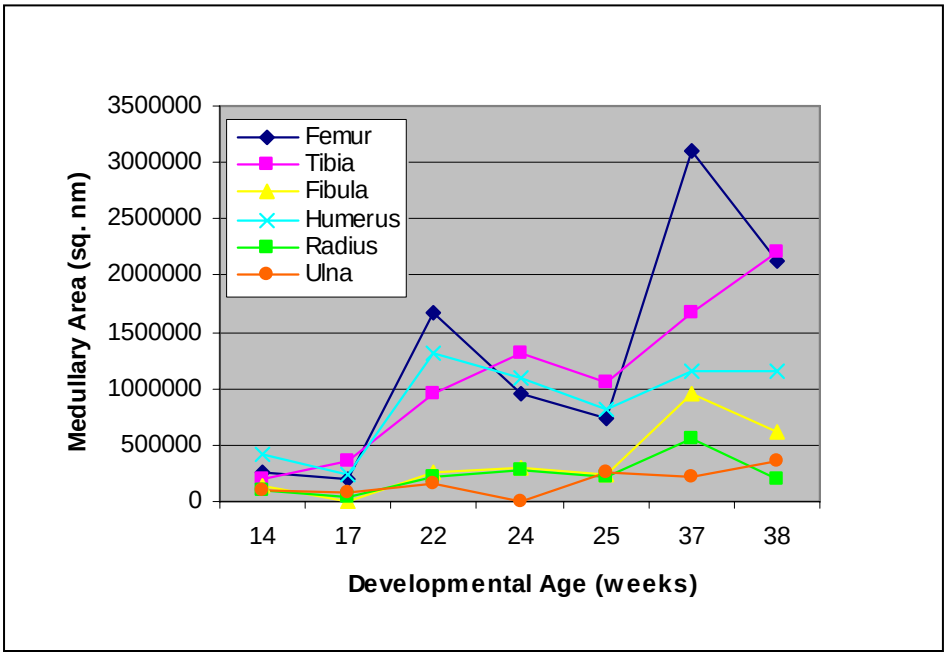


Figure 33: Medullary Area by Bone

thicknesses are presented in graphic form here due to the extreme similarity in trends among these two measurements. Results show that both measurements are equally efficient in explaining a linear relationship with age; thus, only the results for maximum cortical thickness are explored in depth here due to the implications that this measurement has concerning the pattern of growth in fetal long bones. The raw data for both maximum and minimum cortical thicknesses are presented by quadrant for each long bone in the appendix (Table A3).

The maximum cortical thicknesses of each quadrant are presented for each long bone in figures 34-39. For the femur (Figure 34), all quadrants except for the posterior quadrant follow a general positive curvilinear trend with an increase in thickness up to stage 3 (fetus 4), a decline to stage 5, and an increase to a peak at stage 7. The posterior

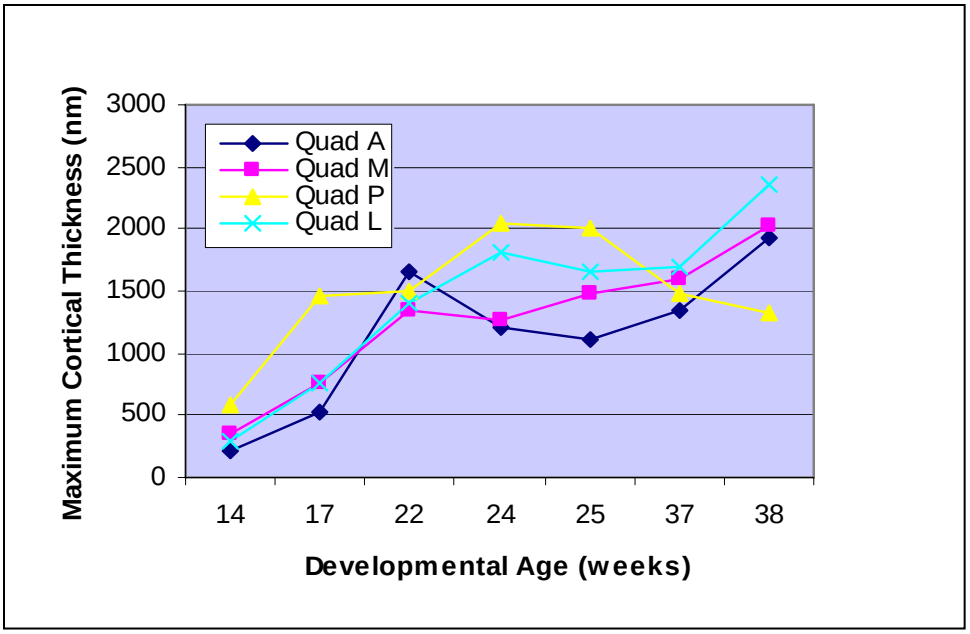


Figure 34: Maximum Cortical Thickness of the Femur by Quadrant

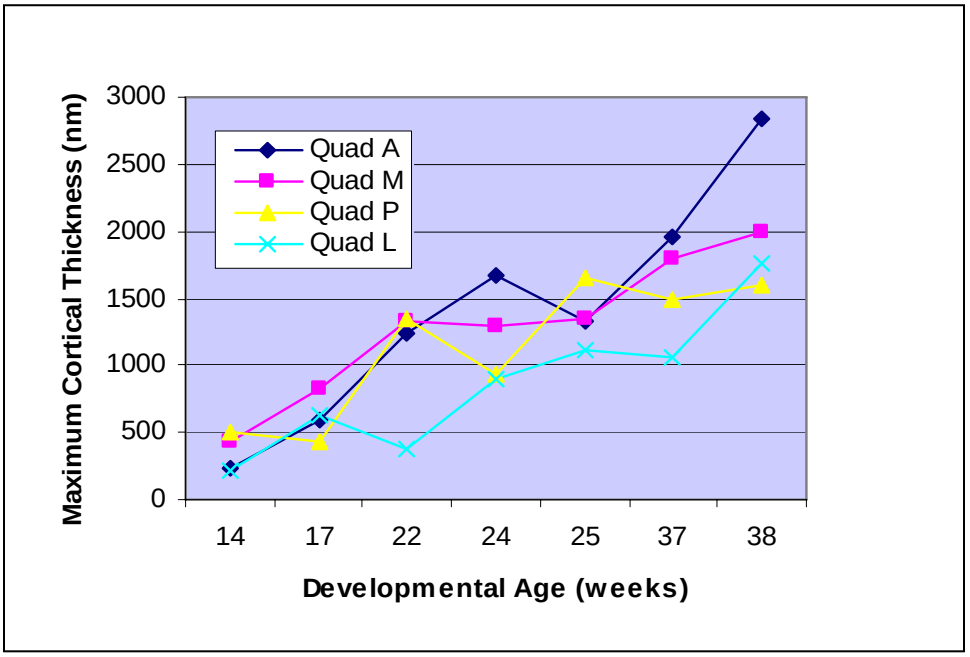


Figure 35: Maximum Cortical Thickness of the Tibia by Quadrant

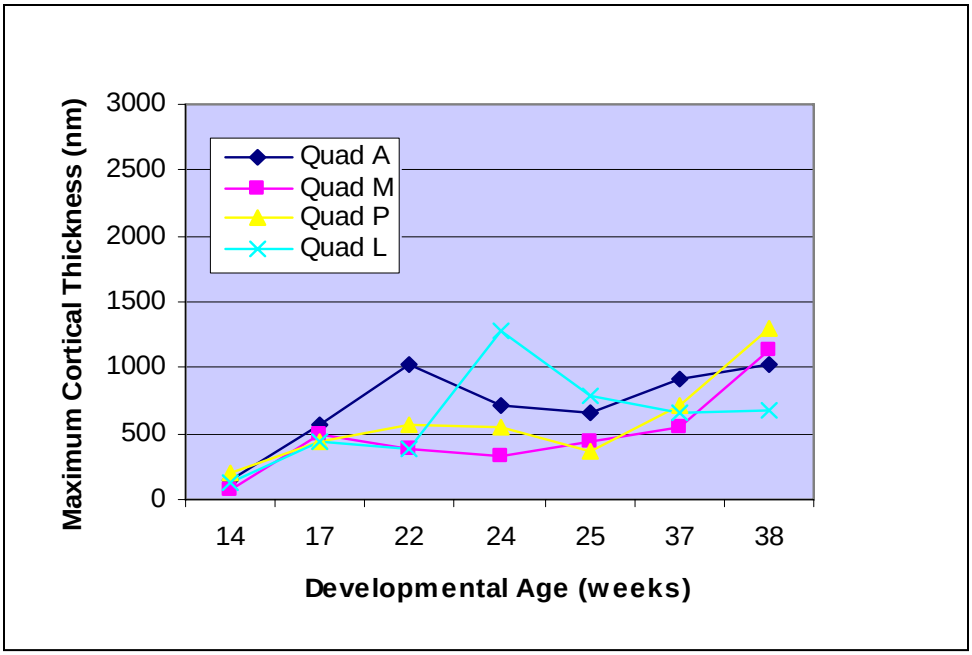


Figure 36: Maximum Cortical Thickness of the Fibula by Quadrant

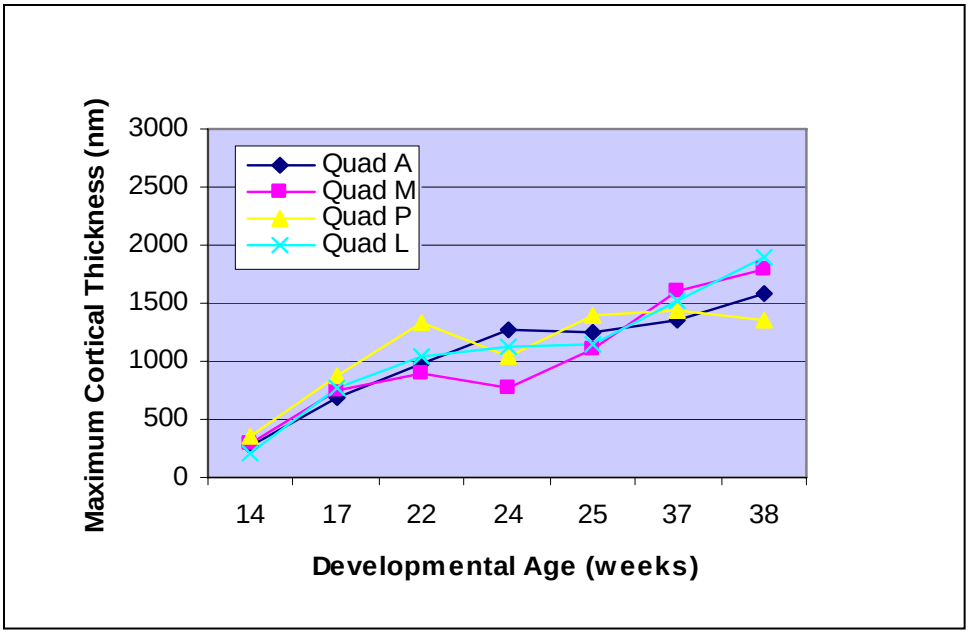


Figure 37: Maximum Cortical Thickness of the Humerus by Quadrant

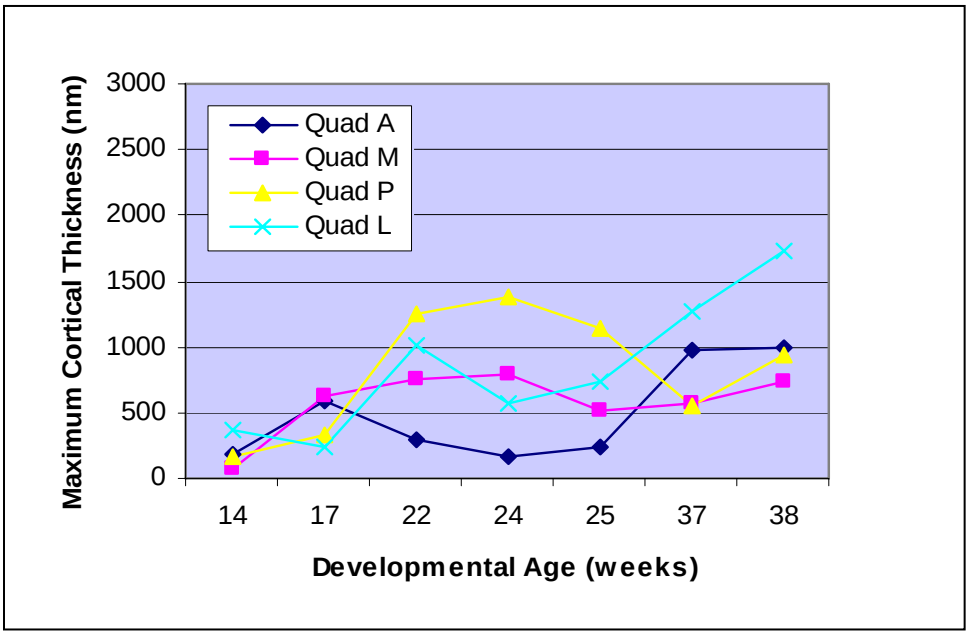


Figure 38: Maximum Cortical Thickness of the Radius by Quadrant

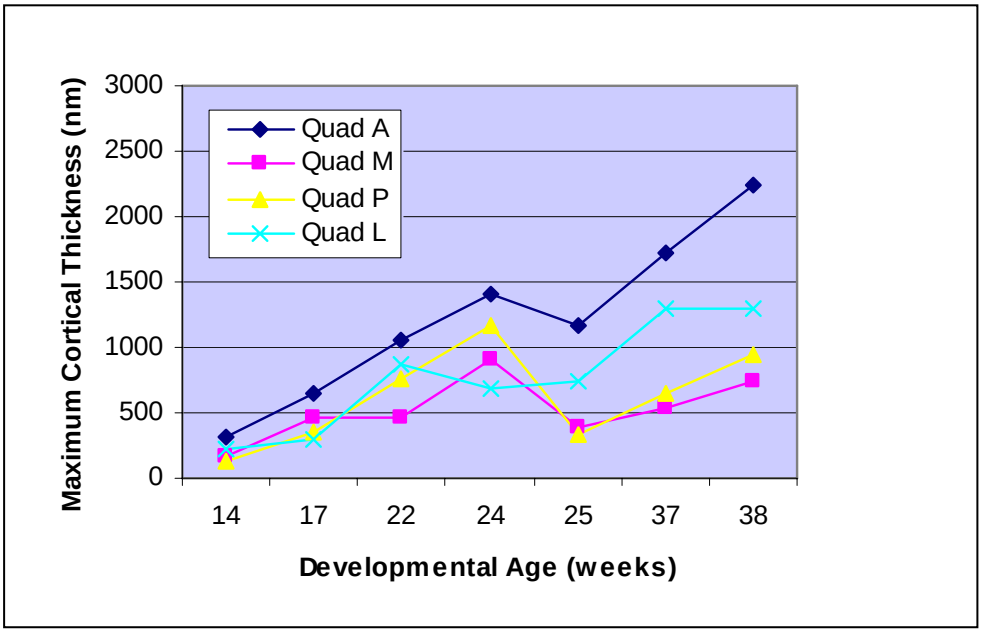


Figure 39: Maximum Cortical Thickness of the Ulna by Quadrant

quadrant tends to be the thickest quadrant up until the sixth stage where the lateral quadrant becomes the largest.

The maximum cortical thicknesses of the tibia (Figure 35) are oriented in a much straighter linear pattern than those of the femur. All of the quadrants tend to increase in thickness up to the third developmental stage, except for the lateral quadrant which decreases in thickness in fetus 4. In general, the lateral quadrant tends to be the thinnest quadrant. In the last developmental stage, the anterior quadrant increases in thickness quite drastically until it is roughly 800 nanometers thicker than the next thickest tibial quadrant, the medial quadrant. Out of all the bones, the anterior tibial quadrant is by far the largest; it is roughly 483 nanometers thicker than the next largest quadrant, the lateral femoral quadrant of fetus 6.

The pattern of maximum cortical thickness in the fibula (Figure 36) is slightly more complex than in other long bones. Interestingly, the cortical thicknesses of each quadrant are almost identical within fetus 1 and fetus 2, with fetus 1 having much larger cortical layers than fetus 2. It appears that the anterior quadrant is the largest in the fibula while the medial quadrant tends to be the smallest. What is unique about the trends in fibular cortical thickness is the increase in the lateral quadrant during the fourth and fifth developmental stages. In the other developmental stages, the lateral quadrant is relatively thin. It is also worth mentioning the increase in thickness of the medial and posterior quadrants above that of the anterior quadrant in the last stage of development (fetus 6).

Like the cortical thickness trends in the tibia, the humeral trends (Figure 37) of all quadrants are oriented in a relatively straight linear pattern. Unlike the tibia, however, the lateral quadrant is never the thinnest. In fact, it appears that no quadrant is consistently

the largest or smallest, and a significant amount of reversals in size order of the quadrants is present. The pattern present in fetus 1 and fetus 2 is identical to that of the fibula, although the cortical thicknesses are larger in size in the humerus.

The radius (Figure 38) is similar to the femur, considering both have similar relationships among relative quadrant sizes during the middle stages of development. In both, the posterior quadrant tends to be the largest during this period, the lateral the next largest, the medial the second smallest, and the anterior the smallest. The drastic increase in size of the lateral quadrant of the femur during the last two stages of development is also present in the radius; however, the rest of the quadrants are not similar in trend to the femur in these two fetuses (fetus 7 and fetus 6). Also, the anterior portion of the radius is the next largest quadrant rather than the medial quadrant, as is the case in the femur.

The maximum cortical thicknesses of the ulna (Figure 39) are quite unique compared to those of the other five long bones. In particular, the anterior quadrant remains the thickest quadrant in all seven fetuses, exceeding the next thickest ulnar quadrant (fetus 6) by about 956 nanometers. In addition, the thicknesses of the medial and posterior quadrants drastically decrease in the fifth fetus and increase thereafter; however, they do not return to their original size.

In figures 40-43, the maximum cortical thicknesses of all the long bones are presented separately for each quadrant. In figure 40, one can see that all six long bones have very similar anterior quadrant thicknesses during the first two developmental stages, and differences among the bones develop thereafter. In the later developmental stages, the tibia tends to have the thickest anterior portion and the ulna the second thickest portion. The fibula and radius tend to have much thinner anterior quadrants than the other

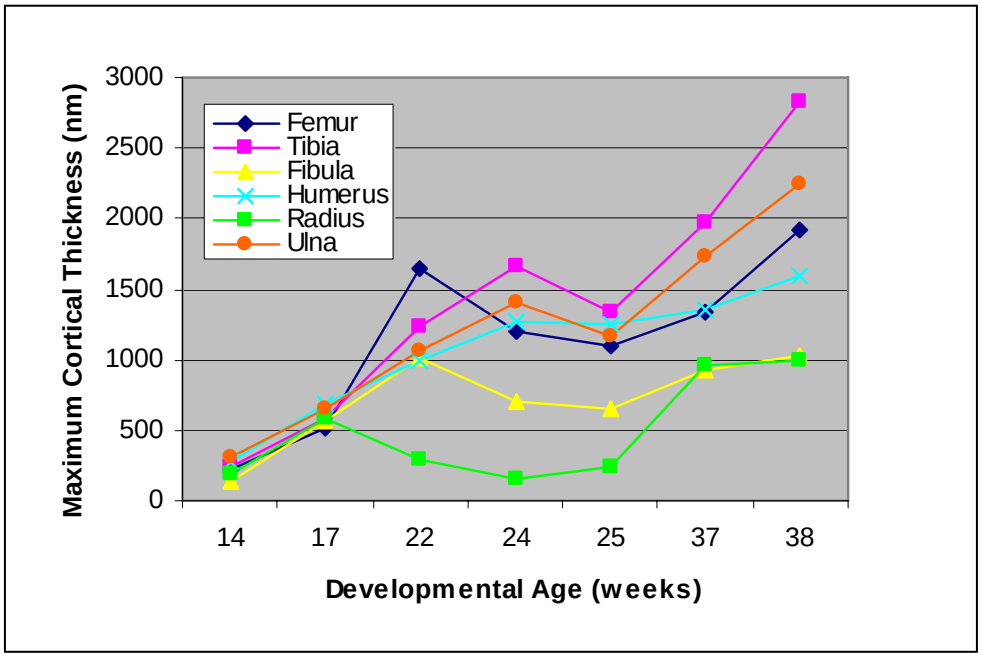


Figure 40: Maximum Cortical Thickness of the Anterior Quadrant by Bone

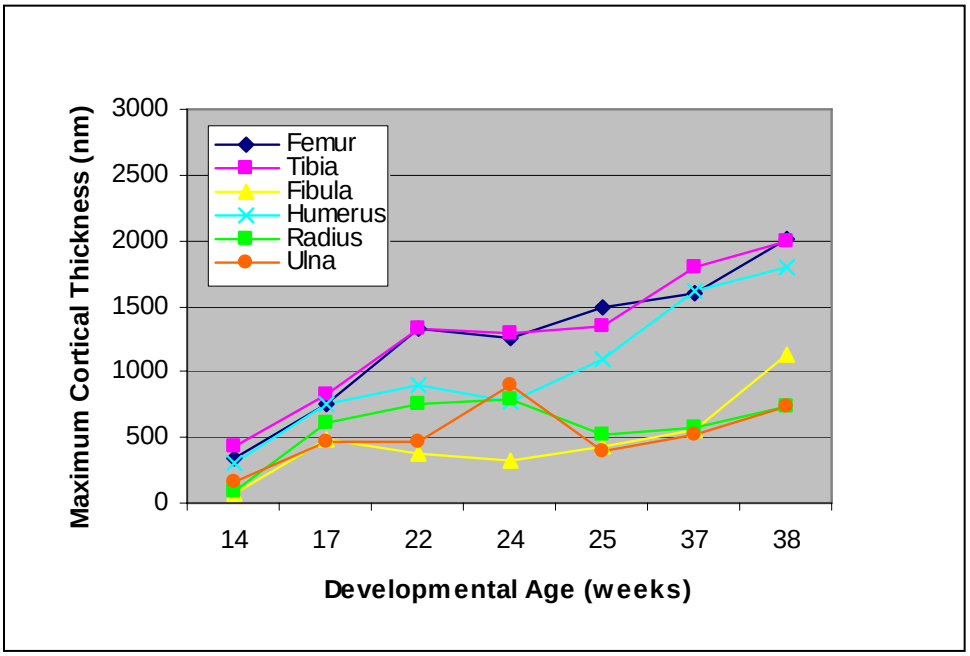


Figure 41: Maximum Cortical Thickness of the Medial Quadrant by Bone

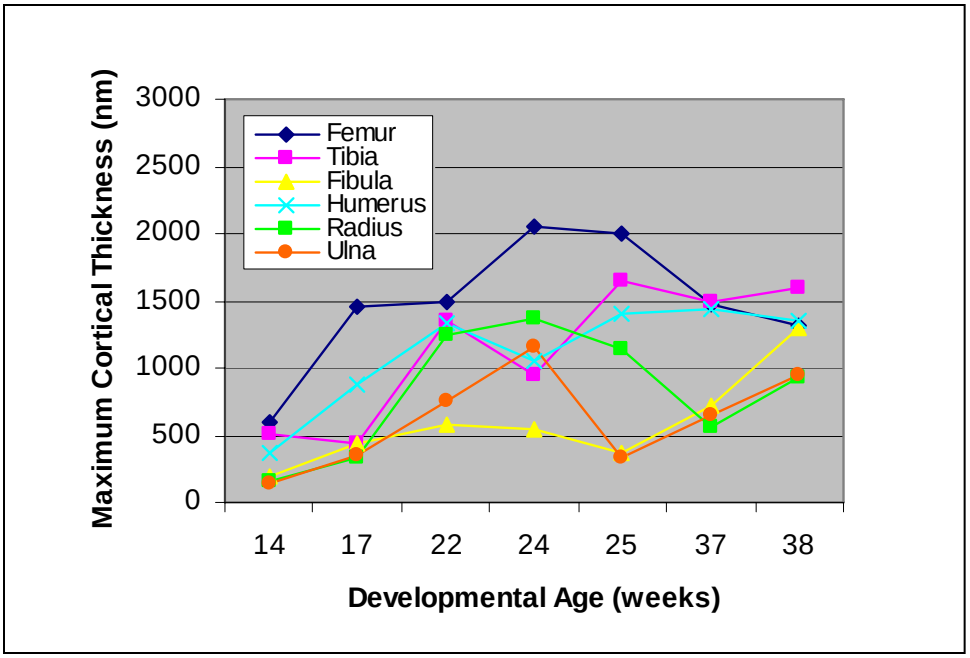


Figure 42: Maximum Cortical Thickness of the Posterior Quadrant by Bone

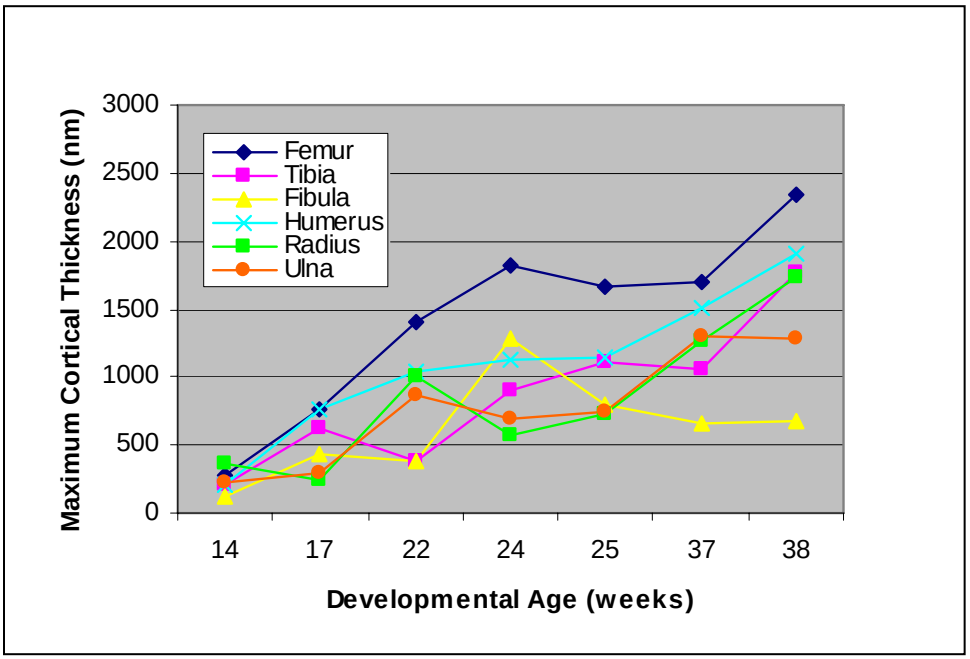


Figure 43: Maximum Cortical Thickness of the Lateral Quadrant by Bone

long bones. For the medial quadrant (Figure 41), the similarity among bones in the first two developmental stages is slightly less than that found in the anterior quadrant, although the medial quadrants in these two fetuses still remain more similar to one another than those of the older fetuses. The medial quadrants of the femur and tibia tend to be the thickest in the later developmental stages, while the medial quadrants of the fibula and ulna remain relatively thin across all fetuses. There is also a distinct separation present between the humerus, femur, and tibia on the one hand and the radius, fibula, and ulna on the other at the fifth, sixth, and seventh developmental stages.

The posterior quadrant (Figure 42) contains the most dissimilarity in maximum cortical thickness among the six long bones. The femur possesses the thickest posterior quadrant up until the sixth and seventh developmental stages where it is usurped by the tibia. Figure 43 shows that the trends in maximum cortical thickness of the lateral quadrant are most similar to those of the medial quadrant minus a few differences. For example, the femur exhibits the largest lateral quadrant in the third through the seventh developmental stages, while the tibia remains relatively thin compared to the femur at these stages. Another dissimilarity between the figures is the lack of separation in the lateral quadrant of the femur, humerus, and tibia from the other long bones in the fifth through seventh developmental stages.

The results of Pearson's rho analysis (Tables 2-3) show that given an alpha of 0.05 there exists a significant correlation of both maximum and minimum cortical thicknesses with age for all six long bones. The R-square values are the squared values of the Pearson's rho for each respective bone; this value represents the amount of variation in the cortical measurement that is explained by its linear relationship with age. Thus, for

Table 2: Pearson's Correlation Coefficients for Maximum Cortical Thickness

Bone	Pearson's Rho	R-square	p-Value
Femur	0.76711	0.58845	**<0.0001***
Tibia	0.84967	0.72194	**<0.0001***
Fibula	0.68620	0.47087	**<0.0001***
Humerus	0.91799	0.84271	**<0.0001***
Radius	0.57222	0.32744	**0.0015***
Ulna	0.63372	0.40160	**0.0003***

Table 3: Pearson's Correlation Coefficients for Minimum Cortical Thickness

Bone	Pearson's Rho	R-square	p-Value
Femur	0.78745	0.62008	**<0.0001***
Tibia	0.80073	0.64117	**<0.0001***
Fibula	0.60811	0.36980	**0.0006***
Humerus	0.89123	0.79429	**<0.0001***
Radius	0.57199	0.32717	**0.0015***
Ulna	0.62778	0.39411	**0.0003***

the femur approximately 59% of the variation in maximum cortical thickness can be explained by its linear relationship with age. The R-square values for the radius, ulna, and fibula are low in relation to the other long bones for both the maximum and minimum cortical thicknesses, suggesting that the cortical thicknesses of the femur, tibia, and humerus are more strongly correlated with age. The humerus and tibia have the strongest correlations between maximum cortical thickness and age, as roughly 84% and 72%, respectively, of the variation in the bone's maximum cortical thickness is explained by its positive linear relationship with age. The radius possesses the weakest correlation with age, as only 33% of the variation in maximum cortical thickness can be explained by its positive linear relationship with age.

Trabecular Thickness

The means of trabecular thicknesses for each quadrant are presented separately for each long bone (Tables A5-A10) and are shown averaged across all quadrants by bone (Table A11) in the appendix. These means are illustrated in the following figures (44-50) in order to show general trends in trabecular thickness across the fetal ages.

In figure 44, one can see that the quadrants of the femur possess very similar values for average trabecular thickness up until the sixth developmental stage (fetus 7). At this stage, the average trabecular thickness of the anterior quadrant drops drastically while the others increase. Also, in the seventh stage (fetus 6), the lateral quadrant decreases in trabecular thickness while all other quadrants increase. It seems that, in general, the anterior quadrant of the femur possesses the smallest trabeculae, while the posterior quadrant more often contains the largest trabeculae.

Regarding the tibia (Figure 45), the lateral quadrant appears to possess a unique pattern of change in average trabecular thickness compared with the other quadrants. Up until the fifth developmental stage, the anterior, medial, and posterior quadrants follow a very similar trend in change. The fifth fetus has a unique pattern of average trabecular thickness, as the anterior and medial quadrants are separated from the posterior and lateral quadrants and values for this variable are almost identical in each group. It seems that no one quadrant in the tibia consistently has the largest or smallest trabeculae. Missing values for trabecular thickness in the fibula (Figure 46) complicate the analysis of average trabecular thickness; yet it is still possible to make some general observations. The remaining quadrants appear similar in size up through six (fetus 7), the medial

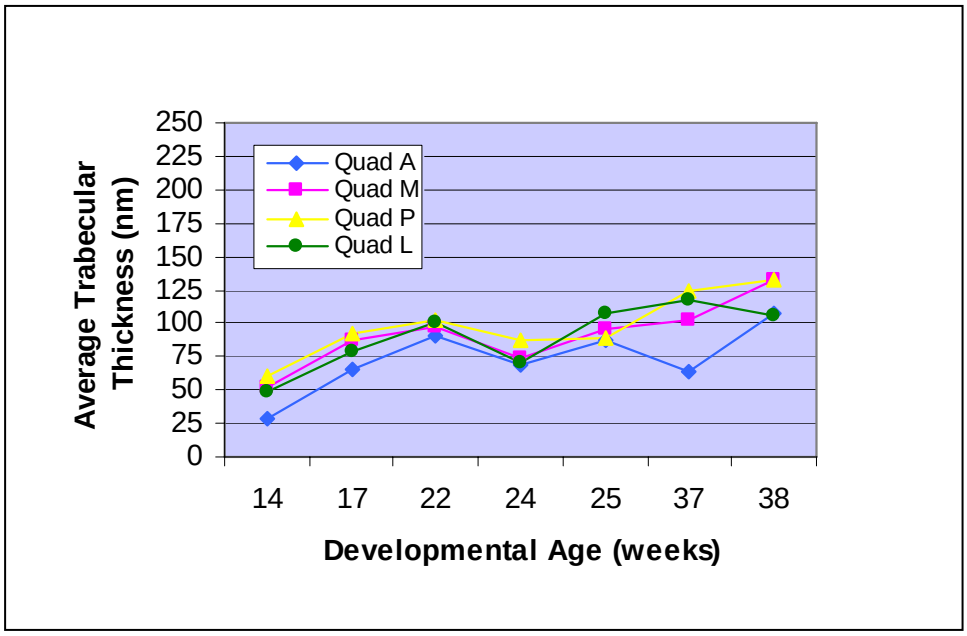


Figure 44: Average Trabecular Thickness in the Femur by Quadrant

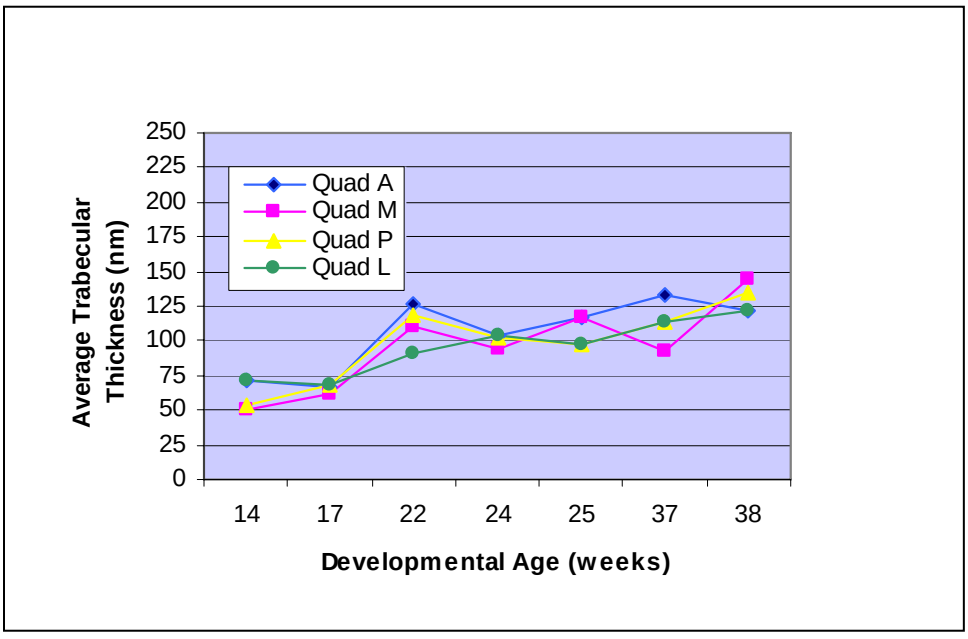


Figure 45: Average Trabecular Thickness in the Tibia by Quadrant

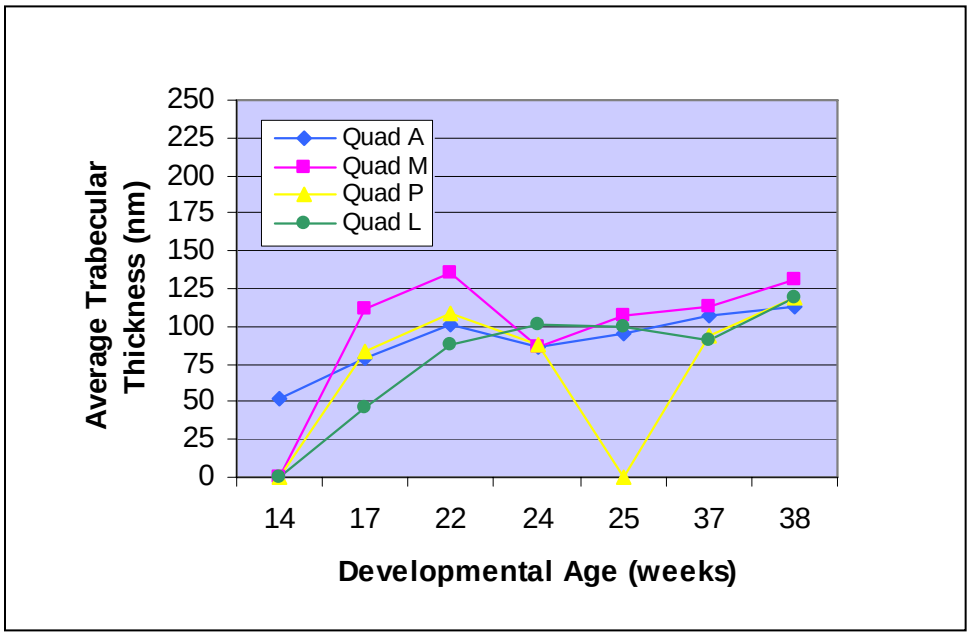


Figure 46: Average Trabecular Thickness in the Fibula by Quadrant

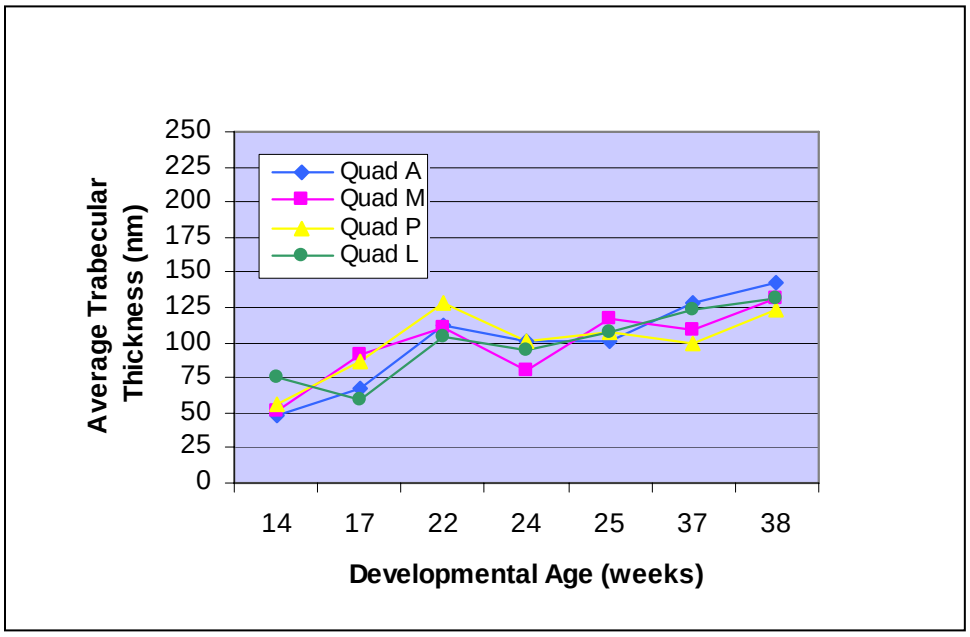


Figure 47: Average Trabecular Thickness in the Humerus by Quadrant

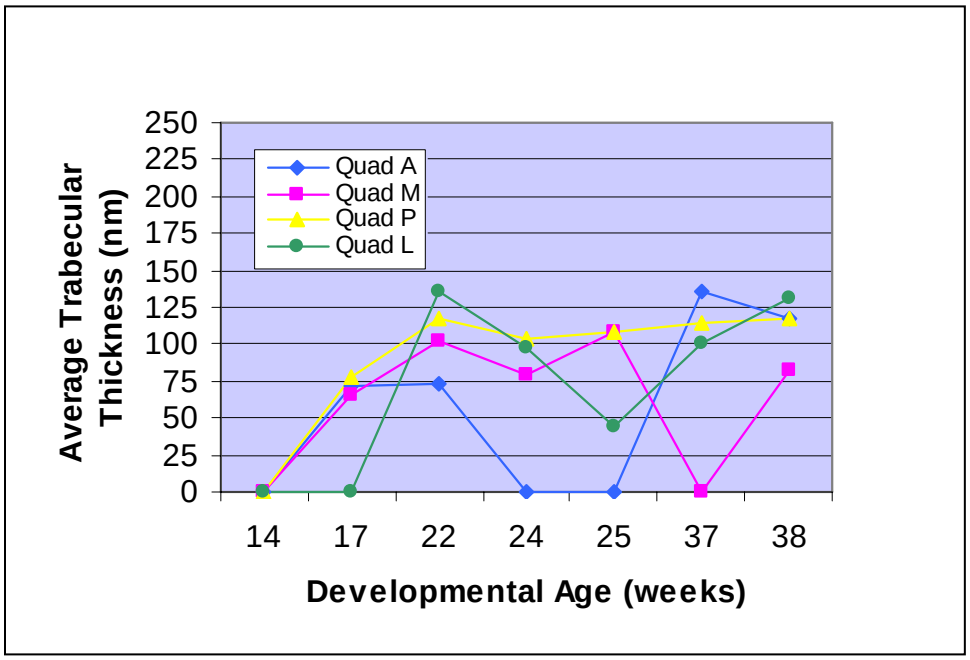


Figure 48: Average Trabecular Thickness in the Radius by Quadrant

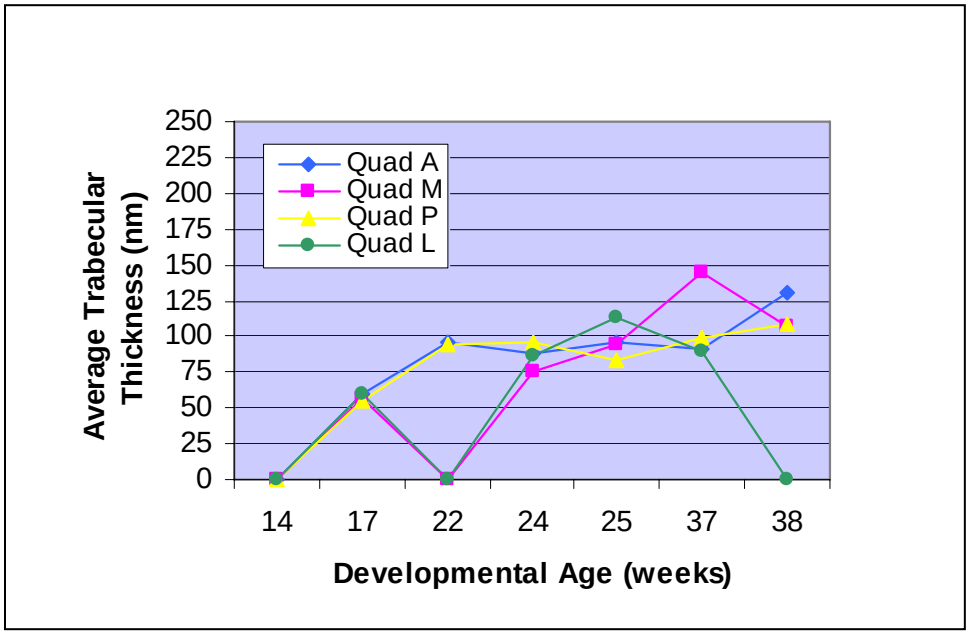


Figure 49: Average Trabecular Thickness in the Ulna by Quadrant

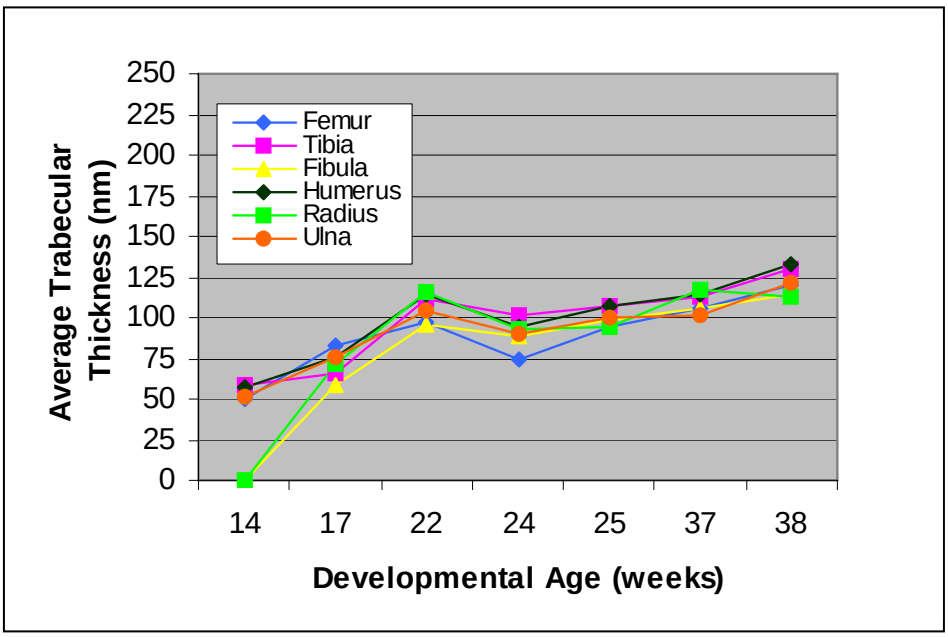


Figure 50: Average Trabecular Thickness Across All Quadrants by Bone

quadrant far exceeds the other three quadrants, which are all clustered around 100 nanometers. However, for the sixth fetus (stage 7), the anterior quadrant exhibits the largest average for trabecular thickness.

At first glance, the humerus (Figure 47) appears to be quite similar in general trend to the femur; however, there exist a few differences. For example, fetus 2 possesses larger trabeculae in its lateral quadrant than in any other quadrants, yet fetus 1 has relatively small trabeculae in its lateral quadrant. This same relationship is also depicted in figure 45 for the tibia but is not found in any other long bone.

Like the fibula, the radius (Figure 48) possesses areas of bone that lack trabeculae, making the analysis of average trabecular thickness difficult. The radius, in particular, has a significant amount of non-trabecular bone. One of the only points that can be made concerning

the radius is the distinct difference in average trabecular thickness present between the lateral quadrant of fetus 5 and its posterior and medial quadrants. This difference far exceeds all other differences present between quadrants of the same fetus. There is also a distinct separation present between the medial quadrant of fetus 6 and its other three quadrants.

In the ulna (Figure 49), the medial quadrant consistently contains the largest trabeculae in the early developmental stages (stage 2 and 3) and later stages (stages 5, 6, and 7). However, in fetus 3 (stage 4), the medial quadrant contains relatively small trabeculae. It is also worth mentioning that in the early stages of development (stages 2 and 3), the lateral quadrant has much smaller trabeculae than any other quadrant, yet this trend is not found in later stages. In fact, within the ulna, the largest variation in average trabecular thickness between the quadrants lies in the early developmental stages, a condition not found in any other bone.

A fixed effects ANCOVA analysis (Tables 4-7) was performed with trabecular thickness as the dependent variable, quadrant as a fixed factor, and age as a covariate. Age was chosen as a covariate because of the potential this variable has for affecting the relationship between quadrant and trabecular thickness. The ANCOVA analysis was run in SAS with two main effects (quadrant and age) and an interaction term of quadrant upon age. Once the model for each long bone was run with the interaction term included, those bones that lacked a significant interaction between age and quadrant were reanalyzed with the interaction term dropped from the model. This approach is seldom employed, yet it returns the most accurate results (Engqvist, 2005).

When the values for trabecular thickness are averaged across all quadrants for each bone, five of the six long bones possess a statistically significant linear relationship

Table 4: ANCOVA Summary for Age Effect of Trabecular Thickness by Bone

Bone	F-Value	p-Value
Femur	14.68	**0.0001***
Tibia	20.12	**<0.0001***
Fibula	15.12	**0.0001***
Humerus	18.79	**<0.0001***
Radius	2.37	0.1246
Ulna	13.10	**0.0003***

Table 5: ANCOVA Summary for Quadrant Effect of Trabecular Thickness by Bone

Bone	F-Value	p-Value
Femur	26.57	**<0.0001***
Tibia	6.32	**0.0003***
Fibula	0.79	0.5017
Humerus	5.62	**0.0008***
Radius	2.06	0.1049
Ulna	5.49	**0.0010***

Table 6: ANCOVA Post Hoc Summary for Trabecular Thickness by Bone

Bone	Quad Comparison	t-Value	p-Value
Femur	A-L	-5.59	**<.0001***
	A-M	-5.85	**<.0001***
	A-P	-8.78	**<.0001***
	L-M	-0.34	0.7329
	L-P	-3.08	**0.0021***
	M-P	-2.69	**0.0073***
Tibia	A-L	4.08	**<.0001***
	A-M	3.33	**0.0009***
	A-P	2.58	**0.0101***
	L-M	-0.84	0.4018
	L-P	-1.52	0.1293
	M-P	-0.71	0.4798
Humerus	A-L	0.93	0.3533
	A-M	0.70	0.4842
	A-P	0.22	0.8287
	L-M	-0.23	0.8219
	L-P	-0.74	0.4615
	M-P	-0.50	0.6142
Ulna	A-L	0.68	0.4938
	A-M	-3.21	**0.0014***
	A-P	-0.50	0.6168
	L-M	-3.85	**0.0001***
	L-P	-1.09	0.2744
	M-P	2.31	**0.0212***

Table 7: ANCOVA Summary for Quadrant/Age Interaction of Trabecular Thickness by Bone

Bone	F-Value	p-Value
Femur	0.60	0.6178
Tibia	1.50	0.2142
Fibula	1.92	0.1253
Humerus	6.74	**0.0002***
Radius	3.34	**0.0195***
Ulna	2.19	0.0889

with age (Table 4). In this instance, the radius is the only bone whose variation in trabecular thickness cannot be explained by differences in age. Four of the six long bones exhibit significant quadrant effects (Table 5); in other words, the mean trabecular thicknesses of the femur, tibia, humerus, and ulna differ by quadrant. Post hoc tests of the least significant differences (LSD) among the means (Table 6) show that for the femur, the posterior quadrant is different from all others, the anterior quadrant is different from all others, and the lateral and medial quadrants are not significantly different from one another. For the tibia, the anterior quadrant is significantly different from the medial, posterior, and lateral quadrants which are no different from one another. In the ulna, the medial quadrant is significantly different from the posterior, lateral, and anterior quadrants which do not differ from one another. Only two long bones, the humerus and

radius, possess age by quadrant interactions (Table 7), meaning that the rate of change in trabecular thickness for every unit increase in age differs by quadrant.

Chapter 6: Discussion

One of the most important points to keep in mind when analyzing the results of this study is that each fetal age is represented by only a single fetus; in other words, the lack of replication for fetal age reduces the statistical validity of these results. Any one of the seven fetuses utilized in this study, whether due to genuine variation or a pathological condition, could fall at either extreme for a particular measurement and alter the comparisons made across fetal ages. For example, in some long bones, fetus 4 possessed consistently larger values for medullary and cortical thickness measurements in comparison to the fetal developmental stages immediately surrounding it. It is not known whether this trend is due to a true increase in these measurements during this developmental stage or a reflection of the fact that this fetus is simply large for its developmental age. Another issue with the structure of this fetal sample involved the very nature in which the sample itself was collected. Given the osteological paradox (Wood et al., 1992), any sample of fetal skeletal material (especially one consisting of stillbirths) will be prone to pathological conditions that could potentially affect skeletal growth. If a larger sample had been incorporated in this study, it would have been possible to eliminate all fetuses that were small-for-gestational-age (SGA) so that these complicating factors could be avoided in analysis. However, given the small sample size, this type of analysis was not practical.

It is also concerning that a significant portion of the fetal period is not represented by these seven fetuses (i.e., 18-21 weeks and 26-36 weeks). Therefore, the trends thus far

discussed are certainly much more complex than this research suggests. The excessive separation between fetus 5 and fetus 7, especially, in developmental age causes there to be a significant portion of the growth period that is not being presented in the line graphs; however, there does not appear to be drastic increases in any measurement values between these two fetuses as would be expected if bone growth rate were constant throughout the fetal period. This seems to suggest a slowing of the rate of bone growth in this age range (i.e., 26-36 weeks) in comparison with earlier developmental stages of this study. This pattern has previously been documented in postmortem radiographs of the femur, tibia, and humerus of newborns and stillbirths (Rodriguez et al., 1992) and may be associated with reduced bone apposition and/or increased bone resorption caused by a combination of the crowding of the fetus within the uterine environment and decreased amniotic fluid volume (Miller, 2003). This hypothesis is supported by the fairly large increase in most measurements between fetus 1 and fetus 4 that would be expected given the gap in developmental ages and a relatively fast growth rate during the earlier developmental stages in comparison with later stages.

Another limitation of this research involves the inclusion of a fetal specimen (fetus 2) that was especially small-for-gestational-age (SGA). Developmentally, this stillborn was almost four weeks younger than its actual age, a red flag for a pathological condition called placental insufficiency. Placental insufficiency is caused by abnormal formation of the placenta, which is crucial in providing the fetus with the proper oxygen and nutrients required for normal growth. Certain health conditions in the mother (e.g., preeclampsia, gestational diabetes, kidney disease) are associated with placental insufficiency and can lead to fetal growth retardation (Baschat and Hecher, 2004).

Calcium levels in SGA newborn infants who have suffered placental insufficiency are lower than appropriate-for-gestational-age (AGA) infants, indicating an increase in fetal parathyroid hormone and, as a result, heightened bone resorption (Mora et al., 1997). This resorption has been shown to occur endosteally, such that these SGA infants have larger medullary canals than actual-age-matched AGA infants (Palacios et al, 1992). If these same conditions are present in the fetus just as they are in newborns, it could explain the larger medullary diameters in the humerus and radius of fetus 2 in comparison with the AGA fetus 1. Yet, the tendency for these two bones to possess this condition over the other four long bones can not presently be explained. The fact that there is a medullary canal present in all long bones of fetus 2 also points to the presence of growth retardation in this fetus, because the medullary canal does not normally form until roughly 16 weeks gestation. The increase in cortical thickness of most long bones between fetus 2 and fetus 1 (Figures 40-43) and the lack of increase in medullary area for most long bones (Figure 33) between these two fetuses speaks to the enhanced endosteal resorption and pathological condition of fetus 2.

Unfortunately, another pathological condition could also be present in two fetuses that each lacked a medullary canal in one of its long bones (i.e., the fibula of Fetus 1 and the ulna of Fetus 3). Malformations of the medullary canal in infants can be associated with a condition known as osteopetrosis (or Albers-Schonberg disease), a rare congenital disorder in which osteoclast function is compromised, resulting in an imbalance between the formation and resorption of bone. Individuals who suffer from osteopetrosis have extremely dense bones that cannot resist average bending stresses and, thus, are prone to fracture. In infantile osteopetrosis, the remodeling of woven bone and subsequent

deposition of lamellar bone is abnormal (Chen et al., 2003). Whether fetus 1 and fetus 3 possessed this pathological condition cannot be presently concluded. The lack of a medullary cavity in only a single long bone among these two fetuses is quite peculiar and may indicate a different pathological condition; however, regardless of the diagnosis, the lack of a medullary canal must be interpreted as indicative of some form of pathology in these fetuses. Therefore, one must consider the possibility that these fetuses may have a significantly negative affect on the outcome of the results of this study. Nevertheless, despite the inclusion of these potentially abnormal fetuses in the skeletal sample, the correlation between trabecular thickness and fetal age remains strong, suggesting that perhaps the severity of any pathological conditions these fetuses may possess is minute.

In this thesis, developmental age was used in all statistical and non-statistical comparisons rather than actual gestational age due to the potential for growth retardation in this fetal collection consisting of stillbirths. The logic behind this type of analysis involves the assumption that any acceleration or retardation of long bone growth that can be detected macroscopically (e.g. via long bone length age estimation) would also be present microscopically. Obviously, this hypothesis has never been formerly tested; however, one would assume that the appearance of microscopic structures in a developing bone would be highly correlated with the macroscopic growth of said bone. The practicality of using developmental age in this research was supported by the existence of stronger correlations between most measurements and fetal age when developmental age was incorporated into statistical analysis rather than actual gestational age. What remains puzzling, however, are the rather large discrepancies present between developmental and actual age for the two oldest fetuses, especially considering that

developmental age is *greater* than actual age. These discrepancies are most likely due either to hospital staff recording errors or maternal errors in reporting of last menstrual period (LMP). Such issues in fetal sampling strongly support the need for employment of developmental age in fetal histomorphometric studies.

At this point in the discussion of the results of this analysis, it becomes necessary to attempt a more detailed examination of the relationship between histological structures and fetal age. To the author's knowledge, this type of description has not been thoroughly and/or properly presented in the literature; therefore, the author attempts to do so here utilizing previous research and the results of this thesis. At 2 ½ lunar months (10 gestational weeks), the long bones consist of mostly cartilage tissue surrounded by a thin layer of periosteal bone, the bony collar. At 3 ½ lunar months (14 gestational weeks), resorption of the cartilage has begun in the central part of the midshaft, forming the primary medullary spaces upon which endochondral bone has formed. Thus, the cross section appears as a continuous layer of periosteal bone surrounding the newly-formed endochondral bone, or primary spongiosa. At this time, no medullary canal is present within the shaft. In the 4-lunar-month-old fetus (16 gestational weeks), the central portion of the endochondral bone has been resorbed to form a medullary canal. At the age of 4 ½ lunar months (18 gestational weeks), endosteal resorption and periosteal apposition have caused a visible decrease in endochondral bone tissue relative to periosteal bone. This periosteally deposited bone is not the circumferential lamellae associated with slow transverse growth of the diaphysis in childhood, but is rather comprised of woven bone trabeculae (Lacroix, 1960; Dhem et al., 1990).

The primary Haversian canals make their first appearance at 5 lunar months (20 gestational weeks), as concentric lamellae are laid down within the spaces between woven bone trabeculae. By 6 lunar months (24 gestational weeks), the open spaces between the trabeculae have narrowed due to lamellar deposition, however, due to the fact that the primary osteons have not completely formed, the open spaces are still relatively elongated in shape. At 6 ½ lunar months (26 gestational weeks), the majority of the Haversian canals of the primary osteons are round in shape like those found in adult bones. By 9 lunar months (36 gestational weeks), the primary osteons are distributed closest to the periosteum in some long bones due to the incorporation of endochondral bone from the growing metaphyses into the diaphysis at the endosteal surface. This bone tissue, which Enlow (1963) calls compacted fine-cancellous bone, is in the form of trabeculae (produced by the replacement of cartilage at the growth plate) that has subsequently been incorporated into the growing diaphysis. In mature fetuses (10 lunar months), this expansion of the endochondral bone and resorption of periosteal bone continues until a small ring of primary osteons are visible at the periosteal surface in most bones.

With this general framework in mind, one can make more informed inferences concerning the results of this thesis. In this fetal sample, the morphology of the femoral and tibial medullary canals appears to be quite unique in comparison to the other long bones. Firstly, the femur possesses the most similar sagittal and transverse dimensions up through the fifth fetus; yet, it also exhibits the largest dissimilarity in these two measurements for the sixth and seventh fetuses. It appears that in the later stages of fetal development, the femur displays a medullary canal more ovoid in shape with the long

axis of the oval in the anterio-posterior plane, a condition present in the adult femur. The presence of this trend in two of the fetuses (fetus 6 and fetus 7) speaks to its validity as a true trend rather than an aberration in growth patterning associated with a single fetus. How exactly the morphology of the femoral medullary canal in the late fetal period relates to adult morphology is beyond the scope of this thesis; however, it can be hypothesized that the morphology of the femoral medullary canal approaches the adult condition rather late in fetal development. In contrast to the femur, the sagittal and transverse medullary diameters of the tibia are consistently dissimilar in comparison with other bones throughout the period of development sampled here. It may be that the unique triangular cross-sectional morphology of the tibia causes its development to be distinct from that of other long bones. Why this distinction is present at such an early stage of development is unknown.

For the two medullary diameters, medullary area, and maximum cortical thickness the ulna, radius, and fibula of all seven fetuses cluster together at lower values than the other three long bones. These three distal long bones also tend to have smaller sagittal and transverse diaphyseal diameters at midshaft in the fetus *and* the adult. The presence of this phenomenon in the human fetus is likely related to the future differential biomechanics associated with these long bones. Because the distal segments of the limbs are located farther away from the axis of rotation, they are energetically more costly to move than the proximal segments; thus, distal segments are oftentimes more slender and will ultimately sustain greater loads, proportionally more micocracks, and a higher incidence of remodeling. This hypothesis explains the smaller medullary sizes of the ulna, radius, and fibula and the relatively weak correlations of their cortical thicknesses

and trabecular thicknesses with developmental age. The tibia, however, is an exception to this rule for humans, because as bipedal, noncursorial animals we possess equal average bending strength and remodeling rates in our femora and tibiae (Drapeau and Streeter, 2006). If one accepts the classification of humans as noncursorial animals, the relationship of medullary shape and cortical thickness among the six long bones of the fetus as outlined in this thesis is remarkable and indicates the presence of a genetic and perhaps biomechanical driving force in the development of proper long bone cross-sectional morphology.

The relatively weak correlations of cortical thickness and trabecular thickness with age in the ulna, radius, and fibula of these fetuses mimics the weak correlations in these three bones between osteon population density and age in the adult. The femur, humerus, and tibia have historically been the most popular long bones for histological age estimation of adults because their microscopic properties appear to be more strongly correlated with age. It seems that the unique cross-sectional morphologies of the femur, humerus, and tibia facilitate their use in such endeavors. The presence of this phenomenon in both the fetus and the adult points to an underlying biomechanical explanation; mainly, that long bones that are less stressed mechanically will remodel less often and, thus, should reveal a more accurate picture of histological changes due to age alone rather than biomechanical stress. The humerus and femur, being proximal limb segments, will certainly remodel less in response to mechanical stress compared with distal segments. Similarly, in humans, the tibia should not differ significantly from the femur and humerus in remodeling rates because of its altered function in bipedal walking (Drapeau and Streeter, 2006). Thus, due to these differential remodeling rates among the

long bones, care should be taken in choosing among the recovered elements of a fetal specimen the long bone that is most significantly correlated with age. This bone should be relied upon for the most accurate estimation of age.

In general, it appears that medullary diameters, medullary area, and maximum cortical thickness are most similar early on in fetal development (in this particular study between 14 and 17 developmental weeks) and that differences in these measurements between the long bones tend to develop thereafter. This pattern would be expected given the recently discovered relationship between fetal bone modeling and intrauterine biomechanics. By approximately 16 weeks gestation, all basic fetal movements characteristic of full term infants can be observed in the fetus (Carter et al., 1996), while bone modeling begins shortly thereafter. Thus, divergence in cross-sectional shape of the six long bones would be expected to develop sometime shortly after 16 weeks gestation (Miller, 2003).

Previous research (Rodriguez et al., 1992) examining postmortem radiographs of the tibia, femur, and humerus detected positive correlations between diaphyseal diameter, medullary diameter, cortical thickness, and cortical area and the gestational age of newborns and stillbirths. Thus, the results outlined in this study for medullary diameters, medullary area, and cortical thickness are not too surprising. However, the histomorphometric relationship of trabecular thickness and age has not been previously documented.

From a forensic anthropology perspective, in the event of complete preservation of a fetal long bone's mid-diaphyseal cross section, the utilization of maximum cortical thickness would be ideal for estimating age. Not only is it easier to measure, but all six

long bones possess significant correlations between maximum cortical thickness and fetal age. However, if taphonomic processes have in some way altered the integrity of the cross section (and the bone fragment is not from the radius), it may be more practical and efficient to use trabecular thickness in estimating fetal age. The non-significant relationship between trabecular thickness of the radius and developmental age is likely a reflection of the lack of woven bone trabeculae in certain quadrants of this long bone. It is also interesting to note that the radius also has the weakest correlation between maximum and minimum cortical thicknesses and age of all the long bones. Some aspect of this bone's morphology obviously precludes its accuracy in histological age estimation.

Several bones possessed quadrant effects in the ANCOVA analysis: femur, tibia, humerus, and ulna. These bones have significantly different values among their quadrants for trabecular thickness. One possible explanation for this phenomenon is the differential biomechanical functions of these long bones compared with the radius and fibula, the lateral elements of the distal pectoral and pelvic limbs, respectively.

The significant difference present in the anterior quadrant of the tibia for trabecular thickness compared to the other three quadrants is not surprising given the morphology of this bone. The increase in growth of the cortical thickness of the anterior tibia in the later stages of fetal development in relation to other long bones has previously been documented (Rodriguez et al, 1992), and in this study, it also tends to have the largest trabecular thicknesses of the quadrants. The anterior quadrant is much larger in the adult due to the increased stress and strain placed on the tibial crest by the tibialis anterior. The relative sizes and morphology of the tibial tuberosity and crest speak to the

great deal of stress applied to this portion of the bone and, thus, the increased remodeling rates associated with this increased bone loading. Thus, it can be concluded that the anterior quadrant of the fetal tibia, like the adult, remodels at a faster rate than other tibial quadrants. The anterior tibial quadrant also does not obtain its relatively large diameter or large trabecular thicknesses until the later stages of fetal development, suggesting that this area of bone must grow at a faster rate than other tibial quadrants in order to achieve its adult form. Differences in rates of growth among the quadrants of long bones will ultimately affect the relative size of woven bone trabeculae deposited and perhaps even the amounts of lamellar bone that are deposited between these woven bone trabeculae. This fact may explain the lack of significant differences in trabecular thickness among the quadrants of the fibula and radius, long bones that are relatively uniform in cortical thickness and cross-sectional morphology in the adult and do not require increased rates of growth to achieve the adult form. The other four long bones, however, have more variation present in quadrant size and shape and thus differential rates of lamellar bone apposition and periosteal deposition.

The ulna also possesses a quadrant, the medial quadrant, with trabecular thicknesses significantly different from all other quadrants. Oddly enough, however, this quadrant is not the thickest of the four but rather the thinnest quadrant, yet it tends to have relatively large trabecular thicknesses. This significant difference in trabecular thickness in this quadrant may be explained by the added stress of the flexor carpi ulnaris muscle, which acts to flex the hand, on this portion of the bone. Despite the small size of this quadrant, it appears that this area undergoes an increased rate of modeling compared to the ulna's other quadrants.

The femur possesses significantly different anterior and posterior quadrants for trabecular thickness with the anterior quadrant consistently having the smallest thicknesses and the posterior quadrant the largest thicknesses. This pattern matches the relative sizes of these quadrants' cortical thicknesses, the anterior being the thinnest and the posterior the thickest. It would appear that the effects of the quadriceps femoris on the linea aspera have already begun in the fetal period, considering that the posterior quadrant has already grown to be the largest quadrant and possesses the fastest rate of lamellar bone apposition.

Chapter 7: Conclusions

Presently, it is difficult to say what factors determine the differential rates of bone growth and modeling among the six long bones of the human fetus. Because each long bone is subjected to the same intrauterine environment, disparities among them are most likely caused by genetic factors that serve to provide each bone with the particular size and shape appropriate for its postnatal function. Thus, the cross-sectional modeling process is specifically coordinated with longitudinal bone growth, which explains the existence of such positive correlations among a growing bone's length and its histomorphometric properties. This research supports the hypothesis that bone strength, and thus bone density and cross-sectional shape, are directly related to fetal biomechanics. This hypothesis states that reduced fetal movement will result in decreased bone strength through changes in bone density (remodeling) and bone shape (modeling). One would assume, however, that fetal movement is inherently different from that of an adult human, so that the processes of fetal modeling and remodeling must differ somewhat from those of postnatal life. Currently, the exact biomechanical mechanisms by which fetal long bones remodel is unknown; there is still even some confusion in the literature as to the initial appearance of remodeling in the fetus. Future research is required to elucidate the relationship between fetal biomechanics in an intrauterine environment and the fetal mechanostat.

Future research, in addition to expanding the fetal skeletal sample size, will focus on distinguishing woven from lamellar bone layers within fetal cross sections, as well as

extend the examination of histomorphometric properties to other sections of the diaphysis. Previous research (Tersigni, 2005) has shown that intra-bone variation along the length of the diaphysis prevents conventional histological aging techniques, normally created from only the midshaft cross section of a particular long bone, from being applied to areas other than the midshaft. In the forensic setting, it is not practical to rely on such conventional methods, since the midshaft of a long bone is not always preserved. In order to properly apply histological aging techniques, the anthropological community must develop a complete understanding of the inter- and intra-bone variation that is present within human long bone histomorphometry.

Despite the growth in histological studies in the past few decades, much remains to be learned concerning the exact nature of our long bone histomorphometry. The recent increase in fragmentary and commingled remains associated with mass disasters and mass grave production has spurred a need for improved histological techniques that has not yet been fully appreciated or acknowledged in the anthropological community. Despite the time-consuming and complex nature of histological studies, the benefits of such research are crucial to expanding the limits of forensic anthropology.

References Cited

Ascenzi A and Bonucci E. The tensile properties of single osteons. Anat Rec 1967;158:375-86.

Balthazard V and Müller . Caractérisation des os de foetus humains. Ann Méd lég 1921;1:49.

Baschat AA and Hecher K. Fetal growth restriction due to placental disease. Semin Perinat 2004;28(1):67-80.

Bloom WB and Fawcett DW. A Textbook of Histology. Philadelphia: W.B. Saunders Company;1968.

Bourne GH. The Biochemistry and Physiology of Bone. New York: Academic Press;1956.

Burton P, Nyssen-Behets C and Dhem A. Haversian bone remodeling in human fetus. Acta Anat 1989;135:171-5.

Carter DR, van der Meulen MCH and Beaupri GS. Mechanical factors in bone growth and development. Bone, Suppl. 1996;18:5S-10S.

Chen CJ, Lee MY, Hsu ML, Lien SH, Cheng SN. Malignant infantile osteopetrosis initially presenting with neonatal hypocalcemia: case report. Annals of Hematology 2003;82:64-67.

Christel P, Cerf C and Pilla A. Time evolution of the mechanical properties of the callus of fresh fractures. Annals of Biomed 1981;9:383-91.

Currey JD. The Mechanical Adaptations of Bones. Princeton: Princeton University Press;1984.

Currey JD. Bones: Structure and Mechanics. Princeton: Princeton University Press;2002.

Demeter G and Mátyás J. Mikroskopische vergleichend-anatomische Studien an Röhrenknochen mit besonderer Rücksicht auf die Unterscheidung menschlicher und tierischer Knochen. Z Anat Entwickl-Gesch 1928;87:45.

Dhem A, Goret - Nicaise M and Lengelé B. Opening address--contribution to the study of skeletal growth. In: Dixon AD, Sarnat BG and Hoyte DAN, editors. Fundamentals of bone growth: methodology and applications. Boca Raton: CRC Press;1990.

Drapeau MSM and Streeter MA. Modeling and remodeling responses to normal loading in the human lower limb. AJPA 2006;129:403-9.

Engfeldt B and Zetterström R. Osteodysmetamorphosis foetalis: a newly discovered characteristic skeletal disease showing low serum and tissue alkaline phosphatase activity (hypophosphatasia). In: Wolstenholme GEW and O'Connor CM, editors. CIBA Foundation Symposium on Bone Structure and Metabolism. London: J. & A. Churchill Ltd.;1956.

Engqvist L. The mistreatment of covariate interaction terms in linear model analyses of behavioural and evolutionary ecology studies. Anim Beh 2005;70:967-71.

Enlow DH. Principles of Bone Remodeling. Springfield: Charles C Thomas;1963.

Fazekas IG and Kósa F. Forensic Fetal Osteology. Budapest: Akadémiai Kiadó;1978.

Frost HM. Bone Remodeling Dynamics. Springfield: Charles C Thomas;1963.

Frost HM. Mathematical Elements of Lamellar Bone Remodeling. Springfield: Charles C Thomas;1964.

Frost HM. Bone Biodynamics. Boston: Little, Brown and Company;1964.

Frost HM. Bone "mass" and the "mechanostat": a proposal. Anat Rec 1987;219:1-9.

Frost HM.a Skeletal structural adaptations to mechanical usage (SATMU): 1. redefining Wolff's law: the bone modeling problem. Anat Rec 1990;226:403-13.

Frost HM.b Structural adaptations to mechanical usage (SATMU): 2. redefining Wolff's Law: the bone remodeling problem. Anat Rec 1990;226:414-22.

Gardner E. Osteogenesis in the human embryo and fetus. In: Bourne GH, editor. The biochemistry and physiology of bone. London: Academic Press;1971.

Giraud-Guille MM. Twisted plywood architecture of collagen fibrils in human compact bone osteons. Calcif Tissue Int 1988;42:167-80.

Glorieux FH, Salle BL, Ravers R and Audra PH. Dynamic histomorphometric evaluation of human fetal bone formation. Bone 1991;12:377-81.

Gruenwald P. Growth of the human fetus: I. normal growth and its variation. Am J Obstet Gynecol 1966;94(8):1112-9.

Hall BK. Bones and Cartilage. San Diego: Elsevier Academic Press;2005.

Hall MC. The Locomotor System: Functional Histology. Springfield: Charles C Thomas;1965.

Ham AW and Cormack DH. Histophysiology of Cartilage, Bone, and Joints. Philadelphia: J.B. Lippincott Company;1979.

Jowsey J. Studies of Haversian systems in man and some animals. J Anat 1966;100:857-64.

Lacroix P. Ca45 autoradiography in the study of bone tissue. In: Rodahl K, Nicholson JT and Brown EM, editors. Bone as a Tissue. New York: McGraw-Hill;1960.

Larsen WJ, Sherman LS, Potter SS and Scott WJ. Human Embryology. New York: Churchill Livingstone;2001.

Lubchenco LO, Hansman C, Dressler M and Boyd E. Intrauterine growth as estimated from liveborn birth-weight data at 24 to 42 weeks of gestation. Pediatrics 1963;32:793-800.

Marks MK, Rose JC and Davenport WD. Technical note: Thin section procedure for enamel histology. AJPA 1996;99:493-8.

Martin RB and Burr DB. Structure, Function, and Adaptation of Compact Bone. New York: Raven Press;1989.

Martin RB, Burr DB and Sharkey NA. Skeletal Tissue Mechanics. New York: Springer-Verlag;1998.

Martini FH, Timmons MJ and Tallitsch RB. Human Anatomy. San Francisco: Pearson Education;2006.

Miller ME. The bone disease of preterm birth: a biomechanical perspective. Pediatr Res 2003;53(1):10-5.

Mora S, Prinster C, Bellini A, Weber G, Proverbio MC, Puzzovio M, Bianchi C and Chiumello G. Bone turnover in neonates: changes of urinary excretion rate of collagen type I cross-linked peptides during the first days of life and influence of gestational age. Bone 1997;20(6):563-6.

Mori S and Burr DB. Increased intracortical remodeling following fatigue damage. Bone 1993;14:102-9.

Netter FH. Atlas of Human Anatomy. Philadelphia: Saunders; 2002.

Palacios J, Rodriguez S and Rodriguez JI. Intra-uterine long bone growth in small-for-gestational-age infants. Eur J Pediatr 1992;151:304-7.

Rodriguez JI, Palacios J and Rodriguez S. Transverse bone growth and cortical bone mass in the human prenatal period. Biol Neonate 1992;62:23-31.

Sadler TW. Langman's Medical Embryology. Philadelphia: Lippincott Williams & Wilkins;2006.

Scheuer L and Black S. Developmental Juvenile Osteology. San Diego: Elsevier Academic Press;2000.

Stout SD. The effects of long-term immobilization on the histomorphology of human cortical bone. Calcif Tissue Int 1982;34:337-42.

Stout SD and Paine RR. Brief communication: histological age estimation using rib and clavicle. AJPA 1992;87:111-5.

Su X, Sun K, Cui FZ and Landis WJ. Organization of apatite crystals in human woven bone. Bone 2003;32:150-62.

Tersigni MA. Serial long bone histology: inter- and intra-bone age estimation. Doctoral dissertation. University of Tennessee, Knoxville; 2005.

Vaughan JM. The Physiology of Bone. Oxford: Clarendon Press;1970.

Wood JW, Milner GR, Harpending HC, Weiss KM. The osteological paradox: problems of inferring prehistoric health from skeletal samples. Curr Anth 1992;33(4):343-70.

Appendix

Key:

A=Anterior	F=Femur	U=Ulna
M=Medial	T=Tibia	Fib=Fibula
P=Posterior	H=Humerus	
L=Lateral	R=Radius	

Quad=Quadrant
Trab=Trabecular Thickness
MedAP=Sagittal Medullary Diameter
MedML=Transverse Medullary Diameter
MedArea=Medullary Area
Std Dev=Standard Deviation
Dev_Age=Developmental Age

Table A1: Osteometric Measurements of the Long Bones of Fetal Specimens

Measurement	Fetus 1	Fetus 2	Fetus 3	Fetus 4	Fetus 5	Fetus 6	Fetus 7
Femur:							
Max. Length	**23.76**	**11.76**	**39.72**	**35.91**	**41.00**	**68.85**	**65.77**
Max. Sag. Mdsht.	**1.97**	**1.32**	**3.85**	**3.60**	**3.71**	**5.21**	**4.45**
Max. Trans. Mdsht.	**1.75**	**1.11**	**3.46**	**3.29**	**3.65**	**5.66**	**4.66**
Tibia:							
Max. Length	**20.79**	**10.03**	**34.13**	**31.90**	**35.53**	**59.52**	**58.82**
Max. Sag. Mdsht.	**1.94**	**0.94**	**3.90**	**3.62**	**3.42**	**5.63**	**4.58**
Max. Trans. Mdsht.	**1.83**	**0.91**	**3.29**	**2.42**	**3.29**	**4.34**	**4.31**
Fibula:							
Max. Length	**20.02**	**8.30**	**33.41**	**30.26**	**34.61**	**56.66**	**53.43**
Max. Sag. Mdsht.	**0.96**	**0.58**	**1.76**	**2.11**	**1.44**	**2.72**	**2.54**
Max. Trans. Mdsht.	**0.90**	**0.51**	**2.10**	**1.13**	**1.81**	**2.53**	**2.75**
Humerus:							
Max. Length	**23.48**	**12.37**	**37.93**	**34.30**	**37.73**	**61.17**	**58.69**
Max. Sag. Mdsht.	**1.86**	**1.35**	**3.04**	**3.39**	**3.13**	**4.26**	**3.79**
Max. Trans. Mdsht.	**1.89**	**1.21**	**3.21**	**2.60**	**3.01**	**4.17**	**4.04**
Radius:							
Max. Length	**18.59**	**9.91**	**29.77**	**28.93**	**31.19**	**47.44**	**47.30**
Max. Sag. Mdsht.	**1.05**	**0.66**	**1.76**	**1.88**	**1.73**	**2.58**	**2.25**
Max. Trans. Mdsht.	**1.21**	**0.75**	**2.18**	**2.07**	**2.00**	**3.01**	**2.94**
Ulna:							
Max. Length	**21.3**	**10.20**	**34.64**	**32.18**	**35.91**	**54.50**	**54.55**
Max. Sag. Mdsht.	**1.13**	**0.71**	**2.63**	**2.14**	**2.29**	**3.58**	**3.06**
Max. Trans. Mdsht.	**1.20**	**0.69**	**1.65**	**1.45**	**1.47**	**2.46**	**2.31**

Table A2: Medullary Diameters and Medullary Area by Bone

Fetus	Measurement	Femur	Tibia	Fibula	Humerus	Radius	Ulna
1	MedAP (nm)	590.64	979.89	-	546.98	253.28	297.88
	MedML (nm)	503.40	580.55	-	684.56	223.04	363.32
	MedArea (nm^2)	207963.6	363688.60	-	245957.40	44694.00	81225.19
2	MedAP (nm)	516.79	504.52	473.78	707.18	307.45	331.35
	MedML (nm)	577.18	613.05	440.70	780.45	380.17	361.60
	MedArea (nm^2)	253555.1	198022.20	148033.00	422112.50	92328.96	96335.57
3	MedAP (nm)	1187.92	1383.14	471.76	1255.11	546.76	-
	MedML (nm)	1080.54	1174.67	808.74	1214.84	694.24	-
	MedArea (nm^2)	953245.3	1312745	294018.20	1103475	286053.90	-
4	MedAP (nm)	1336.18	1268.05	540.36	1298.70	606.62	479.88
	MedML (nm)	1530.57	1423.21	597.55	1083.89	489.17	466.49
	MedArea (nm^2)	1675961	945509.20	249605.90	1308837	224438.30	162267.50
5	MedAP (nm)	953.02	1000.20	593.48	1248.39	609.01	510.07
	MedML (nm)	1013.42	1570.99	561.48	1436.49	515.24	460.17
	MedArea (nm^2)	734403.9	1053657	243453.40	814501.60	223052.90	249256.80
6	MedAP (nm)	2574.33	1899.38	833.98	1302.17	467.05	827.73
	MedML (nm)	1047.07	1662.82	952.33	1228.26	600.10	621.88
	MedArea (nm^2)	2133474	2216646	610419.40	1155139	207482.30	354079.60
7	MedAP (nm)	2551.83	1167.79	1068.28	1107.57	691.28	528.42
	MedML (nm)	1718.17	1604.53	1195.72	1322.30	765.17	469.75
	MedArea (nm^2)	3107146	1671817	948103.70	1144385	554569.60	223679.10

Table A3: Maximum and Minimum Cortical Thickness by Quadrant

		Femur		Tibia		Fibula		Humerus		Radius		Ulna	
Fetus	Quad	Max	Min	Max	Min	Max	Min	Max	Min	Max	Min	Max	Min
1	A	520.23	278.54	587.33	520.40	565.11	449.56	684.60	553.70	581.85	244.57	651.09	486.41
	M	751.69	567.11	818.80	550.35	492.54	449.43	758.46	385.96	618.50	614.18	471.84	413.16
	P	1459.87	1218.16	430.00	181.33	446.11	269.81	882.56	734.93	333.84	226.11	354.35	222.12
	L	768.46	600.68	627.53	476.52	435.15	354.03	768.72	637.59	244.76	168.51	294.57	218.48
2	A	217.39	115.22	236.96	134.78	137.48	81.18	280.51	202.17	190.48	154.82	317.13	185.52
	M	343.51	280.47	428.26	334.81	72.58	51.42	300.01	223.92	81.35	41.48	164.68	147.29
	P	282.68	176.10	502.48	215.23	198.24	151.83	363.05	274.05	165.59	80.27	132.11	98.49
	L	593.58	365.28	213.14	71.77	122.31	89.42	204.36	178.26	362.99	129.34	222.13	186.15
3	A	1208.52	550.34	1664.44	1242.26	706.61	445.84	1261.91	979.89	158.70	89.13	1402.69	932.98
	M	1261.75	892.62	1288.66	1167.96	321.75	267.39	778.52	724.86	794.15	700.86	906.05	849.95
	P	2046.99	1416.11	939.81	610.89	547.98	467.40	1048.03	912.75	1376.11	1119.78	1157.72	812.19
	L	1818.80	1503.37	899.43	785.23	1278.29	1250.09	1134.31	865.77	574.18	411.01	691.28	684.56
4	A	1652.11	1120.89	1234.90	993.38	1017.71	694.92	986.94	819.04	293.49	180.45	1060.42	842.61
	M	1335.57	1041.05	1335.84	1161.09	378.32	218.15	899.33	470.23	758.90	547.90	459.84	362.61
	P	1490.48	624.20	1355.71	1228.65	573.92	460.17	1335.89	1067.11	1248.25	889.45	761.77	590.60
	L	1402.70	503.40	382.61	255.39	385.92	332.28	1033.75	832.24	1005.11	904.44	862.47	664.57
5	A	1100.67	771.81	1335.57	751.71	657.23	552.21	1248.36	1073.96	247.91	161.40	1171.22	1067.75
	M	1483.28	1026.87	1355.85	718.15	437.30	422.19	1100.67	892.64	514.22	282.64	396.48	137.62
	P	2000.01	1798.77	1651.23	1276.60	370.08	293.55	1396.12	1144.30	1137.21	1130.69	329.01	107.38
	L	1657.73	1510.07	1114.42	792.06	795.66	728.52	1140.98	570.51	732.66	645.95	745.72	456.43

Table A3: Maximum and Minimum Cortical Thickness by Quadrant (cont.)

		Femur		Tibia		Fibula		Humerus		Radius		Ulna	
Fetus	Quad	Max	Min	Max	Min	Max	Min	Max	Min	Min	Max	Min	Max
6	A	1926.19	1592.13	2832.86	2000.00	1024.43	641.44	1590.66	1583.91	986.78	726.35	2247.56	1800.31
	M	2020.24	1959.74	1993.39	1516.91	1135.70	876.36	1792.15	1422.96	734.97	526.94	732.04	671.98
	P	1315.45	1268.62	1590.66	1308.88	1306.61	668.41	1355.72	1061.17	932.38	803.05	944.48	779.24
	L	2349.03	2094.65	1765.42	1033.64	669.62	491.32	1899.76	1328.86	1729.36	1563.76	1291.32	1232.62
7	A	1342.30	825.50	1966.55	1369.39	918.05	665.39	1355.72	1228.26	966.50	748.51	1730.44	1556.91
	M	1590.96	1328.88	1805.38	1698.04	556.52	419.84	1610.75	1409.40	577.18	473.20	528.30	432.70
	P	1478.04	1087.27	1485.06	1120.99	717.51	678.26	1436.26	1073.91	557.30	443.16	641.44	406.67
	L	1691.33	1504.09	1053.88	973.25	652.26	519.58	1517.02	1268.47	1268.46	1073.96	1293.89	1158.94

Table A4: Mean Maximum and Minimum Cortical Thickness Across All Quadrants by Bone

		Mean		Std Dev	
Fetus	**Bone**	**Max**	**Min**	**Max**	**Min**
1	Femur	875.06	666.13	405.99	395.41
	Tibia	615.92	432.15	159.87	169.94
	Fibula	484.73	380.71	59.08	86.55
	Humerus	773.58	578.05	81.74	147.93
	Radius	444.74	313.34	183.74	203.16
	Ulna	442.96	335.04	157.08	135.83
2	Femur	359.29	234.27	164.46	110.84
	Tibia	345.21	189.15	142.35	113.48
	Fibula	132.66	93.46	51.77	42.20
	Humerus	286.98	219.60	65.38	40.81
	Radius	200.10	101.48	118.21	50.57
	Ulna	209.01	154.36	81.12	41.44
3	Femur	1584.02	1090.61	414.06	449.97
	Tibia	1198.09	951.59	356.65	302.80
	Fibula	713.66	607.68	408.21	437.55
	Humerus	1055.69	870.82	204.60	107.99
	Radius	725.78	580.20	507.34	437.98
	Ulna	1039.43	819.92	308.19	103.39
4	Femur	1470.21	822.38	136.85	304.38
	Tibia	1077.26	909.63	466.11	447.23
	Fibula	588.97	426.38	299.81	204.51
	Humerus	1063.98	797.16	189.64	245.95
	Radius	826.44	630.56	407.62	342.28
	Ulna	786.13	615.10	250.41	198.80
5	Femur	1560.42	1276.88	374.18	463.45
	Tibia	1364.27	884.63	220.35	263.05
	Fibula	565.07	499.12	196.65	185.85
	Humerus	1221.53	920.35	132.03	256.19
	Radius	658.00	555.17	375.97	435.43
	Ulna	660.61	442.30	386.30	445.86

Table A4: Mean Maximum and Minimum Cortical Thickness Across All Quadrants by Bone (cont.)

		Mean		Std Dev	
Fetus	**Bone**	**Max**	**Min**	**Max**	**Min**
6	Femur	1902.73	1728.78	431.45	373.11
	Tibia	2045.58	1464.86	550.14	407.99
	Fibula	1034.09	669.38	269.27	158.46
	Humerus	1659.57	1349.22	239.68	219.02
	Radius	1095.87	905.03	435.96	454.31
	Ulna	1303.85	1121.04	670.04	513.92
7	Femur	1525.66	1186.43	150.11	295.13
	Tibia	1577.72	1290.42	402.49	317.12
	Fibula	711.09	570.77	153.00	123.70
	Humerus	1479.94	1245.01	109.28	138.00
	Radius	842.36	684.71	340.86	293.64
	Ulna	1048.52	888.80	566.14	565.64

Table A5: Mean Trabecular Thickness of the Femur by Quadrant

Fetus	Quad	N	Mean	Std Dev
1	A	15	65.00	19.95
	M	16	86.51	20.37
	P	25	92.91	29.73
	L	18	78.39	25.21
2	A	11	28.75	5.10
	M	10	52.04	9.44
	P	25	59.58	15.19
	L	8	49.25	16.02
3	A	25	68.58	10.23
	M	24	73.56	20.21
	P	25	87.21	23.06
	L	25	69.90	14.71
4	A	24	90.09	26.66
	M	25	96.68	18.88
	P	24	102.04	24.29
	L	25	100.45	24.49
5	A	25	87.20	30.75
	M	18	95.18	22.83
	P	25	89.24	21.98
	L	25	108.18	24.90
6	A	25	108.09	25.80
	M	25	132.40	24.42
	P	25	131.88	16.36
	L	25	105.74	18.99
7	A	16	63.69	12.12
	M	25	102.66	24.21
	P	25	124.70	22.91
	L	25	118.03	20.94

Table A6: Mean Trabecular Thickness of the Tibia by Quadrant

Fetus	Quad	N	Mean	Std Dev
1	A	25	66.82	14.49
	M	23	62.27	13.17
	P	17	67.39	16.68
	L	18	67.73	17.76
2	A	14	70.65	17.00
	M	22	50.24	14.51
	P	18	53.35	19.58
	L	10	70.99	11.87
3	A	25	104.22	19.47
	M	25	93.65	27.45
	P	25	101.90	20.75
	L	25	104.29	22.84
4	A	25	127.19	33.29
	M	25	111.18	21.48
	P	25	118.15	27.43
	L	25	90.93	24.64
5	A	25	117.09	26.24
	M	25	117.07	19.51
	P	25	96.64	21.39
	L	25	97.51	19.61
6	A	25	121.02	30.52
	M	24	144.56	29.03
	P	25	135.08	24.88
	L	25	121.62	29.38
7	A	25	133.21	45.48
	M	25	92.02	25.52
	P	25	113.16	22.49
	L	25	114.39	20.33

Table A7: Mean Trabecular Thickness of the Fibula by Quadrant

Fetus	Quad	N	Mean	Std Dev
1	A	16	60.33	16.60
	M	25	56.38	17.66
	P	11	55.26	13.52
	L	14	60.45	24.80
2	A	-	-	-
	M	-	-	-
	P	-	-	-
	L	-	-	-
3	A	25	87.58	20.45
	M	11	76.14	13.59
	P	25	95.48	26.77
	L	25	86.21	21.62
4	A	21	95.94	36.42
	M	-	-	-
	P	15	93.77	19.47
	L	-	-	-
5	A	25	96.06	18.99
	M	21	94.89	25.22
	P	6	83.20	29.58
	L	18	112.54	30.07
6	A	18	130.37	32.67
	M	24	107.13	26.20
	P	25	109.21	26.70
	L	-	-	-
7	A	25	91.88	24.53
	M	21	145.33	48.17
	P	25	99.19	39.27
	L	11	89.49	31.45

Table A8: Mean Trabecular Thickness of the Humerus by Quadrant

Fetus	Quad	N	Mean	Std Dev
1	A	22	66.97	24.16
	M	21	91.00	25.33
	P	25	87.15	25.56
	L	24	59.81	16.91
2	A	12	48.84	16.52
	M	17	51.12	10.98
	P	21	55.30	17.44
	L	11	75.77	21.42
3	A	25	100.69	28.77
	M	25	79.91	15.31
	P	25	101.54	23.67
	L	25	93.86	24.18
4	A	24	112.45	44.09
	M	17	109.81	33.66
	P	23	128.70	28.69
	L	25	104.29	35.29
5	A	23	100.74	27.86
	M	25	116.49	32.80
	P	25	106.95	18.91
	L	25	106.67	19.42
6	A	25	143.42	19.82
	M	25	131.94	39.73
	P	25	122.93	41.55
	L	25	132.17	31.34
7	A	18	128.66	27.41
	M	25	109.21	28.48
	P	25	98.71	13.96
	L	24	122.65	22.58

Table A9: Mean Trabecular Thickness of the Radius by Quadrant

Fetus	Quad	N	Mean	Std Dev
1	A	18	70.98	24.46
	M	10	66.02	17.42
	P	14	77.95	18.54
	L	-	-	-
2	A	-	-	-
	M	-	-	-
	P	-	-	-
	L	-	-	-
3	A	6	73.71	22.88
	M	17	102.04	32.18
	P	25	116.75	34.90
	L	24	136.23	37.36
4	A	-	-	-
	M	23	78.77	21.98
	P	25	104.28	23.07
	L	25	96.86	38.15
5	A	-	-	-
	M	14	107.76	28.62
	P	25	107.99	43.10
	L	10	44.46	14.52
6	A	19	116.98	40.63
	M	16	82.33	41.47
	P	25	117.61	32.71
	L	18	131.29	34.50
7	A	25	135.15	41.85
	M	-	-	-
	P	10	114.71	38.40
	L	25	100.03	25.60

Table A10: Mean Trabecular Thickness of the Ulna by Quadrant

Fetus	Quad	N	Mean	Std Dev
1	A	13	79.10	24.71
	M	7	111.45	47.37
	P	9	82.75	22.84
	L	12	45.56	18.77
2	A	12	51.66	21.17
	M	-	-	-
	P	-	-	-
	L	-	-	-
3	A	25	86.48	23.47
	M	25	86.22	27.53
	P	21	88.17	26.66
	L	25	101.17	22.84
4	A	18	100.76	35.33
	M	8	135.46	21.15
	P	25	108.07	27.08
	L	20	88.34	26.66
5	A	25	94.76	26.56
	M	25	106.57	30.39
	P	-	-	-
	L	24	99.74	23.68
6	A	25	113.07	30.23
	M	25	130.22	35.16
	P	-	-	-
	L	25	119.50	28.09
7	A	25	106.59	34.19
	M	20	113.64	28.80
	P	25	94.38	23.68
	L	25	90.92	30.96

Table A11: Mean Trabecular Thickness Across Quadrants by Bone

Fetus	Bone	N	Mean	Std Dev
1	Femur	74	82.34	26.61
	Tibia	83	65.87	15.26
	Fibula	66	58.01	18.29
	Humerus	92	76.07	26.37
	Radius	42	72.12	21.09
	Ulna	41	75.61	35.10
2	Femur	54	50.37	17.21
	Tibia	64	58.82	18.50
	Fibula	-	-	-
	Humerus	61	56.55	18.67
	Radius	-	-	-
	Ulna	12	51.66	21.17
3	Femur	99	74.82	18.99
	Tibia	100	101.01	22.90
	Fibula	86	88.02	22.58
	Humerus	100	94.00	24.71
	Radius	73	93.21	30.04
	Ulna	96	90.61	25.54
4	Femur	98	97.34	23.79
	Tibia	100	111.86	29.84
	Fibula	36	95.04	30.18
	Humerus	89	113.85	36.70
	Radius	72	116.18	38.35
	Ulna	71	103.75	31.37
5	Femur	93	94.93	26.52
	Tibia	100	107.08	23.76
	Fibula	70	98.84	25.95
	Humerus	98	107.85	25.61
	Radius	49	94.96	43.10
	Ulna	71	100.10	26.95

Table A11: Mean Trabecular Thickness Across Quadrants by Bone (cont.)

Fetus	Bone	N	Mean	Std Dev
6	Femur	100	119.53	24.89
	Tibia	100	130.57	29.79
	Fibula	67	114.15	29.53
	Humerus	100	132.61	34.46
	Radius	78	113.38	40.02
	Ulna	82	120.78	33.84
7	Femur	91	106.08	29.94
	Tibia	99	113.41	33.12
	Fibula	82	105.82	42.28
	Humerus	92	113.67	25.83
	Radius	60	117.11	38.30
	Ulna	95	100.74	30.58

TableA12: Raw Data for Trabecular Thickness (nm)

Fetus	Dev_Age	Bone	Quad	Trab(nm)
1	17	H	A	63.42028
1	17	H	A	84.22806
1	17	H	A	53.73243
1	17	H	A	42.02703
1	17	H	A	39.02112
1	17	H	A	41.77545
1	17	H	A	45.67305
1	17	H	A	45.50605
1	17	H	A	90.0092
1	17	H	A	84.83772
1	17	H	A	58.2408
1	17	H	A	49.35824
1	17	H	A	75.05862
1	17	H	A	78.94501
1	17	H	A	104.447
1	17	H	A	82.77629
1	17	H	A	102.1968
1	17	H	A	84.30451
1	17	H	A	46.08153
1	17	H	A	38.96104
1	17	H	A	45.77551
1	17	H	A	117.0634
1	17	H	M	99.77862
1	17	H	M	129.441
1	17	H	M	78.43148
1	17	H	M	74.14012
1	17	H	M	98.77579
1	17	H	M	67.08211
1	17	H	M	73.59307
1	17	H	M	83.39656
1	17	H	M	135.0908
1	17	H	M	95.80826
1	17	H	M	69.16253
1	17	H	M	75.88116
1	17	H	M	132.4819
1	17	H	M	95.26269
1	17	H	M	44.37229
1	17	H	M	52.36351
1	17	H	M	95.53893
1	17	H	M	127.9072
1	17	H	M	89.8855
1	17	H	M	83.58594
1	17	H	M	108.9693
1	17	H	P	89.48063

Fetus	Dev_Age	Bone	Quad	Trab(nm)
1	17	H	P	69.1456
1	17	H	P	78.37919
1	17	H	P	63.49411
1	17	H	P	68.25908
1	17	H	P	80.24729
1	17	H	P	89.67676
1	17	H	P	129.8701
1	17	H	P	53.9174
1	17	H	P	104.6431
1	17	H	P	82.42179
1	17	H	P	70.91016
1	17	H	P	75.37007
1	17	H	P	108.9693
1	17	H	P	127.8431
1	17	H	P	104.8444
1	17	H	P	143.4013
1	17	H	P	55.91165
1	17	H	P	68.89104
1	17	H	P	81.34901
1	17	H	P	69.47512
1	17	H	P	100.9689
1	17	H	P	131.0775
1	17	H	P	53.07446
1	17	H	L	69.21332
1	17	H	L	74.54974
1	17	H	L	51.44963
1	17	H	L	53.5687
1	17	H	L	59.61229
1	17	H	L	66.44176
1	17	H	L	48.8094
1	17	H	L	55.45943
1	17	H	L	64.83578
1	17	H	L	52.06066
1	17	H	L	60.65436
1	17	H	L	106.7266
1	17	H	L	69.27252
1	17	H	L	61.07771
1	17	H	L	80.15237
1	17	H	L	39.39453
1	17	H	L	58.45158
1	17	H	L	56.49517
1	17	H	L	35.97569
1	17	H	L	44.49092
1	17	H	L	46.48643

Table A12, cont.

Fetus	Dev_Age	Bone	Quad	Trab(nm)
1	17	H	P	77.17444
1	17	H	L	49.287
1	17	H	L	37.19229
2	14	H	A	69.34857
2	14	H	A	62.02913
2	14	H	A	58.88082
2	14	H	A	68.83151
2	14	H	A	32.43144
2	14	H	A	41.13978
2	14	H	A	23.83411
2	14	H	A	61.6978
2	14	H	A	62.02913
2	14	H	A	41.2535
2	14	H	A	30.32235
2	14	H	A	34.22378
2	14	H	M	43.62694
2	14	H	M	42.92323
2	14	H	M	43.62694
2	14	H	M	51.18716
2	14	H	M	60.23775
2	14	H	M	49.13229
2	14	H	M	40.40726
2	14	H	M	60.29605
2	14	H	M	44.21363
2	14	H	M	76.7712
2	14	H	M	43.10023
2	14	H	M	48.39974
2	14	H	M	47.58214
2	14	H	M	74.7302
2	14	H	M	40.6673
2	14	H	M	52.77569
2	14	H	M	49.35824
2	14	H	P	74.54974
2	14	H	P	79.89623
2	14	H	P	27.40041
2	14	H	P	56.27706
2	14	H	P	49.03684
2	14	H	P	39.02112
2	14	H	P	53.45926
2	14	H	P	54.76875
2	14	H	P	39.09609
2	14	H	P	39.02112
2	14	H	P	78.07225
2	14	H	P	46.04339
1	17	H	L	93.83186
2	14	H	P	52.86439
2	14	H	P	41.80348
2	14	H	P	38.29395
2	14	H	P	49.97141
2	14	H	P	56.44331
2	14	H	L	92.04862
2	14	H	L	81.313
2	14	H	L	94.16206
2	14	H	L	89.04763
2	14	H	L	99.95454
2	14	H	L	81.63646
2	14	H	L	48.05975
2	14	H	L	47.1688
2	14	H	L	89.13152
2	14	H	L	72.29894
2	14	H	L	38.61538
3	24	H	A	122.2234
3	24	H	A	87.39022
3	24	H	A	97.07441
3	24	H	A	65.21739
3	24	H	A	126.6106
3	24	H	A	138.7222
3	24	H	A	148.4004
3	24	H	A	92.56378
3	24	H	A	90.07978
3	24	H	A	74.04081
3	24	H	A	77.68508
3	24	H	A	133.0889
3	24	H	A	100.7064
3	24	H	A	86.98369
3	24	H	A	52.62486
3	24	H	A	86.79333
3	24	H	A	83.51901
3	24	H	A	111.1038
3	24	H	A	41.36152
3	24	H	A	133.2486
3	24	H	A	130.6701
3	24	H	A	105.3619
3	24	H	A	72.39489
3	24	H	A	132.7334
3	24	H	A	126.5546
3	24	H	M	64.19488
3	24	H	M	72.91526

Table A12, cont.

Fetus	Dev_Age	Bone	Quad	Trab(nm)
2	14	H	P	87.66902
2	14	H	P	75.98913
2	14	H	P	81.3634
2	14	H	P	40.1747
3	24	H	M	75.05512
3	24	H	M	45.85875
3	24	H	M	99.00259
3	24	H	M	90.00105
3	24	H	M	91.40781
3	24	H	M	76.9209
3	24	H	M	56.56353
3	24	H	M	76.58224
3	24	H	M	80.55221
3	24	H	M	85.03307
3	24	H	M	88.03677
3	24	H	M	97.92266
3	24	H	M	61.21795
3	24	H	M	79.81548
3	24	H	M	77.77628
3	24	H	M	97.63266
3	24	H	M	74.96061
3	24	H	M	117.2503
3	24	H	M	66.36668
3	24	H	P	120.5885
3	24	H	P	88.03677
3	24	H	P	115.7902
3	24	H	P	118.2737
3	24	H	P	108.7174
3	24	H	P	81.16589
3	24	H	P	121.8167
3	24	H	P	123.7795
3	24	H	P	83.00819
3	24	H	P	139.8926
3	24	H	P	75.46328
3	24	H	P	93.88184
3	24	H	P	144.7245
3	24	H	P	88.73188
3	24	H	P	104.0303
3	24	H	P	76.58224
3	24	H	P	106.7212
3	24	H	P	33.74821
3	24	H	P	81.16589
3	24	H	P	99.55003
3	24	H	P	103.3009

Fetus	Dev_Age	Bone	Quad	Trab(nm)
3	24	H	M	81.4855
3	24	H	M	77.59378
3	24	H	M	70.0054
3	24	H	M	93.57932
3	24	H	L	93.37709
3	24	H	L	74.96061
3	24	H	L	75.05512
3	24	H	L	48.2687
3	24	H	L	97.85024
3	24	H	L	89.23642
3	24	H	L	164.4864
3	24	H	L	58.00724
3	24	H	L	109.2378
3	24	H	L	91.74325
3	24	H	L	65.79455
3	24	H	L	96.48844
3	24	H	L	92.48716
3	24	H	L	69.59918
3	24	H	L	113.2314
3	24	H	L	98.23586
3	24	H	L	105.7872
3	24	H	L	113.0644
3	24	H	L	127.67
3	24	H	L	115.2994
3	24	H	L	85.22737
3	24	H	L	78.56222
4	22	H	A	81.39846
4	22	H	A	93.65504
4	22	H	A	64.37866
4	22	H	A	57.39295
4	22	H	A	61.25653
4	22	H	A	64.52531
4	22	H	A	72.39489
4	22	H	A	128.3345
4	22	H	A	178.2609
4	22	H	A	104.574
4	22	H	A	171.1879
4	22	H	A	109.3243
4	22	H	A	113.0644
4	22	H	A	97.43885
4	22	H	A	142.1048
4	22	H	A	152.1894
4	22	H	A	217.7606
4	22	H	A	46.52377

Table A12, cont.

Fetus	Dev_Age	Bone	Quad	Trab(nm)
3	24	H	P	116.7656
3	24	H	P	86.00018
3	24	H	P	117.7129
3	24	H	P	109.1729
3	24	H	L	110.2069
3	24	H	L	79.13163
3	24	H	L	93.50354
4	22	H	M	116.5226
4	22	H	M	111.4011
4	22	H	M	49.28602
4	22	H	M	67.95
4	22	H	M	67.42636
4	22	H	M	110.7843
4	22	H	M	120.9993
4	22	H	M	129.4528
4	22	H	M	116.218
4	22	H	M	68.74517
4	22	H	M	129.4346
4	22	H	M	189.5797
4	22	H	M	134.1676
4	22	H	M	108.6957
4	22	H	M	89.15694
4	22	H	M	137.3872
4	22	H	P	172.0313
4	22	H	P	133.6647
4	22	H	P	114.4148
4	22	H	P	101.3379
4	22	H	P	96.35365
4	22	H	P	177.7033
4	22	H	P	141.6926
4	22	H	P	133.8061
4	22	H	P	99.48473
4	22	H	P	123.0615
4	22	H	P	117.8985
4	22	H	P	124.6024
4	22	H	P	176.653
4	22	H	P	183.5155
4	22	H	P	139.5417
4	22	H	P	106.9645
4	22	H	P	89.13706
4	22	H	P	164.7878
4	22	H	P	118.3785
4	22	H	P	94.23982
4	22	H	P	108.7174
4	22	H	A	123.3205
4	22	H	A	148.3686
4	22	H	A	161.4707
4	22	H	A	130.9049
4	22	H	A	96.24323
4	22	H	A	82.6087
4	22	H	M	119.5652
4	22	H	L	124.5218
4	22	H	L	99.92909
4	22	H	L	62.2514
4	22	H	L	63.19323
4	22	H	L	81.86161
4	22	H	L	86.57525
4	22	H	L	106.9424
4	22	H	L	153.9953
4	22	H	L	186.868
4	22	H	L	87.06515
4	22	H	L	122.9751
4	22	H	L	139.1984
4	22	H	L	108.6957
4	22	H	L	97.3418
4	22	H	L	112.2253
4	22	H	L	92.28254
4	22	H	L	124.3509
5	25	H	A	105.7872
5	25	H	A	155.02
5	25	H	A	160.4725
5	25	H	A	108.7174
5	25	H	A	94.70879
5	25	H	A	65.25361
5	25	H	A	104.7095
5	25	H	A	97.82609
5	25	H	A	84.58729
5	25	H	A	129.1421
5	25	H	A	97.82609
5	25	H	A	85.03307
5	25	H	A	88.81173
5	25	H	A	67.53141
5	25	H	A	123.0711
5	25	H	A	139.0795
5	25	H	A	85.42123
5	25	H	A	126.0307
5	25	H	A	79.042
5	25	H	A	98.88318

Table A12, cont.

Fetus	Dev_Age	Bone	Quad	Trab(nm)
4	22	H	P	124.0512
4	22	H	P	118.0187
4	22	H	L	81.86161
4	22	H	L	54.86708
4	22	H	L	141.0533
4	22	H	L	48.85262
4	22	H	L	141.1705
4	22	H	L	76.21108
4	22	H	L	150.1417
4	22	H	L	62.74291
5	25	H	M	72.91526
5	25	H	M	68.22763
5	25	H	M	148.7503
5	25	H	M	171.8629
5	25	H	M	155.5526
5	25	H	M	130.0174
5	25	H	M	116.8668
5	25	H	M	95.3057
5	25	H	M	97.85024
5	25	H	M	149.0043
5	25	H	M	132.7334
5	25	H	M	148.3526
5	25	H	M	144.4957
5	25	H	M	111.0612
5	25	H	M	107.9321
5	25	H	M	59.05686
5	25	H	M	101.3379
5	25	H	M	98.81146
5	25	H	P	121.8361
5	25	H	P	110.9548
5	25	H	P	83.0651
5	25	H	P	142.1048
5	25	H	P	109.4107
5	25	H	P	110.2069
5	25	H	P	120.0386
5	25	H	P	95.35527
5	25	H	P	110.4425
5	25	H	P	88.73188
5	25	H	P	76.85943
5	25	H	P	117.0688
5	25	H	P	140.5666
5	25	H	P	115.5655
5	25	H	P	110.8483

Fetus	Dev_Age	Bone	Quad	Trab(nm)
5	25	H	A	49.19004
5	25	H	A	93.85667
5	25	H	A	77.10499
5	25	H	M	115.9534
5	25	H	M	165.7457
5	25	H	M	140.9695
5	25	H	M	92.25694
5	25	H	M	123.913
5	25	H	M	111.74
5	25	H	M	51.53595
5	25	H	L	127.5959
5	25	H	L	118.1137
5	25	H	L	87.63324
5	25	H	L	129.7081
5	25	H	L	111.0399
5	25	H	L	129.1238
5	25	H	L	78.77248
5	25	H	L	111.21
5	25	H	L	75.93152
5	25	H	L	93.50354
5	25	H	L	127.8919
5	25	H	L	111.4011
5	25	H	L	118.3735
5	25	H	L	138.6711
5	25	H	L	123.5884
5	25	H	L	69.08804
5	25	H	L	80.90345
5	25	H	L	88.03677
5	25	H	L	88.09043
5	25	H	L	104.0303
5	25	H	L	101.8264
6	38	H	A	123.9893
6	38	H	A	148.8456
6	38	H	A	171.4224
6	38	H	A	136.5245
6	38	H	A	165.2746
6	38	H	A	113.4191
6	38	H	A	175.6032
6	38	H	A	151.7696
6	38	H	A	132.234
6	38	H	A	144.8061
6	38	H	A	158.3379
6	38	H	A	119.585

Table A12, cont.

Fetus	Dev_Age	Bone	Quad	Trab(nm)
5	25	H	P	99.92909
5	25	H	P	113.4816
5	25	H	P	131.3195
5	25	H	P	100.3774
5	25	H	P	95.3057
5	25	H	P	98.23586
5	25	H	P	87.95621
5	25	H	P	75.71337
5	25	H	P	135.2202
5	25	H	P	83.0651
5	25	H	L	108.1071
5	25	H	L	126.5546
5	25	H	L	112.3095
5	25	H	L	105.1824
6	38	H	M	117.0688
6	38	H	M	71.77206
6	38	H	M	113.1271
6	38	H	M	95.67687
6	38	H	M	95.08229
6	38	H	M	185.4973
6	38	H	M	147.8261
6	38	H	M	115.5655
6	38	H	M	150.6915
6	38	H	M	141.4548
6	38	H	M	58.7359
6	38	H	M	136.5245
6	38	H	M	132.8935
6	38	H	M	58.00724
6	38	H	M	153.7496
6	38	H	M	155.1876
6	38	H	M	112.9808
6	38	H	M	203.9427
6	38	H	M	136.8184
6	38	H	M	102.3357
6	38	H	M	152.5616
6	38	H	M	193.7102
6	38	H	M	155.02
6	38	H	M	194.4407
6	38	H	L	117.8935
6	38	H	L	117.0688
6	38	H	L	129.2702
6	38	H	L	117.8333
6	38	H	L	106.1662
6	38	H	L	137.2839
6	38	H	A	120.5885
6	38	H	A	148.9249
6	38	H	A	113.8973
6	38	H	A	164.6587
6	38	H	A	149.2578
6	38	H	A	128.3345
6	38	H	A	124.5218
6	38	H	A	128.6288
6	38	H	A	119.3872
6	38	H	A	153.9186
6	38	H	A	161.5877
6	38	H	A	173.1096
6	38	H	A	156.7932
6	38	H	M	117.8935
6	38	H	L	81.4855
6	38	H	L	164.5869
6	38	H	P	155.4614
6	38	H	P	109.1512
6	38	H	P	138.3299
6	38	H	P	169.5792
6	38	H	P	160.8696
6	38	H	P	115.4018
6	38	H	P	135.1503
6	38	H	P	140.2132
6	38	H	P	121.6809
6	38	H	P	181.271
6	38	H	P	112.9808
6	38	H	P	78.26087
6	38	H	P	213.6305
6	38	H	P	146.6868
6	38	H	P	137.6621
6	38	H	P	110.8483
6	38	H	P	117.6728
6	38	H	P	111.1038
6	38	H	P	27.23905
6	38	H	P	97.63266
6	38	H	P	45.2362
6	38	H	P	110.8483
6	38	H	P	152.3756
6	38	H	P	125.4482
6	38	H	P	58.49402
7	37	H	A	100.0945
7	37	H	A	71.73913
7	37	H	A	139.7574

Table A12, cont.

Fetus	Dev_Age	Bone	Quad	Trab(nm)
6	38	H	L	158.3379
6	38	H	L	170.5102
6	38	H	L	134.9403
6	38	H	L	159.2308
6	38	H	L	92.56378
6	38	H	L	126.2555
6	38	H	L	97.65686
6	38	H	L	134.8527
6	38	H	L	173.3823
6	38	H	L	122.0493
6	38	H	L	182.3108
6	38	H	L	196.628
6	38	H	L	161.3975
6	38	H	L	91.40781
6	38	H	L	126.7598
6	38	H	L	95.57803
6	38	H	L	108.7826
7	37	H	M	108.7826
7	37	H	M	126.2555
7	37	H	M	99.57376
7	37	H	M	127.2807
7	37	H	M	133.3195
7	37	H	M	121.3114
7	37	H	M	143.4947
7	37	H	M	40.08498
7	37	H	M	136.4553
7	37	H	M	117.8333
7	37	H	M	183.0868
7	37	H	M	86.2197
7	37	H	M	130.471
7	37	H	M	95.97278
7	37	H	M	93.85667
7	37	H	M	85.64224
7	37	H	M	82.63729
7	37	H	M	81.22409
7	37	H	M	125.8055
7	37	H	M	111.0612
7	37	H	M	90.07978
7	37	H	M	107.5593
7	37	H	M	110.0137
7	37	H	P	90.83731
7	37	H	P	106.1662
7	37	H	P	90.78527
7	37	H	P	107.954

Fetus	Dev_Age	Bone	Quad	Trab(nm)
7	37	H	A	144.283
7	37	H	A	110.8909
7	37	H	A	158.8296
7	37	H	A	131.3375
7	37	H	A	147.8421
7	37	H	A	104.7095
7	37	H	A	140.2469
7	37	H	A	83.23561
7	37	H	A	136.1432
7	37	H	A	143.9387
7	37	H	A	126.0495
7	37	H	A	187.8392
7	37	H	A	120.0583
7	37	H	A	130.0901
7	37	H	A	138.7222
7	37	H	M	69.87026
7	37	H	M	122.3973
7	37	H	P	82.63729
7	37	H	L	128.7757
7	37	H	L	84.67105
7	37	H	L	148.3526
7	37	H	L	136.4553
7	37	H	L	135.6389
7	37	H	L	124.5028
7	37	H	L	96.26778
7	37	H	L	116.2789
7	37	H	L	98.88318
7	37	H	L	115.0532
7	37	H	L	142.2543
7	37	H	L	109.7557
7	37	H	L	151.8942
7	37	H	L	107.9321
7	37	H	L	131.6071
7	37	H	L	142.3706
7	37	H	L	143.7415
7	37	H	L	135.3599
7	37	H	L	167.0663
7	37	H	L	87.63324
7	37	H	L	119.585
7	37	H	L	91.30435
7	37	H	L	93.65504
7	37	H	L	134.4491
2	14	F	A	32.09744
2	14	F	A	24.52286

Table A12, cont.

Fetus	Dev_Age	Bone	Quad	Trab(nm)
7	37	H	P	82.03462
7	37	H	P	113.4191
7	37	H	P	100.0236
7	37	H	P	106.8761
7	37	H	P	111.74
7	37	H	P	108.3036
7	37	H	P	88.278
7	37	H	P	117.4718
7	37	H	P	87.63324
7	37	H	P	91.64017
7	37	H	P	112.8761
7	37	H	P	136.8184
7	37	H	P	81.68824
7	37	H	P	90.8113
7	37	H	P	104.5288
7	37	H	P	91.25257
7	37	H	P	76.85943
7	37	H	P	103.1177
7	37	H	P	94.70879
7	37	H	P	89.20993
2	14	F	P	41.53255
2	14	F	P	48.13389
2	14	F	P	63.90898
2	14	F	P	35.85309
2	14	F	P	53.30522
2	14	F	P	57.40324
2	14	F	P	41.81605
2	14	F	P	52.93824
2	14	F	P	76.52822
2	14	F	P	49.57284
2	14	F	P	83.72388
2	14	F	P	101.1103
2	14	F	P	60.12746
2	14	F	P	54.87785
2	14	F	P	69.59918
2	14	F	P	76.31952
2	14	F	P	51.04068
2	14	F	P	55.55188
2	14	F	P	63.6125
2	14	F	P	79.99291
2	14	F	P	52.45621
2	14	F	P	67.04857
2	14	F	P	60.12746
2	14	F	P	50.01181

Fetus	Dev_Age	Bone	Quad	Trab(nm)
2	14	F	A	27.94557
2	14	F	A	24.01165
2	14	F	A	22.92937
2	14	F	A	21.43813
2	14	F	A	28.94245
2	14	F	A	30.06373
2	14	F	A	33.05849
2	14	F	A	33.81815
2	14	F	A	37.40141
2	14	F	M	61.57395
2	14	F	M	52.89359
2	14	F	M	43.81662
2	14	F	M	44.24594
2	14	F	M	60.65568
2	14	F	M	44.56522
2	14	F	M	60.01929
2	14	F	M	39.19077
2	14	F	M	66.19735
2	14	F	M	47.24199
2	14	F	P	43.00009
1	17	F	M	97.07441
1	17	F	M	82.17851
1	17	F	M	98.4281
1	17	F	M	113.752
1	17	F	M	84.58729
1	17	F	M	56.89675
1	17	F	M	79.75624
1	17	F	M	69.59918
1	17	F	M	63.37991
1	17	F	M	103.278
1	17	F	M	81.4855
1	17	F	M	86.2197
1	17	F	M	87.39022
1	17	F	M	138.1761
1	17	F	M	69.08804
1	17	F	M	72.91526
1	17	F	P	53.07198
1	17	F	P	84.55935
1	17	F	P	131.5891
1	17	F	P	96.09581
1	17	F	P	80.90345
1	17	F	P	131.894
1	17	F	P	103.0031
1	17	F	P	102.7505

Table A12, cont.

Fetus	Dev_Age	Bone	Quad	Trab(nm)
2	14	F	L	83.91417
2	14	F	L	46.12847
2	14	F	L	46.12847
2	14	F	L	61.21795
2	14	F	L	41.66036
2	14	F	L	36.90854
2	14	F	L	36.53856
2	14	F	L	41.50409
1	17	F	A	46.06439
1	17	F	A	44.81637
1	17	F	A	81.68824
1	17	F	A	36.95652
1	17	F	A	41.53255
1	17	F	A	54.4781
1	17	F	A	106.6104
1	17	F	A	46.52377
1	17	F	A	70.97751
1	17	F	A	77.92804
1	17	F	A	72.36225
1	17	F	A	59.97006
1	17	F	A	68.26225
1	17	F	A	87.63324
1	17	F	A	79.13163
1	17	F	L	51.67332
1	17	F	L	53.82356
1	17	F	L	132.769
1	17	F	L	100.8471
1	17	F	L	30.89711
1	17	F	L	107.0528
1	17	F	L	89.63273
1	17	F	L	83.66035
1	17	F	L	58.33221
1	17	F	L	83.6321
1	17	F	L	73.84908
1	17	F	L	65.54267
3	24	F	A	80.69874
3	24	F	A	64.85406
3	24	F	A	76.335
3	24	F	A	78.38155
3	24	F	A	61.48755
3	24	F	A	76.335
3	24	F	A	51.67332
3	24	F	A	58.5344
3	24	F	A	70.77748

Fetus	Dev_Age	Bone	Quad	Trab(nm)
1	17	F	P	102.8194
1	17	F	P	78.38155
1	17	F	P	95.67687
1	17	F	P	144.3648
1	17	F	P	50.42354
1	17	F	P	84.89402
1	17	F	P	100.5185
1	17	F	P	80.66946
1	17	F	P	152.9329
1	17	F	P	113.4816
1	17	F	P	81.71716
1	17	F	P	61.56436
1	17	F	P	101.1512
1	17	F	P	127.67
1	17	F	P	41.81605
1	17	F	P	63.04348
1	17	F	P	57.76231
1	17	F	L	80.46415
1	17	F	L	69.32704
1	17	F	L	54.34783
1	17	F	L	66.25979
1	17	F	L	106.9424
1	17	F	L	101.896
3	24	F	M	73.94501
3	24	F	M	71.77206
3	24	F	M	105.07
3	24	F	M	85.75253
3	24	F	M	78.38155
3	24	F	M	34.02712
3	24	F	M	78.38155
3	24	F	M	32.09744
3	24	F	M	61.21795
3	24	F	M	54.52146
3	24	F	M	72.00215
3	24	F	M	62.28934
3	24	F	M	83.0651
3	24	F	M	90.83731
3	24	F	P	103.278
3	24	F	P	107.2513
3	24	F	P	106.7212
3	24	F	P	52.35476
3	24	F	P	78.26087
3	24	F	P	102.5433
3	24	F	P	89.13043

Table A12, cont.

Fetus	Dev_Age	Bone	Quad	Trab(nm)
3	24	F	A	72.39489
3	24	F	A	68.26225
3	24	F	A	73.94501
3	24	F	A	85.47654
3	24	F	A	83.91417
3	24	F	A	70.0054
3	24	F	A	72.91526
3	24	F	A	57.39295
3	24	F	A	53.47119
3	24	F	A	58.85646
3	24	F	A	67.95
3	24	F	A	85.66983
3	24	F	A	63.19323
3	24	F	A	59.97006
3	24	F	A	52.35476
3	24	F	A	69.59918
3	24	F	M	41.75951
3	24	F	M	59.05686
3	24	F	M	90.8113
3	24	F	M	115.4018
3	24	F	M	92.56378
3	24	F	M	71.70618
3	24	F	M	74.42279
3	24	F	M	68.64197
3	24	F	M	80.69874
3	24	F	M	86.98369
3	24	F	L	67.42636
3	24	F	L	39.96691
3	24	F	L	77.92804
3	24	F	L	87.20074
3	24	F	L	71.87076
3	24	F	L	54.34783
3	24	F	L	77.04367
3	24	F	L	63.97365
3	24	F	L	77.19687
3	24	F	L	59.81225
3	24	F	L	60.55821
3	24	F	L	53.69169
3	24	F	L	82.86573
3	24	F	L	53.07198
3	24	F	L	50.04724
3	24	F	L	85.22737
3	24	F	L	102.4511
4	22	F	A	91.74325
3	24	F	P	127.8919
3	24	F	P	74.86598
3	24	F	P	89.13043
3	24	F	P	95.67687
3	24	F	P	76.58224
3	24	F	P	61.02465
3	24	F	P	98.2118
3	24	F	P	70.24128
3	24	F	P	110.4425
3	24	F	P	93.88184
3	24	F	P	79.60797
3	24	F	P	65.21739
3	24	F	P	79.60797
3	24	F	P	142.9172
3	24	F	P	54.34783
3	24	F	P	85.66983
3	24	F	P	45.7039
3	24	F	P	89.79077
3	24	F	L	80.43478
3	24	F	L	66.96923
3	24	F	L	54.52146
3	24	F	L	69.87026
3	24	F	L	69.19057
3	24	F	L	93.57932
3	24	F	L	73.94501
3	24	F	L	74.20021
4	22	F	M	108.7174
4	22	F	M	87.06515
4	22	F	M	83.91417
4	22	F	M	92.28254
4	22	F	M	116.1976
4	22	F	M	97.05006
4	22	F	M	108.3036
4	22	F	M	78.38155
4	22	F	M	90.49851
4	22	F	M	84.67105
4	22	F	M	113.7935
4	22	F	M	93.70549
4	22	F	M	73.56054
4	22	F	M	100.0945
4	22	F	M	95.57803
4	22	F	M	95.75094
4	22	F	M	52.35476
4	22	F	M	83.91417

Table A12, cont.

Fetus	Dev_Age	Bone	Quad	Trab(nm)
4	22	F	A	107.7787
4	22	F	A	115.2994
4	22	F	A	113.4191
4	22	F	A	77.68508
4	22	F	A	113.1271
4	22	F	A	49.57284
4	22	F	A	51.67332
4	22	F	A	58.41317
4	22	F	A	91.43366
4	22	F	A	108.7174
4	22	F	A	108.8911
4	22	F	A	116.8668
4	22	F	A	95.87425
4	22	F	A	58.5344
4	22	F	A	48.2687
4	22	F	A	69.08804
4	22	F	A	59.69361
4	22	F	A	137.2839
4	22	F	A	100.8471
4	22	F	A	93.50354
4	22	F	A	131.3195
4	22	F	A	93.50354
4	22	F	A	69.59918
4	22	F	M	107.4054
4	22	F	M	129.6535
4	22	F	M	102.5433
4	22	F	M	117.4718
4	22	F	M	92.56378
4	22	F	M	139.4358
4	22	F	L	133.8149
4	22	F	L	99.00259
4	22	F	L	89.13043
4	22	F	L	110.8483
4	22	F	L	111.4011
4	22	F	L	87.44428
4	22	F	L	104.461
4	22	F	L	132.769
4	22	F	L	98.09143
4	22	F	L	126.6293
4	22	F	L	145.4086
4	22	F	L	75.08659
4	22	F	L	59.69361
4	22	F	L	58.7359
4	22	F	L	86.54795

Fetus	Dev_Age	Bone	Quad	Trab(nm)
4	22	F	M	71.96933
4	22	F	P	94.08298
4	22	F	P	78.41169
4	22	F	P	110.0137
4	22	F	P	105.6531
4	22	F	P	102.197
4	22	F	P	72.00215
4	22	F	P	77.59378
4	22	F	P	97.22035
4	22	F	P	135.4297
4	22	F	P	110.0137
4	22	F	P	100.495
4	22	F	P	94.38388
4	22	F	P	115.7086
4	22	F	P	63.19323
4	22	F	P	101.8728
4	22	F	P	96.53741
4	22	F	P	109.6696
4	22	F	P	137.1117
4	22	F	P	70.10659
4	22	F	P	118.2737
4	22	F	P	103.0948
4	22	F	P	175.2665
4	22	F	P	99.35996
4	22	F	P	81.16589
4	22	F	L	117.2503
4	22	F	L	108.129
4	22	F	L	89.52722
4	22	F	L	89.52722
5	25	F	M	103.5522
5	25	F	M	93.65504
5	25	F	M	39.96691
5	25	F	M	138.6711
5	25	F	M	129.5988
5	25	F	M	89.55361
5	25	F	M	122.6095
5	25	F	M	85.22737
5	25	F	M	88.6786
5	25	F	M	81.71716
5	25	F	M	70.0054
5	25	F	M	74.29568
5	25	F	M	87.39022
5	25	F	M	107.9321
5	25	F	M	94.30875

Table A12, cont.

Fetus	Dev_Age	Bone	Quad	Trab(nm)
4	22	F	L	95.97278
4	22	F	L	135.5692
4	22	F	L	130.2354
4	22	F	L	70.54339
4	22	F	L	70.77748
4	22	F	L	84.67105
5	25	F	A	82.17851
5	25	F	A	65.14489
5	25	F	A	70.10659
5	25	F	A	63.3053
5	25	F	A	59.05686
5	25	F	A	80.16995
5	25	F	A	73.04477
5	25	F	A	76.58224
5	25	F	A	70.10659
5	25	F	A	68.08896
5	25	F	A	63.9367
5	25	F	A	59.81225
5	25	F	A	102.4511
5	25	F	A	86.13745
5	25	F	A	80.66946
5	25	F	A	149.3053
5	25	F	A	194.0758
5	25	F	A	107.0528
5	25	F	A	124.9764
5	25	F	A	80.69874
5	25	F	A	109.1729
5	25	F	A	77.77628
5	25	F	A	78.53214
5	25	F	A	80.87424
5	25	F	A	76.85943
5	25	F	M	106.6104
5	25	F	L	134.3788
5	25	F	L	146.9604
5	25	F	L	152.639
5	25	F	L	106.3441
5	25	F	L	82.29345
5	25	F	L	72.26422
5	25	F	L	114.2494
5	25	F	L	115.2174
5	25	F	L	123.3779
5	25	F	L	152.5616
5	25	F	L	108.5434
5	25	F	L	113.918

Fetus	Dev_Age	Bone	Quad	Trab(nm)
5	25	F	M	92.86961
5	25	F	M	106.6104
5	25	F	P	100.5185
5	25	F	P	110.4425
5	25	F	P	50.04724
5	25	F	P	68.74517
5	25	F	P	85.03307
5	25	F	P	44.60497
5	25	F	P	95.50384
5	25	F	P	72.91526
5	25	F	P	109.2378
5	25	F	P	61.02465
5	25	F	P	48.61017
5	25	F	P	79.13163
5	25	F	P	121.5254
5	25	F	P	96.85508
5	25	F	P	72.26422
5	25	F	P	85.03307
5	25	F	P	100.2124
5	25	F	P	109.6696
5	25	F	P	95.57803
5	25	F	P	106.6104
5	25	F	P	107.5593
5	25	F	P	121.2139
5	25	F	P	97.05006
5	25	F	P	96.95262
5	25	F	P	94.70879
5	25	F	L	99.14569
5	25	F	L	115.2174
5	25	F	L	95.65217
5	25	F	L	108.7174
5	25	F	L	93.57932
6	38	F	M	163.4054
6	38	F	M	108.7174
6	38	F	M	95.65217
6	38	F	M	141.9717
6	38	F	M	120.2746
6	38	F	M	99.00259
6	38	F	M	158.7552
6	38	F	M	153.4265
6	38	F	M	161.7631
6	38	F	M	174.8075
6	38	F	M	144.1027
6	38	F	M	96.53741

Table A12, cont.

Fetus	Dev_Age	Bone	Quad	Trab(nm)
5	25	F	L	120.2746
5	25	F	L	63.97365
5	25	F	L	126.3865
5	25	F	L	127.9842
5	25	F	L	97.1474
5	25	F	L	66.25979
5	25	F	L	80.46415
5	25	F	L	86.87496
6	38	F	A	76.21108
6	38	F	A	131.894
6	38	F	A	105.2497
6	38	F	A	90.8113
6	38	F	A	83.20721
6	38	F	A	109.2378
6	38	F	A	90.70716
6	38	F	A	97.3418
6	38	F	A	104.1892
6	38	F	A	104.0303
6	38	F	A	115.2994
6	38	F	A	111.3587
6	38	F	A	111.0612
6	38	F	A	138.347
6	38	F	A	124.4458
6	38	F	A	80.55221
6	38	F	A	80.19942
6	38	F	A	80.69874
6	38	F	A	156.7631
6	38	F	A	78.38155
6	38	F	A	166.4712
6	38	F	A	156.5368
6	38	F	A	114.7859
6	38	F	A	107.0528
6	38	F	A	87.44428
6	38	F	M	124.3889
6	38	F	M	117.6527
6	38	F	P	158.2633
6	38	F	L	112.2253
6	38	F	L	102.2664
6	38	F	L	74.35927
6	38	F	L	78.77248
6	38	F	L	117.5723
6	38	F	L	70.10659
6	38	F	L	139.0285
6	38	F	L	114.3734

Fetus	Dev_Age	Bone	Quad	Trab(nm)
6	38	F	M	91.30435
6	38	F	M	148.5914
6	38	F	M	126.3865
6	38	F	M	104.5288
6	38	F	M	171.8629
6	38	F	M	126.6479
6	38	F	M	129.5988
6	38	F	M	129.3067
6	38	F	M	141.6217
6	38	F	M	136.9738
6	38	F	M	142.6193
6	38	F	P	136.0564
6	38	F	P	122.2234
6	38	F	P	139.1474
6	38	F	P	125.1275
6	38	F	P	134.8001
6	38	F	P	123.9893
6	38	F	P	121.5254
6	38	F	P	129.7081
6	38	F	P	102.2664
6	38	F	P	123.9321
6	38	F	P	117.8333
6	38	F	P	110.4425
6	38	F	P	134.1676
6	38	F	P	101.1512
6	38	F	P	132.234
6	38	F	P	143.0164
6	38	F	P	139.5544
6	38	F	P	157.1244
6	38	F	P	128.5553
6	38	F	P	163.9684
6	38	F	P	148.1614
6	38	F	P	148.3686
6	38	F	P	141.0868
6	38	F	P	114.3734
7	37	F	M	82.78014
7	37	F	M	68.26225
7	37	F	M	104.5288
7	37	F	M	122.3973
7	37	F	M	73.94501
7	37	F	M	106.0103
7	37	F	M	102.6124
7	37	F	M	144.5284
7	37	F	M	152.8092

Table A12, cont.

Fetus	Dev_Age	Bone	Quad	Trab(nm)
6	38	F	L	87.52531
6	38	F	L	113.0435
6	38	F	L	125.4858
6	38	F	L	106.9645
6	38	F	L	132.769
6	38	F	L	106.8761
6	38	F	L	111.7823
6	38	F	L	116.2789
6	38	F	L	128.3345
6	38	F	L	85.03307
6	38	F	L	97.70524
6	38	F	L	112.7505
6	38	F	L	82.29345
6	38	F	L	104.0303
6	38	F	L	127.5959
6	38	F	L	112.9808
6	38	F	L	83.23561
7	37	F	A	76.08696
7	37	F	A	78.29106
7	37	F	A	63.19323
7	37	F	A	68.64197
7	37	F	A	52.89359
7	37	F	A	71.77206
7	37	F	A	48.61017
7	37	F	A	63.19323
7	37	F	A	85.22737
7	37	F	A	70.24128
7	37	F	A	52.17391
7	37	F	A	40.84412
7	37	F	A	51.16784
7	37	F	A	61.83245
7	37	F	A	62.28934
7	37	F	A	72.55791
7	37	F	M	107.9321
7	37	F	M	109.1512
7	37	F	M	104.7095
7	37	F	M	108.7826
7	37	F	M	123.0519
7	37	F	L	93.37709
7	37	F	L	139.0795
7	37	F	L	159.0675
7	37	F	L	133.0179
7	37	F	L	130.0356
7	37	F	L	106.0772
7	37	F	M	112.2253
7	37	F	M	63.97365
7	37	F	M	128.4266
7	37	F	M	125.2785
7	37	F	M	120.8234
7	37	F	M	90.42015
7	37	F	M	73.91304
7	37	F	M	56.52174
7	37	F	M	87.63324
7	37	F	M	97.92266
7	37	F	M	97.82609
7	37	F	P	103.0031
7	37	F	P	143.3135
7	37	F	P	144.8061
7	37	F	P	132.6087
7	37	F	P	163.0435
7	37	F	P	80.55221
7	37	F	P	104.0303
7	37	F	P	107.6471
7	37	F	P	148.4004
7	37	F	P	163.058
7	37	F	P	133.3727
7	37	F	P	120.3531
7	37	F	P	136.4553
7	37	F	P	125.4482
7	37	F	P	133.8855
7	37	F	P	120.5297
7	37	F	P	155.5526
7	37	F	P	118.8516
7	37	F	P	118.2737
7	37	F	P	96.29232
7	37	F	P	80.43478
7	37	F	P	144.5284
7	37	F	P	104.3705
7	37	F	P	128.0396
7	37	F	P	110.7203
7	37	F	L	94.95796
7	37	F	L	85.55943
2	14	T	P	45.85779
2	14	T	P	29.40307
2	14	T	P	59.26229
2	14	T	P	50.27155
2	14	T	P	34.27196
2	14	T	P	46.2322

Table A12, cont.

Fetus	Dev_Age	Bone	Quad	Trab(nm)
7	37	F	L	99.14569
7	37	F	L	125.1464
7	37	F	L	130.7966
7	37	F	L	110.4425
7	37	F	L	123.0711
7	37	F	L	91.40781
7	37	F	L	143.6922
7	37	F	L	150.9266
7	37	F	L	141.7218
7	37	F	L	116.5226
7	37	F	L	117.0082
7	37	F	L	114.7859
7	37	F	L	132.3947
7	37	F	L	113.3774
7	37	F	L	121.9137
7	37	F	L	92.56378
7	37	F	L	84.58729
2	14	T	A	45.91989
2	14	T	A	50.37347
2	14	T	A	57.02757
2	14	T	A	60.60541
2	14	T	A	63.24215
2	14	T	A	87.79962
2	14	T	A	61.93091
2	14	T	A	68.36076
2	14	T	A	92.3503
2	14	T	A	68.69756
2	14	T	A	91.91731
2	14	T	A	103.494
2	14	T	A	67.10285
2	14	T	A	70.30271
2	14	T	L	68.0716
2	14	T	L	78.38155
2	14	T	L	80.78654
2	14	T	L	77.18157
2	14	T	L	68.0716
2	14	T	L	83.19301
2	14	T	L	68.44375
2	14	T	L	41.01731
2	14	T	L	73.92104
2	14	T	L	70.8609
1	17	T	A	96.41758
1	17	T	A	66.23872
1	17	T	A	51.2786

Fetus	Dev_Age	Bone	Quad	Trab(nm)
2	14	T	P	27.35472
2	14	T	P	45.69595
2	14	T	P	23.63871
2	14	T	P	81.7162
2	14	T	P	92.29783
2	14	T	P	77.18093
2	14	T	P	52.73632
2	14	T	P	64.02579
2	14	T	P	50.93321
2	14	T	P	46.95689
2	14	T	P	51.65815
2	14	T	P	80.8362
2	14	T	M	54.45102
2	14	T	M	39.77853
2	14	T	M	29.84076
2	14	T	M	36.36168
2	14	T	M	31.08944
2	14	T	M	36.30286
2	14	T	M	60.47833
2	14	T	M	43.7755
2	14	T	M	64.73177
2	14	T	M	41.21052
2	14	T	M	51.24555
2	14	T	M	77.82069
2	14	T	M	66.70035
2	14	T	M	60.00057
2	14	T	M	31.71555
2	14	T	M	63.82744
2	14	T	M	52.93318
2	14	T	M	65.22948
2	14	T	M	26.51902
2	14	T	M	65.04575
2	14	T	M	52.00176
2	14	T	M	54.12822
1	14	T	A	73.5692
1	14	T	A	93.41275
1	14	T	A	66.30941
1	14	T	A	62.43379
1	14	T	A	68.75489
1	14	T	A	76.38117
1	14	T	A	70.17962
1	17	T	P	76.65669
1	17	T	P	62.96618
1	17	T	P	62.36809

Table A12, cont.

Fetus	Dev_Age	Bone	Quad	Trab(nm)
1	17	T	A	65.41131
1	17	T	A	49.88931
1	17	T	A	38.71979
1	17	T	A	51.04968
1	17	T	A	69.21332
1	17	T	A	65.41131
1	17	T	A	57.61399
1	17	T	A	70.55414
1	17	T	A	52.30756
1	17	T	A	45.46743
1	17	T	A	90.0092
1	17	T	A	78.53594
1	17	T	A	73.92654
1	17	T	A	79.01174
1	17	T	A	58.37137
1	17	T	M	67.80284
1	17	T	M	90.7608
1	17	T	M	37.89425
1	17	T	M	46.01795
1	17	T	M	79.58778
1	17	T	M	65.51866
1	17	T	M	43.2088
1	17	T	M	55.23723
1	17	T	M	41.2535
1	17	T	M	75.6183
1	17	T	M	56.27706
1	17	T	M	71.21508
1	17	T	M	68.21617
1	17	T	M	75.30788
1	17	T	M	72.41384
1	17	T	M	55.36431
1	17	T	M	56.93916
1	17	T	M	57.64448
1	17	T	M	64.9531
1	17	T	M	50.13522
1	17	T	M	64.57331
1	17	T	M	65.11519
1	17	T	M	71.20686
1	17	T	P	56.8156
1	17	T	P	57.11374
1	17	T	P	75.05862
1	17	T	P	56.31867
1	17	T	P	82.37914
1	17	T	P	73.879

Fetus	Dev_Age	Bone	Quad	Trab(nm)
1	17	T	P	52.86439
1	17	T	P	74.70669
1	17	T	P	119.7343
1	17	T	P	73.879
1	17	T	P	54.76875
1	17	T	P	58.88082
1	17	T	P	52.59785
1	17	T	P	54.72596
1	17	T	L	72.58347
1	17	T	L	33.40985
1	17	T	L	79.01174
1	17	T	L	77.45471
1	17	T	L	98.25266
1	17	T	L	57.52243
1	17	T	L	78.49865
1	17	T	L	71.20686
1	17	T	L	68.53307
1	17	T	L	53.59056
1	17	T	L	41.48002
1	17	T	L	77.92959
1	17	T	L	81.50723
1	17	T	L	91.4294
1	17	T	L	49.19185
1	17	T	L	75.38561
1	17	T	L	42.70437
1	17	T	L	69.47512
3	24	T	A	112.8761
3	24	T	A	84.89402
3	24	T	A	104.574
3	24	T	A	89.36872
3	24	T	A	135.1678
3	24	T	A	115.2994
3	24	T	A	97.43885
3	24	T	A	78.04923
3	24	T	A	141.6217
3	24	T	A	111.295
3	24	T	A	98.57204
3	24	T	A	107.954
3	24	T	A	133.0534
3	24	T	A	122.6865
3	24	T	A	76.335
3	24	T	A	81.22409
3	24	T	A	69.08804
3	24	T	A	116.0145

Table A12, cont.

Fetus	Dev_Age	Bone	Quad	Trab(nm)
3	24	T	A	84.89402
3	24	T	A	102.197
3	24	T	A	94.38388
3	24	T	A	120.7452
3	24	T	A	126.4986
3	24	T	A	101.0577
3	24	T	A	100.0945
3	24	T	M	100.2124
3	24	T	M	149.3053
3	24	T	M	63.19323
3	24	T	M	115.5451
3	24	T	M	91.74325
3	24	T	M	113.7935
3	24	T	M	66.11698
3	24	T	M	137.2839
3	24	T	M	96.24323
3	24	T	M	64.85406
3	24	T	M	72.91526
3	24	T	M	127.9473
3	24	T	M	95.2809
3	24	T	M	116.7656
3	24	T	M	109.4755
3	24	T	M	88.278
3	24	T	M	113.3774
3	24	T	M	53.29413
3	24	T	M	35.05329
3	24	T	M	67.91521
3	24	T	M	81.16589
3	24	T	M	98.4281
3	24	T	M	106.5217
3	24	T	M	106.7212
3	24	T	M	69.70095
3	24	T	P	113.3774
3	24	T	P	110.8696
3	24	T	P	91.25257
3	24	T	P	112.3095
3	24	T	P	87.20074
3	24	T	P	111.3587
3	24	T	P	108.9562
3	24	T	P	137.3872
3	24	T	P	83.6321
3	24	T	P	78.38155
3	24	T	P	81.39846
3	24	T	P	67.91521

Fetus	Dev_Age	Bone	Quad	Trab(nm)
3	24	T	P	122.8597
3	24	T	P	150.1732
3	24	T	P	89.86968
3	24	T	P	74.35927
3	24	T	P	70.10659
3	24	T	P	109.2378
3	24	T	P	127.5959
3	24	T	P	108.6957
3	24	T	P	91.94907
3	24	T	P	110.9548
3	24	T	L	88.73188
3	24	T	L	109.8633
3	24	T	L	79.72661
3	24	T	L	97.92266
3	24	T	L	75.61968
3	24	T	L	76.36595
3	24	T	L	121.9137
3	24	T	L	117.8333
3	24	T	L	159.2308
3	24	T	L	93.04754
3	24	T	L	70.24128
3	24	T	L	88.03677
3	24	T	L	95.75094
3	24	T	L	94.95796
3	24	T	L	119.881
3	24	T	L	147.2656
3	24	T	L	116.5226
3	24	T	L	98.4281
3	24	T	L	98.4281
3	24	T	L	98.57204
3	24	T	L	121.3114
3	24	T	L	91.53697
3	24	T	L	127.5959
3	24	T	L	82.86573
3	24	T	L	135.6389
4	22	T	A	102.5433
4	22	T	A	140.4994
4	22	T	A	96.85508
4	22	T	A	113.5649
4	22	T	A	146.9604
4	22	T	A	143.7415
4	22	T	A	97.05006
4	22	T	A	133.479
4	22	T	A	83.6321

Table A12, cont.

Fetus	Dev_Age	Bone	Quad	Trab(nm)
3	24	T	P	94.70879
3	24	T	P	99.16952
3	24	T	P	113.8143
4	22	T	A	133.9385
4	22	T	A	136.9738
4	22	T	A	102.2664
4	22	T	A	168.0816
4	22	T	A	150.063
4	22	T	A	182.2071
4	22	T	A	91.25257
4	22	T	A	198.4105
4	22	T	A	138.0563
4	22	T	A	129.1604
4	22	T	A	58.00724
4	22	T	A	90.07978
4	22	T	A	96.53741
4	22	T	M	119.09
4	22	T	M	137.2495
4	22	T	M	108.6957
4	22	T	M	145.1158
4	22	T	M	99.73974
4	22	T	M	98.69182
4	22	T	M	115.2994
4	22	T	M	79.34038
4	22	T	M	106.7212
4	22	T	M	87.06515
4	22	T	M	97.1474
4	22	T	M	98.30799
4	22	T	M	139.8926
4	22	T	M	161.5877
4	22	T	M	97.65686
4	22	T	M	123.0711
4	22	T	M	133.1954
4	22	T	M	125.6552
4	22	T	M	93.57932
4	22	T	M	87.63324
4	22	T	M	109.2378
4	22	T	M	86.54795
4	22	T	M	93.65504
4	22	T	M	99.76343
4	22	T	M	135.6389
4	22	T	P	93.88184
4	22	T	P	89.36872
4	22	T	P	108.6957

Fetus	Dev_Age	Bone	Quad	Trab(nm)
4	22	T	A	137.8508
4	22	T	A	158.6808
4	22	T	A	149.8739
4	22	T	P	80.19942
4	22	T	P	105.8765
4	22	T	P	82.72303
4	22	T	P	137.8508
4	22	T	P	119.6442
4	22	T	P	138.0563
4	22	T	P	163.9828
4	22	T	P	78.26087
4	22	T	P	95.75094
4	22	T	P	171.1327
4	22	T	P	152.5616
4	22	T	P	138.6541
4	22	T	P	141.555
4	22	T	P	127.9842
4	22	T	P	127.5959
4	22	T	P	139.5713
4	22	T	L	47.82609
4	22	T	L	47.67764
4	22	T	L	72.03496
4	22	T	L	113.4816
4	22	T	L	130.7966
4	22	T	L	70.0054
4	22	T	L	106.0103
4	22	T	L	141.4214
4	22	T	L	68.74517
4	22	T	L	109.4755
4	22	T	L	109.0429
4	22	T	L	83.51901
4	22	T	L	85.03307
4	22	T	L	75.8381
4	22	T	L	113.4816
4	22	T	L	116.7656
4	22	T	L	90.42015
4	22	T	L	112.2253
4	22	T	L	108.6957
4	22	T	L	81.16589
4	22	T	L	68.64197
4	22	T	L	81.60141
4	22	T	L	61.25653
4	22	T	L	98.38007
4	22	T	L	79.60797

Table A12, cont.

Fetus	Dev_Age	Bone	Quad	Trab(nm)
4	22	T	P	91.53697
4	22	T	P	91.30435
4	22	T	P	119.881
4	22	T	P	105.3619
4	22	T	P	99.73974
4	22	T	P	152.67
5	25	T	A	90.8113
5	25	T	A	139.7574
5	25	T	A	85.75253
5	25	T	A	115.5451
5	25	T	A	89.36872
5	25	T	A	131.3914
5	25	T	A	138.1077
5	25	T	A	116.2789
5	25	T	A	155.02
5	25	T	A	70.71068
5	25	T	A	95.87425
5	25	T	A	90.70716
5	25	T	A	101.896
5	25	T	A	136.9738
5	25	T	A	100.7064
5	25	T	A	161.3096
5	25	T	A	120.0583
5	25	T	A	152.9174
5	25	T	A	111.3587
5	25	T	M	117.7129
5	25	T	M	135.3075
5	25	T	M	155.02
5	25	T	M	130.5072
5	25	T	M	109.1729
5	25	T	M	112.0567
5	25	T	M	140.3479
5	25	T	M	103.3009
5	25	T	M	87.52531
5	25	T	M	122.2234
5	25	T	M	130.0174
5	25	T	M	105.7872
5	25	T	M	103.5522
5	25	T	M	94.05786
5	25	T	M	65.36216
5	25	T	M	107.3834
5	25	T	M	99.00259
5	25	T	M	119.1693
5	25	T	M	127.5959

Fetus	Dev_Age	Bone	Quad	Trab(nm)
5	25	T	A	119.5652
5	25	T	A	100.2124
5	25	T	A	100.0236
5	25	T	A	175.3473
5	25	T	A	116.7656
5	25	T	A	110.8483
5	25	T	P	103.7118
5	25	T	P	74.04081
5	25	T	P	121.7585
5	25	T	P	116.7656
5	25	T	P	90.00105
5	25	T	P	106.3441
5	25	T	P	95.50384
5	25	T	P	115.5246
5	25	T	P	108.6957
5	25	T	P	56.56353
5	25	T	P	113.5649
5	25	T	P	110.4425
5	25	T	P	132.68
5	25	T	P	101.2446
5	25	T	P	54.34783
5	25	T	P	79.93381
5	25	T	P	93.50354
5	25	T	P	105.7872
5	25	T	P	115.0532
5	25	T	P	71.96933
5	25	T	P	116.8668
5	25	T	P	101.8728
5	25	T	L	130.4348
5	25	T	L	111.3587
5	25	T	L	96.95262
5	25	T	L	102.197
5	25	T	L	114.2494
5	25	T	L	98.30799
5	25	T	L	71.50819
5	25	T	L	116.218
5	25	T	L	58.5344
5	25	T	L	113.8973
5	25	T	L	106.1885
5	25	T	L	89.36872
5	25	T	L	87.63324
5	25	T	L	122.4359
5	25	T	L	127.5959
5	25	T	L	93.85667

Table A12, cont.

Fetus	Dev_Age	Bone	Quad	Trab(nm)
5	25	T	M	128.7757
5	25	T	M	122.5324
5	25	T	M	120.3531
5	25	T	M	127.5959
5	25	T	M	114.3734
5	25	T	M	147.9699
5	25	T	P	56.89675
5	25	T	P	85.03307
5	25	T	P	87.95621
6	38	T	A	161.3096
6	38	T	A	131.3375
6	38	T	A	113.5649
6	38	T	A	97.3418
6	38	T	A	120.8234
6	38	T	A	150.1102
6	38	T	A	120.3531
6	38	T	A	143.4947
6	38	T	A	61.83245
6	38	T	A	89.13043
6	38	T	A	106.0103
6	38	T	A	107.0749
6	38	T	A	141.4214
6	38	T	A	132.68
6	38	T	A	102.0814
6	38	T	A	146.235
6	38	T	A	175.226
6	38	T	A	192.5356
6	38	T	A	107.9321
6	38	T	A	129.1604
6	38	T	A	76.36595
6	38	T	A	81.16589
6	38	T	A	119.585
6	38	T	A	113.1271
6	38	T	A	105.5412
6	38	T	M	139.9602
6	38	T	M	122.2234
6	38	T	M	144.5284
6	38	T	M	167.617
6	38	T	M	102.7505
6	38	T	M	165.1316
6	38	T	M	89.23642
6	38	T	M	117.4114
6	38	T	M	111.4011
6	38	T	M	136.8875

Fetus	Dev_Age	Bone	Quad	Trab(nm)
5	25	T	L	72.65554
5	25	T	L	94.38388
5	25	T	L	97.3418
5	25	T	L	105.7872
5	25	T	L	117.8935
5	25	T	L	76.335
5	25	T	L	83.6321
5	25	T	L	63.37991
5	25	T	L	85.64224
6	38	T	M	137.2323
6	38	T	M	130.7966
6	38	T	M	149.1152
6	38	T	P	153.4265
6	38	T	P	127.9473
6	38	T	P	154.959
6	38	T	P	120.8234
6	38	T	P	160.7079
6	38	T	P	121.8167
6	38	T	P	128.7206
6	38	T	P	115.2379
6	38	T	P	139.5713
6	38	T	P	139.0285
6	38	T	P	161.1924
6	38	T	P	101.8728
6	38	T	P	132.2518
6	38	T	P	113.3774
6	38	T	P	123.1287
6	38	T	P	82.17851
6	38	T	P	128.4266
6	38	T	P	117.5723
6	38	T	P	128.7757
6	38	T	P	151.5671
6	38	T	P	149.0043
6	38	T	P	118.2737
6	38	T	P	202.1856
6	38	T	P	128.9224
6	38	T	P	176.0735
6	38	T	L	128.4634
6	38	T	L	149.8897
6	38	T	L	123.9321
6	38	T	L	122.2234
6	38	T	L	136.4553
6	38	T	L	95.35527
6	38	T	L	122.5131

Table A12, cont.

Fetus	Dev_Age	Bone	Quad	Trab(nm)
6	38	T	M	181.6746
6	38	T	M	145.4574
6	38	T	M	139.4019
6	38	T	M	185.5992
6	38	T	M	138.1761
6	38	T	M	200.9077
6	38	T	M	178.4331
6	38	T	M	174.8075
6	38	T	M	123.6076
6	38	T	M	103.0719
6	38	T	M	148.8615
6	38	T	M	179.8051
6	38	T	L	133.8149
6	38	T	L	141.555
6	38	T	L	124.0845
6	38	T	L	93.57932
6	38	T	L	116.8263
6	38	T	L	149.3053
7	37	T	A	121.6226
7	37	T	A	134.4491
7	37	T	A	107.3173
7	37	T	A	100.3067
7	37	T	A	50.56393
7	37	T	A	122.0493
7	37	T	A	167.4712
7	37	T	A	135.2202
7	37	T	A	262.0445
7	37	T	A	206.0062
7	37	T	A	151.2706
7	37	T	A	109.4107
7	37	T	A	207.2869
7	37	T	A	68.64197
7	37	T	A	144.0699
7	37	T	A	124.7493
7	37	T	A	138.1932
7	37	T	A	135.1678
7	37	T	A	98.23586
7	37	T	A	136.4553
7	37	T	A	66.25979
7	37	T	A	155.3245
7	37	T	A	121.3114
7	37	T	A	115.8922
7	37	T	A	150.8796
7	37	T	M	93.65504

Fetus	Dev_Age	Bone	Quad	Trab(nm)
6	38	T	L	138.0563
6	38	T	L	78.80247
6	38	T	L	97.22035
6	38	T	L	113.8973
6	38	T	L	72.26422
6	38	T	L	92.69133
6	38	T	L	127.9473
6	38	T	L	115.5451
6	38	T	L	86.87496
6	38	T	L	203.3045
6	38	T	L	171.9042
6	38	T	L	103.9167
7	37	T	M	45.39264
7	37	T	M	74.20021
7	37	T	M	70.54339
7	37	T	M	110.7843
7	37	T	M	62.2514
7	37	T	M	60.40193
7	37	T	M	81.86161
7	37	T	M	48.02331
7	37	T	P	113.0644
7	37	T	P	126.9833
7	37	T	P	85.03307
7	37	T	P	124.9764
7	37	T	P	69.08804
7	37	T	P	131.3195
7	37	T	P	111.74
7	37	T	P	120.7452
7	37	T	P	123.4737
7	37	T	P	146.8156
7	37	T	P	102.7505
7	37	T	P	128.4266
7	37	T	P	135.6389
7	37	T	P	164.7878
7	37	T	P	139.4019
7	37	T	P	94.95796
7	37	T	P	80.90345
7	37	T	P	101.896
7	37	T	P	117.6728
7	37	T	P	114.7241
7	37	T	P	90.07978
7	37	T	P	122.4359
7	37	T	P	95.65217
7	37	T	P	93.50354

Table A12, cont.

Fetus	Dev_Age	Bone	Quad	Trab(nm)
7	37	T	M	109.4755
7	37	T	M	106.5439
7	37	T	M	123.9321
7	37	T	M	133.0179
7	37	T	M	87.63324
7	37	T	M	87.06515
7	37	T	M	97.63266
7	37	T	M	103.6435
7	37	T	M	99.00259
7	37	T	M	71.07732
7	37	T	M	91.40781
7	37	T	M	113.4191
7	37	T	M	130.0901
7	37	T	M	132.4482
7	37	T	M	75.05512
7	37	T	L	92.28254
7	37	T	L	101.896
7	37	T	L	73.94501
7	37	T	L	121.3114
7	37	T	L	119.8021
7	37	T	L	149.2578
7	37	T	L	93.57932
7	37	T	L	102.6124
7	37	T	L	100.5185
7	37	T	L	128.1318
7	37	T	L	82.72303
1	17	R	A	91.46595
1	17	R	A	54.44556
1	17	R	A	97.22035
1	17	R	A	89.29598
1	17	R	A	69.98008
1	17	R	A	36.00108
1	17	R	A	118.4982
1	17	R	A	102.963
1	17	R	A	55.86999
1	17	R	A	67.61009
1	17	R	A	34.13113
1	17	R	A	56.02837
1	17	R	A	67.49641
1	17	R	A	36.45763
1	17	R	A	83.27109
1	17	R	A	58.94673
1	17	R	A	94.78984
1	17	R	A	63.23995

Fetus	Dev_Age	Bone	Quad	Trab(nm)
7	37	T	P	92.86961
7	37	T	L	76.11801
7	37	T	L	100.2124
7	37	T	L	107.9321
7	37	T	L	118.4533
7	37	T	L	124.8439
7	37	T	L	118.2137
7	37	T	L	129.0506
7	37	T	L	134.4491
7	37	T	L	125.8055
7	37	T	L	128.5553
7	37	T	L	124.9007
7	37	T	L	132.8224
7	37	T	L	146.0572
7	37	T	L	126.1619
1	17	R	P	45.87163
1	17	R	P	91.64017
1	17	R	P	76.28081
1	17	R	P	81.12221
1	17	R	P	75.28302
1	17	R	P	71.21847
3	24	R	M	58.41317
3	24	R	M	67.53141
3	24	R	M	110.2069
3	24	R	M	77.92804
3	24	R	M	82.4942
3	24	R	M	56.68872
3	24	R	M	75.71337
3	24	R	M	71.50819
3	24	R	M	85.22737
3	24	R	M	73.81707
3	24	R	M	67.53141
3	24	R	M	98.69182
3	24	R	M	70.0054
3	24	R	M	64.37866
3	24	R	M	101.501
3	24	R	M	71.07732
3	24	R	M	91.74325
3	24	R	M	49.66809
3	24	R	M	152.3756
3	24	R	M	84.78261
3	24	R	M	51.67332
3	24	R	M	51.85591
3	24	R	M	87.44428

Table A12, cont.

Fetus	Dev_Age	Bone	Quad	Trab(nm)
1	17	R	M	42.44701
1	17	R	M	73.56857
1	17	R	M	67.71486
1	17	R	M	67.61009
1	17	R	M	66.22411
1	17	R	M	79.72661
1	17	R	M	30.60897
1	17	R	M	65.30791
1	17	R	M	78.02652
1	17	R	M	88.9513
1	17	R	P	74.04081
1	17	R	P	99.34212
1	17	R	P	66.65977
1	17	R	P	89.63273
1	17	R	P	82.15695
1	17	R	P	55.47739
1	17	R	P	63.19323
1	17	R	P	119.3179
3	24	R	P	89.36872
3	24	R	P	114.8065
3	24	R	P	106.7212
3	24	R	P	124.7493
3	24	R	P	75.08659
3	24	R	P	70.24128
3	24	R	P	64.85406
3	24	R	P	70.0054
3	24	R	P	81.60141
3	24	R	L	50.89
3	24	R	L	138.8925
3	24	R	L	117.5723
3	24	R	L	67.53141
3	24	R	L	63.3053
3	24	R	L	202.0921
3	24	R	L	77.59378
3	24	R	L	148.1614
3	24	R	L	110.2069
3	24	R	L	104.7095
3	24	R	L	96.29232
3	24	R	L	88.49188
3	24	R	L	52.57994
3	24	R	L	100.2124
3	24	R	L	68.22763
3	24	R	L	93.47826
3	24	R	L	89.63273

Fetus	Dev_Age	Bone	Quad	Trab(nm)
3	24	R	M	83.97047
3	24	R	M	83.0651
3	24	R	P	89.63273
3	24	R	P	146.235
3	24	R	P	128.0396
3	24	R	P	72.65554
3	24	R	P	124.5787
3	24	R	P	84.67105
3	24	R	P	101.896
3	24	R	P	116.5226
3	24	R	P	137.2323
3	24	R	P	129.9447
3	24	R	P	112.3095
3	24	R	P	116.5226
3	24	R	P	108.7826
3	24	R	P	109.0429
3	24	R	P	113.8143
3	24	R	P	117.5723
4	22	R	M	92.28254
4	22	R	M	161.1924
4	22	R	M	65.21739
4	22	R	M	99.00259
4	22	R	M	89.36872
4	22	R	M	71.96933
4	22	R	M	170.5102
4	22	R	M	139.5544
4	22	R	P	99.57376
4	22	R	P	128.7757
4	22	R	P	163.2752
4	22	R	P	153.9953
4	22	R	P	74.20021
4	22	R	P	52.26441
4	22	R	P	132.234
4	22	R	P	147.7781
4	22	R	P	84.81047
4	22	R	P	94.08298
4	22	R	P	110.8696
4	22	R	P	109.2378
4	22	R	P	146.1057
4	22	R	P	104.3931
4	22	R	P	101.1279
4	22	R	P	83.20721
4	22	R	P	82.03462
4	22	R	P	112.4777

Table A12, cont.

Fetus	Dev_Age	Bone	Quad	Trab(nm)
3	24	R	L	147.6982
3	24	R	L	88.51858
3	24	R	L	59.33628
3	24	R	L	48.61017
3	24	R	L	137.5762
3	24	R	L	76.21108
4	22	R	A	69.59918
4	22	R	A	44.01838
4	22	R	A	84.41951
4	22	R	A	55.89113
4	22	R	A	109.1729
4	22	R	A	79.13163
4	22	R	M	83.91417
4	22	R	M	68.74517
4	22	R	M	134.1676
4	22	R	M	70.10659
4	22	R	M	120.3531
4	22	R	M	101.1279
4	22	R	M	94.38388
4	22	R	M	92.56378
4	22	R	M	80.16995
4	22	R	L	58.5344
4	22	R	L	135.6389
4	22	R	L	116.8668
4	22	R	L	66.00968
4	22	R	L	192.3022
4	22	R	L	188.7678
4	22	R	L	152.003
4	22	R	L	111.909
4	22	R	L	107.0528
4	22	R	L	111.295
5	25	R	M	86.52747
5	25	R	M	88.81173
5	25	R	M	161.6681
5	25	R	M	74.42279
5	25	R	M	94.10809
5	25	R	M	128.817
5	25	R	M	111.8298
5	25	R	M	131.791
5	25	R	M	90.2763
5	25	R	M	85.87644
5	25	R	M	103.0547
5	25	R	M	150.566
5	25	R	M	130.8869

Fetus	Dev_Age	Bone	Quad	Trab(nm)
4	22	R	P	126.0307
4	22	R	P	65.25361
4	22	R	P	103.0948
4	22	R	P	144.0699
4	22	R	P	134.1676
4	22	R	P	190.7105
4	22	R	P	175.0101
4	22	R	L	141.4548
4	22	R	L	157.2597
4	22	R	L	192.2039
4	22	R	L	126.1994
4	22	R	L	158.7552
4	22	R	L	180.7619
4	22	R	L	134.1676
4	22	R	L	122.0493
4	22	R	L	171.7529
4	22	R	L	141.7718
4	22	R	L	178.3801
4	22	R	L	98.4281
4	22	R	L	129.7081
4	22	R	L	96.29232
5	25	R	P	107.9321
5	25	R	P	54.58643
5	25	R	L	26.64707
5	25	R	L	50.07084
5	25	R	L	35.12064
5	25	R	L	66.50895
5	25	R	L	28.69648
5	25	R	L	42.82112
5	25	R	L	66.19735
5	25	R	L	47.67764
5	25	R	L	30.20097
5	25	R	L	50.66897
6	38	R	A	112.8395
6	38	R	A	100.7064
6	38	R	A	41.50409
6	38	R	A	135.8739
6	38	R	A	146.4288
6	38	R	A	134.8001
6	38	R	A	56.7408
6	38	R	A	80.35395
6	38	R	A	69.44623
6	38	R	A	106.5273
6	38	R	A	77.24277

Table A12, cont.

Fetus	Dev_Age	Bone	Quad	Trab(nm)
5	25	R	M	70.01384
5	25	R	P	226.0896
5	25	R	P	94.61518
5	25	R	P	100.4303
5	25	R	P	45.09232
5	25	R	P	50.42354
5	25	R	P	83.04376
5	25	R	P	168.2362
5	25	R	P	149.4358
5	25	R	P	117.4768
5	25	R	P	101.7394
5	25	R	P	149.2973
5	25	R	P	112.2148
5	25	R	P	88.47185
5	25	R	P	125.4905
5	25	R	P	82.01301
5	25	R	P	167.55
5	25	R	P	68.54724
5	25	R	P	80.61818
5	25	R	P	145.3964
5	25	R	P	51.27164
5	25	R	P	123.7461
5	25	R	P	90.24358
5	25	R	P	115.7902
6	38	R	P	148.0337
6	38	R	P	97.3418
6	38	R	P	121.9331
6	38	R	P	127.5403
6	38	R	P	130.5072
6	38	R	P	91.64017
6	38	R	P	94.30875
6	38	R	P	124.9007
6	38	R	P	86.30188
6	38	R	P	176.1406
6	38	R	P	150.6759
6	38	R	P	91.40781
6	38	R	P	91.25257
6	38	R	P	94.05786
6	38	R	P	111.74
6	38	R	P	97.70524
6	38	R	P	91.74325
6	38	R	P	115.8922
6	38	R	P	150.2676
6	38	R	P	42.71061

Fetus	Dev_Age	Bone	Quad	Trab(nm)
6	38	R	A	195.5465
6	38	R	A	100.495
6	38	R	A	145.3477
6	38	R	A	164.0008
6	38	R	A	124.7019
6	38	R	A	144.7245
6	38	R	A	113.7623
6	38	R	A	171.5602
6	38	R	M	102.2259
6	38	R	M	86.95652
6	38	R	M	148.1654
6	38	R	M	28.34436
6	38	R	M	91.95549
6	38	R	M	172.0862
6	38	R	M	97.0318
6	38	R	M	76.36595
6	38	R	M	47.35439
6	38	R	M	66.73948
6	38	R	M	57.20738
6	38	R	M	71.15208
6	38	R	M	19.59539
6	38	R	M	37.17963
6	38	R	M	119.1941
6	38	R	M	95.75094
7	37	R	A	169.1187
7	37	R	A	130.7966
7	37	R	A	138.8925
7	37	R	A	167.4054
7	37	R	A	142.9007
7	37	R	A	82.78014
7	37	R	A	152.9329
7	37	R	A	102.3357
7	37	R	A	157.7548
7	37	R	A	134.7826
7	37	R	A	204.1743
7	37	R	A	215.2613
7	37	R	A	150.2518
7	37	R	A	99.00259
7	37	R	A	173.1505
7	37	R	A	72.55791
7	37	R	A	80.69874
7	37	R	A	189.9159
7	37	R	A	137.3872
7	37	R	A	181.4924

Table A12, cont.

Fetus	Dev_Age	Bone	Quad	Trab(nm)
6	38	R	P	130.7966
6	38	R	P	118.7522
6	38	R	P	178.0088
6	38	R	P	176.3015
6	38	R	P	100.2124
6	38	R	L	130.914
6	38	R	L	124.4316
6	38	R	L	157.6087
6	38	R	L	83.18591
6	38	R	L	121.5254
6	38	R	L	159.8418
6	38	R	L	153.3842
6	38	R	L	143.8114
6	38	R	L	113.5701
6	38	R	L	119.0006
6	38	R	L	96.85508
6	38	R	L	59.13683
6	38	R	L	89.20993
6	38	R	L	147.2656
6	38	R	L	201.9868
6	38	R	L	159.3828
6	38	R	L	141.8551
6	38	R	L	160.2957
7	37	R	A	116.7656
7	37	R	A	115.2379
7	37	R	A	58.49402
7	37	R	A	111.1038
7	37	R	L	134.7475
7	37	R	L	107.9321
7	37	R	L	113.3774
7	37	R	L	46.82752
7	37	R	L	120.5297
7	37	R	L	39.67019
7	37	R	L	114.7241
7	37	R	L	111.21
7	37	R	L	96.85508
2	14	U	A	43.82783
2	14	U	A	64.62997
2	14	U	A	46.70638
2	14	U	A	57.60382
2	14	U	A	27.31478
2	14	U	A	50.45252
2	14	U	A	56.74341
2	14	U	A	64.67526

Fetus	Dev_Age	Bone	Quad	Trab(nm)
7	37	R	A	93.65504
7	37	R	P	161.3389
7	37	R	P	51.53595
7	37	R	P	111.21
7	37	R	P	114.4148
7	37	R	P	142.2543
7	37	R	P	102.197
7	37	R	P	135.2202
7	37	R	P	80.16995
7	37	R	P	171.1879
7	37	R	P	77.59378
7	37	R	L	67.53141
7	37	R	L	77.10499
7	37	R	L	73.84908
7	37	R	L	83.0651
7	37	R	L	92.12878
7	37	R	L	88.70524
7	37	R	L	98.69182
7	37	R	L	90.8113
7	37	R	L	96.26778
7	37	R	L	107.3834
7	37	R	L	117.4114
7	37	R	L	116.8668
7	37	R	L	135.7086
7	37	R	L	108.1945
7	37	R	L	143.758
7	37	R	L	117.4718
1	17	U	P	79.56423
1	17	U	P	108.8968
1	17	U	P	81.17566
1	17	U	L	40.99213
1	17	U	L	71.6755
1	17	U	L	39.93582
1	17	U	L	44.22881
1	17	U	L	26.17836
1	17	U	L	56.45507
1	17	U	L	69.1008
1	17	U	L	56.30344
1	17	U	L	9.741079
1	17	U	L	61.97691
1	17	U	L	25.01503
1	17	U	L	45.09649
3	24	U	A	75.93152
3	24	U	A	69.56522

Table A12, cont.

Fetus	Dev_Age	Bone	Quad	Trab(nm)
2	14	U	A	26.44881
2	14	U	A	25.26541
2	14	U	A	101.7834
2	14	U	A	54.49271
1	17	U	A	79.34038
1	17	U	A	117.4114
1	17	U	A	82.39389
1	17	U	A	47.45409
1	17	U	A	82.15695
1	17	U	A	39.28111
1	17	U	A	101.5301
1	17	U	A	61.57395
1	17	U	A	88.9513
1	17	U	A	99.29453
1	17	U	A	52.57994
1	17	U	A	65.00872
1	17	U	A	111.295
1	17	U	M	31.1257
1	17	U	M	80.93995
1	17	U	M	91.33022
1	17	U	M	122.6143
1	17	U	M	134.8264
1	17	U	M	146.336
1	17	U	M	172.9764
1	17	U	P	58.71886
1	17	U	P	92.54448
1	17	U	P	60.5372
1	17	U	P	90.8305
1	17	U	P	52.92241
1	17	U	P	119.5741
3	24	U	M	59.33628
3	24	U	M	70.77748
3	24	U	M	68.74517
3	24	U	M	91.74325
3	24	U	M	93.65504
3	24	U	M	33.81815
3	24	U	M	100.2124
3	24	U	M	86.54795
3	24	U	M	72.26422
3	24	U	M	120.5885
3	24	U	M	57.76231
3	24	U	M	82.78014
3	24	U	M	117.0688
3	24	U	M	147.8421

Fetus	Dev_Age	Bone	Quad	Trab(nm)
3	24	U	A	106.6104
3	24	U	A	134.0971
3	24	U	A	112.8133
3	24	U	A	70.77748
3	24	U	A	42.82112
3	24	U	A	77.19687
3	24	U	A	97.70524
3	24	U	A	81.4855
3	24	U	A	98.09143
3	24	U	A	52.53498
3	24	U	A	60.28445
3	24	U	A	61.21795
3	24	U	A	65.21739
3	24	U	A	94.30875
3	24	U	A	77.92804
3	24	U	A	107.9321
3	24	U	A	81.86161
3	24	U	A	76.58224
3	24	U	A	91.43366
3	24	U	A	136.1432
3	24	U	A	112.2253
3	24	U	A	96.53741
3	24	U	A	80.69874
3	24	U	M	108.5434
3	24	U	M	71.77206
3	24	U	M	118.1137
3	24	U	M	77.04367
3	24	U	M	55.33879
3	24	U	M	54.86708
3	24	U	M	63.97365
3	24	U	L	115.1148
3	24	U	L	67.11021
3	24	U	L	93.35179
3	24	U	L	117.0082
3	24	U	L	95.35527
3	24	U	L	93.37709
3	24	U	L	122.2234
3	24	U	L	84.78261
3	24	U	L	128.4266
3	24	U	L	120.0583
3	24	U	L	87.74103
3	24	U	L	51.53595
3	24	U	L	88.49188
3	24	U	L	135.3075

Table A12, cont.

Fetus	Dev_Age	Bone	Quad	Trab(nm)
3	24	U	M	133.0534
3	24	U	M	73.33534
3	24	U	M	92.48716
3	24	U	M	103.9167
3	24	U	P	59.37609
3	24	U	P	145.8305
3	24	U	P	112.5827
3	24	U	P	81.71716
3	24	U	P	74.80283
3	24	U	P	84.89402
3	24	U	P	41.81605
3	24	U	P	120.0386
3	24	U	P	74.04081
3	24	U	P	95.08229
3	24	U	P	81.4855
3	24	U	P	67.95
3	24	U	P	83.0651
3	24	U	P	128.4634
3	24	U	P	68.22763
3	24	U	P	92.69133
3	24	U	P	100.495
3	24	U	P	54.34783
3	24	U	P	127.818
3	24	U	P	89.36872
3	24	U	P	67.49641
3	24	U	L	106.1662
3	24	U	L	107.9321
3	24	U	L	102.197
3	24	U	L	141.3211
3	24	U	L	95.75094
3	24	U	L	96.24323
3	24	U	L	121.9137
3	24	U	L	79.81548
4	22	U	P	104.2175
4	22	U	P	159.0526
4	22	U	P	78.53214
4	22	U	P	89.36872
4	22	U	P	51.63902
4	22	U	P	152.3756
4	22	U	P	110.1694
4	22	U	P	86.55478
4	22	U	P	99.00855
4	22	U	P	129.3524
4	22	U	P	74.18428

Fetus	Dev_Age	Bone	Quad	Trab(nm)
3	24	U	L	68.08896
3	24	U	L	80.19942
3	24	U	L	129.7446
4	22	U	A	201.087
4	22	U	A	102.963
4	22	U	A	103.6776
4	22	U	A	109.1566
4	22	U	A	90.53767
4	22	U	A	89.36872
4	22	U	A	96.78797
4	22	U	A	53.8016
4	22	U	A	51.16784
4	22	U	A	140.4237
4	22	U	A	71.65674
4	22	U	A	73.48019
4	22	U	A	88.07031
4	22	U	A	88.31814
4	22	U	A	97.85628
4	22	U	A	98.05529
4	22	U	A	105.0531
4	22	U	A	152.1778
4	22	U	M	110.8749
4	22	U	M	138.253
4	22	U	M	115.3301
4	22	U	M	125.2691
4	22	U	M	141.4297
4	22	U	M	176.7834
4	22	U	M	126.5826
4	22	U	M	149.1667
4	22	U	P	102.1739
4	22	U	P	86.62982
4	22	U	P	72.91526
4	22	U	P	115.4479
5	25	U	A	65.25361
5	25	U	A	70.97751
5	25	U	A	88.03677
5	25	U	A	83.91417
5	25	U	A	61.48755
5	25	U	A	91.01922
5	25	U	A	129.7081
5	25	U	A	77.19687
5	25	U	A	103.0719
5	25	U	A	93.70549
5	25	U	A	132.8224

Table A12, cont.

Fetus	Dev_Age	Bone	Quad	Trab(nm)
4	22	U	P	93.61088
4	22	U	P	122.7491
4	22	U	P	123.6314
4	22	U	P	105.261
4	22	U	P	143.9263
4	22	U	P	107.5867
4	22	U	P	151.5905
4	22	U	P	98.57204
4	22	U	P	135.1503
4	22	U	P	108.0524
4	22	U	L	92.25694
4	22	U	L	58.43339
4	22	U	L	84.60126
4	22	U	L	91.00624
4	22	U	L	112.4409
4	22	U	L	80.5962
4	22	U	L	128.7206
4	22	U	L	106.7212
4	22	U	L	67.65377
4	22	U	L	116.4871
4	22	U	L	70.71068
4	22	U	L	75.12592
4	22	U	L	42.20976
4	22	U	L	88.05019
4	22	U	L	96.00355
4	22	U	L	93.57932
4	22	U	L	61.99465
4	22	U	L	48.5372
4	22	U	L	104.1495
4	22	U	L	147.6101
5	25	U	A	115.9534
5	25	U	A	111.7823
5	25	U	A	104.4384
5	25	U	A	63.64035
5	25	U	A	76.58224
5	25	U	A	70.97751
5	25	U	L	123.9321
5	25	U	L	119.8021
5	25	U	L	88.70524
5	25	U	L	88.09043
5	25	U	L	107.0749
5	25	U	L	145.9115
5	25	U	L	116.1163
5	25	U	L	89.52722

Fetus	Dev_Age	Bone	Quad	Trab(nm)
5	25	U	A	176.4221
5	25	U	A	109.2378
5	25	U	A	84.78261
5	25	U	A	66.11698
5	25	U	A	78.56222
5	25	U	A	100.7064
5	25	U	A	113.4816
5	25	U	A	99.00259
5	25	U	M	89.63273
5	25	U	M	128.4266
5	25	U	M	150.566
5	25	U	M	97.1474
5	25	U	M	104.5288
5	25	U	M	104.3705
5	25	U	M	134.7475
5	25	U	M	84.55935
5	25	U	M	112.5827
5	25	U	M	74.96061
5	25	U	M	106.6104
5	25	U	M	46.06439
5	25	U	M	92.23132
5	25	U	M	160.1335
5	25	U	M	115.5451
5	25	U	M	101.6406
5	25	U	M	81.86161
5	25	U	M	87.20074
5	25	U	M	68.64197
5	25	U	M	176.7834
5	25	U	M	113.0644
5	25	U	M	113.2314
5	25	U	L	62.74291
5	25	U	L	117.0688
5	25	U	L	80.90345
5	25	U	L	111.0612
5	25	U	L	93.35179
5	25	U	L	109.3243
6	38	U	M	87.20074
6	38	U	M	130.5072
6	38	U	M	104.9124
6	38	U	M	124.5028
6	38	U	M	143.9551
6	38	U	M	102.0814
6	38	U	M	152.3756
6	38	U	M	180.3824

Table A12, cont.

Fetus	Dev_Age	Bone	Quad	Trab(nm)
5	25	U	L	56.56353
5	25	U	L	115.2379
5	25	U	L	103.278
5	25	U	L	145.9115
5	25	U	L	59.33628
5	25	U	L	87.20074
5	25	U	L	88.278
5	25	U	L	75.61968
5	25	U	L	106.6104
5	25	U	L	102.197
6	38	U	A	141.3043
6	38	U	A	92.56378
6	38	U	A	159.468
6	38	U	A	78.04923
6	38	U	A	146.235
6	38	U	A	112.2253
6	38	U	A	110.6989
6	38	U	A	159.5865
6	38	U	A	75.33793
6	38	U	A	111.6342
6	38	U	A	122.7443
6	38	U	A	58.5344
6	38	U	A	99.33617
6	38	U	A	103.7118
6	38	U	A	67.14541
6	38	U	A	97.05006
6	38	U	A	87.39022
6	38	U	A	100.5185
6	38	U	A	115.2994
6	38	U	A	106.9424
6	38	U	A	114.2494
6	38	U	A	152.3756
6	38	U	A	105.1599
6	38	U	A	132.1803
6	38	U	A	177.1039
6	38	U	M	80.19942
6	38	U	M	151.3955
6	38	U	M	85.03307
6	38	U	M	145.3273
6	38	U	L	96.48844
6	38	U	L	121.3114
6	38	U	L	136.9738
6	38	U	L	103.9167
6	38	U	L	138.1932
6	38	U	M	173.8723
6	38	U	M	163.6655
6	38	U	M	124.5977
6	38	U	M	203.0602
6	38	U	M	127.8734
6	38	U	M	121.6226
6	38	U	M	104.4384
6	38	U	M	169.1187
6	38	U	M	102.197
6	38	U	M	137.7136
6	38	U	M	86.79333
6	38	U	M	174.1303
6	38	U	M	78.53214
6	38	U	P	219.721
6	38	U	P	59.07941
6	38	U	P	135.6748
6	38	U	P	61.62182
6	38	U	P	146.5881
6	38	U	P	101.8754
6	38	U	P	109.5696
6	38	U	L	129.2702
6	38	U	L	124.8439
6	38	U	L	161.7485
6	38	U	L	120.5689
6	38	U	L	100.0236
6	38	U	L	123.913
6	38	U	L	108.5434
6	38	U	L	85.42123
6	38	U	L	107.9978
6	38	U	L	76.85943
6	38	U	L	149.3053
6	38	U	L	135.6389
6	38	U	L	145.6522
6	38	U	L	157.1244
6	38	U	L	87.39022
6	38	U	L	180.7619
6	38	U	L	135.1678
6	38	U	L	100.3774
6	38	U	L	69.87026
7	37	U	M	128.7757
7	37	U	M	100.0295
7	37	U	M	71.51645
7	37	U	M	112.0409
7	37	U	P	59.46556

Table A12, cont.

Fetus	Dev_Age	Bone	Quad	Trab(nm)
6	38	U	L	90.07978
7	37	U	A	91.08238
7	37	U	A	97.67292
7	37	U	A	119.8165
7	37	U	A	94.53042
7	37	U	A	40.49691
7	37	U	A	85.90693
7	37	U	A	92.02174
7	37	U	A	166.9731
7	37	U	A	147.2005
7	37	U	A	144.0139
7	37	U	A	95.70789
7	37	U	A	145.6709
7	37	U	A	47.41308
7	37	U	A	102.1763
7	37	U	A	156.1153
7	37	U	A	95.60335
7	37	U	A	145.2309
7	37	U	A	100.1798
7	37	U	A	60.82763
7	37	U	A	74.96666
7	37	U	A	68.02941
7	37	U	A	138.2317
7	37	U	A	134.8481
7	37	U	A	106.3015
7	37	U	A	113.7717
7	37	U	M	119.9401
7	37	U	M	127.081
7	37	U	M	85.55943
7	37	U	M	86.11687
7	37	U	M	157.6087
7	37	U	M	118.4832
7	37	U	M	123.4785
7	37	U	M	166.5457
7	37	U	M	121.1554
7	37	U	M	119.9401
7	37	U	M	115.9432
7	37	U	M	102.3414
7	37	U	M	38.29112
7	37	U	M	106.1106
7	37	U	M	135.5867
7	37	U	M	136.1779
7	37	U	L	90.22394
7	37	U	L	31.82018
7	37	U	P	76.37368
7	37	U	P	40.69923
7	37	U	P	76.44327
7	37	U	P	76.05589
7	37	U	P	92.64671
7	37	U	P	105.07
7	37	U	P	78.38155
7	37	U	P	124.2083
7	37	U	P	146.9162
7	37	U	P	103.4666
7	37	U	P	75.94708
7	37	U	P	105.4404
7	37	U	P	95.43577
7	37	U	P	126.8204
7	37	U	P	135.8696
7	37	U	P	97.88042
7	37	U	P	88.10384
7	37	U	P	73.05286
7	37	U	P	105.8876
7	37	U	P	78.80247
7	37	U	P	105.8765
7	37	U	P	98.28996
7	37	U	P	95.31809
7	37	U	P	97.12916
7	37	U	L	101.2446
7	37	U	L	51.65045
7	37	U	L	57.77253
7	37	U	L	104.6249
7	37	U	L	114.358
7	37	U	L	86.206
7	37	U	L	103.1464
7	37	U	L	133.8767
7	37	U	L	177.3372
7	37	U	L	52.35476
7	37	U	L	74.55761
7	37	U	L	77.10499
7	37	U	L	118.2137
7	37	U	L	112.0409
7	37	U	L	100.7064
7	37	U	L	88.47185
7	37	U	L	89.34888
7	37	U	L	105.188
1	17	Fib	M	63.0707
1	17	Fib	P	53.81143

Table A12, cont.

Fetus	Dev_Age	Bone	Quad	Trab(nm)
7	37	U	L	40.34937
7	37	U	L	109.135
7	37	U	L	90.74622
7	37	U	L	84.11808
7	37	U	L	78.47947
1	17	Fib	A	66.32978
1	17	Fib	A	61.92171
1	17	Fib	A	71.21885
1	17	Fib	A	59.64332
1	17	Fib	A	62.56264
1	17	Fib	A	59.05758
1	17	Fib	A	38.22601
1	17	Fib	A	58.80615
1	17	Fib	A	62.85346
1	17	Fib	A	49.53783
1	17	Fib	A	41.23817
1	17	Fib	A	104.3536
1	17	Fib	A	83.52003
1	17	Fib	A	43.03696
1	17	Fib	A	56.86494
1	17	Fib	A	46.10567
1	17	Fib	M	33.44296
1	17	Fib	M	41.57537
1	17	Fib	M	34.16787
1	17	Fib	M	56.94006
1	17	Fib	M	40.87727
1	17	Fib	M	82.30514
1	17	Fib	M	89.72101
1	17	Fib	M	77.84265
1	17	Fib	M	47.52089
1	17	Fib	M	67.61051
1	17	Fib	M	70.68269
1	17	Fib	M	44.10299
1	17	Fib	M	35.70532
1	17	Fib	M	62.172
1	17	Fib	M	43.73642
1	17	Fib	M	43.87952
1	17	Fib	M	58.13606
1	17	Fib	M	82.57474
1	17	Fib	M	80.99292
1	17	Fib	M	48.08421
1	17	Fib	M	64.96904
1	17	Fib	M	55.51601
1	17	Fib	M	58.08457

Fetus	Dev_Age	Bone	Quad	Trab(nm)
1	17	Fib	P	76.15513
1	17	Fib	P	74.88926
1	17	Fib	P	61.9792
1	17	Fib	P	65.64968
1	17	Fib	P	42.51738
1	17	Fib	P	40.82845
1	17	Fib	P	55.51601
1	17	Fib	P	53.27926
1	17	Fib	P	48.81351
1	17	Fib	P	34.38402
1	17	Fib	L	83.50126
1	17	Fib	L	110.1832
1	17	Fib	L	95.48597
1	17	Fib	L	77.01831
1	17	Fib	L	49.66995
1	17	Fib	L	56.94006
1	17	Fib	L	50.14669
1	17	Fib	L	30.23445
1	17	Fib	L	81.37024
1	17	Fib	L	34.13867
1	17	Fib	L	47.9596
1	17	Fib	L	40.38989
1	17	Fib	L	53.22308
1	17	Fib	L	35.99148
3	24	Fib	A	106.1103
3	24	Fib	A	69.06085
3	24	Fib	A	94.94248
3	24	Fib	A	72.801
3	24	Fib	A	97.81059
3	24	Fib	A	98.34799
3	24	Fib	A	108.8779
3	24	Fib	A	100.905
3	24	Fib	A	81.94435
3	24	Fib	A	111.2405
3	24	Fib	A	73.35395
3	24	Fib	A	90.0092
3	24	Fib	A	80.53141
3	24	Fib	A	51.73341
3	24	Fib	A	76.4195
3	24	Fib	A	119.0673
3	24	Fib	A	116.1039
3	24	Fib	A	33.42737
3	24	Fib	A	79.44784
3	24	Fib	A	79.8229

Table A12, cont.

Fetus	Dev_Age	Bone	Quad	Trab(nm)
1	17	Fib	M	25.8001
3	24	Fib	A	96.53291
3	24	Fib	A	73.02589
3	24	Fib	A	110.2091
3	24	Fib	A	72.25191
3	24	Fib	M	90.66397
3	24	Fib	M	93.24961
3	24	Fib	M	71.43677
3	24	Fib	M	79.01174
3	24	Fib	M	77.05293
3	24	Fib	M	65.59013
3	24	Fib	M	97.05325
3	24	Fib	M	71.65777
3	24	Fib	M	68.11307
3	24	Fib	M	50.20525
3	24	Fib	M	73.54531
3	24	Fib	P	34.64894
3	24	Fib	P	74.30582
3	24	Fib	P	69.29788
3	24	Fib	P	72.73661
3	24	Fib	P	93.90048
3	24	Fib	P	112.6009
3	24	Fib	P	102.0133
3	24	Fib	P	124.6282
3	24	Fib	P	82.42179
3	24	Fib	P	171.16
3	24	Fib	P	117.1284
3	24	Fib	P	84.69954
3	24	Fib	P	127.2646
3	24	Fib	P	118.9738
3	24	Fib	P	98.69869
3	24	Fib	P	90.30152
3	24	Fib	P	108.1818
3	24	Fib	P	78.28948
3	24	Fib	P	85.01012
3	24	Fib	P	82.99532
3	24	Fib	P	64.86287
3	24	Fib	P	77.75656
3	24	Fib	P	92.97286
3	24	Fib	P	118.4459
3	24	Fib	P	103.6308
3	24	Fib	L	97.42664
3	24	Fib	L	43.62694
3	24	Fib	L	94.92397

Fetus	Dev_Age	Bone	Quad	Trab(nm)
3	24	Fib	A	95.51441
3	24	Fib	L	70.55414
3	24	Fib	L	102.9562
3	24	Fib	L	62.55561
3	24	Fib	L	95.73488
3	24	Fib	L	68.14745
3	24	Fib	L	82.59923
3	24	Fib	L	116.7879
3	24	Fib	L	50.53081
3	24	Fib	L	93.83186
3	24	Fib	L	89.69635
3	24	Fib	L	81.13275
3	24	Fib	L	71.50232
3	24	Fib	L	89.51335
3	24	Fib	L	124.4353
3	24	Fib	L	91.83205
3	24	Fib	L	74.89459
3	24	Fib	L	140.7467
3	24	Fib	L	99.48472
4	22	Fib	A	66.75831
4	22	Fib	A	63.33712
4	22	Fib	A	103.789
4	22	Fib	A	46.98765
4	22	Fib	A	103.9863
4	22	Fib	A	75.72665
4	22	Fib	A	86.64094
4	22	Fib	A	35.71429
4	22	Fib	A	77.02253
4	22	Fib	A	36.1219
4	22	Fib	A	96.17431
4	22	Fib	A	99.78449
4	22	Fib	A	129.7844
4	22	Fib	A	127.6919
4	22	Fib	A	143.3809
4	22	Fib	A	110.14
4	22	Fib	A	166.7229
4	22	Fib	A	160.9391
4	22	Fib	A	102.6485
4	22	Fib	A	84.42252
4	22	Fib	A	96.92645
4	22	Fib	P	104.7095
4	22	Fib	P	109.0429
4	22	Fib	P	89.36872
4	22	Fib	P	118.6726

Table A12, cont.

Fetus	Dev_Age	Bone	Quad	Trab(nm)
3	24	Fib	L	82.77629
3	24	Fib	L	77.95965
3	24	Fib	L	69.1456
3	24	Fib	L	82.54958
4	22	Fib	P	102.2664
4	22	Fib	P	99.16952
4	22	Fib	P	85.03307
4	22	Fib	P	108.1945
4	22	Fib	P	100.495
4	22	Fib	P	119.585
4	22	Fib	P	73.07711
5	25	Fib	A	80.24729
5	25	Fib	A	121.0671
5	25	Fib	A	96.95665
5	25	Fib	A	60.11123
5	25	Fib	A	96.70869
5	25	Fib	A	115.228
5	25	Fib	A	77.17444
5	25	Fib	A	124.0583
5	25	Fib	A	100.7424
5	25	Fib	A	108.0355
5	25	Fib	A	91.83205
5	25	Fib	A	66.01732
5	25	Fib	A	107.5847
5	25	Fib	A	70.17962
5	25	Fib	A	77.95213
5	25	Fib	A	110.4108
5	25	Fib	A	116.386
5	25	Fib	A	73.76
5	25	Fib	A	109.1948
5	25	Fib	A	82.48571
5	25	Fib	A	122.9106
5	25	Fib	A	86.80976
5	25	Fib	A	112.2884
5	25	Fib	A	107.0937
5	25	Fib	A	86.2548
5	25	Fib	M	110.7762
5	25	Fib	M	64.83578
5	25	Fib	M	80.65494
5	25	Fib	M	104.5535
5	25	Fib	M	82.84701
5	25	Fib	M	116.9482
5	25	Fib	M	101.0906
5	25	Fib	M	50.72745

Fetus	Dev_Age	Bone	Quad	Trab(nm)
4	22	Fib	P	60.12746
4	22	Fib	P	74.20021
4	22	Fib	P	59.37609
4	22	Fib	P	103.278
5	25	Fib	M	127.9118
5	25	Fib	M	112.6009
5	25	Fib	M	122.1554
5	25	Fib	M	120.7474
5	25	Fib	M	103.8566
5	25	Fib	M	123.8977
5	25	Fib	P	51.41547
5	25	Fib	P	77.27303
5	25	Fib	P	51.15282
5	25	Fib	P	104.9784
5	25	Fib	P	88.82374
5	25	Fib	P	125.5831
5	25	Fib	L	89.53952
5	25	Fib	L	139.4761
5	25	Fib	L	114.7646
5	25	Fib	L	82.0015
5	25	Fib	L	91.2242
5	25	Fib	L	67.75964
5	25	Fib	L	90.7608
5	25	Fib	L	125.5131
5	25	Fib	L	85.01012
5	25	Fib	L	120.2078
5	25	Fib	L	60.03324
5	25	Fib	L	149.2722
5	25	Fib	L	126.6742
5	25	Fib	L	175.8483
5	25	Fib	L	135.4371
5	25	Fib	L	125.0223
5	25	Fib	L	126.8082
5	25	Fib	L	120.2809
6	38	Fib	A	109.9484
6	38	Fib	A	182.7595
6	38	Fib	A	128.3141
6	38	Fib	A	80.18889
6	38	Fib	A	73.66466
6	38	Fib	A	112.5749
6	38	Fib	A	141.2286
6	38	Fib	A	107.9271
6	38	Fib	A	140.9172
6	38	Fib	A	145.4007

Table A12, cont.

Fetus	Dev_Age	Bone	Quad	Trab(nm)
5	25	Fib	M	88.03565
5	25	Fib	M	126.665
5	25	Fib	M	79.27074
5	25	Fib	M	51.42686
5	25	Fib	M	92.08679
5	25	Fib	M	62.29293
5	25	Fib	M	69.39922
6	38	Fib	A	136.7796
6	38	Fib	M	118.6386
6	38	Fib	M	102.4544
6	38	Fib	M	81.47849
6	38	Fib	M	89.8855
6	38	Fib	M	120.563
6	38	Fib	M	116.386
6	38	Fib	M	98.57995
6	38	Fib	M	107.8022
6	38	Fib	M	121.3859
6	38	Fib	M	117.6024
6	38	Fib	M	96.81158
6	38	Fib	M	48.64114
6	38	Fib	M	55.57546
6	38	Fib	M	118.3816
6	38	Fib	M	127.7102
6	38	Fib	M	103.4272
6	38	Fib	M	114.8309
6	38	Fib	M	65.74174
6	38	Fib	M	93.06101
6	38	Fib	M	130.9703
6	38	Fib	M	166.8914
6	38	Fib	M	134.8434
6	38	Fib	M	113.4713
6	38	Fib	M	125.9324
6	38	Fib	P	124.7268
6	38	Fib	P	117.8064
6	38	Fib	P	125.5878
6	38	Fib	P	91.34609
6	38	Fib	P	102.8309
6	38	Fib	P	74.14012
6	38	Fib	P	109.3877
6	38	Fib	P	105.9999
6	38	Fib	P	75.64153
6	38	Fib	P	74.74587
6	38	Fib	P	97.78664
6	38	Fib	P	154.8792

Fetus	Dev_Age	Bone	Quad	Trab(nm)
6	38	Fib	A	152.5206
6	38	Fib	A	178.6272
6	38	Fib	A	128.8424
6	38	Fib	A	134.138
6	38	Fib	A	133.9414
6	38	Fib	A	79.06361
6	38	Fib	A	179.8394
6	38	Fib	P	145.5256
6	38	Fib	P	100.0834
6	38	Fib	P	104.7941
7	37	Fib	A	142.0225
7	37	Fib	A	83.60696
7	37	Fib	A	106.3969
7	37	Fib	A	117.3881
7	37	Fib	A	126.4568
7	37	Fib	A	132.6056
7	37	Fib	A	82.70551
7	37	Fib	A	76.86269
7	37	Fib	A	78.19217
7	37	Fib	A	76.66433
7	37	Fib	A	90.7608
7	37	Fib	A	85.22341
7	37	Fib	A	88.80396
7	37	Fib	A	80.55322
7	37	Fib	A	117.7616
7	37	Fib	A	68.39621
7	37	Fib	A	86.6477
7	37	Fib	A	93.41275
7	37	Fib	A	120.5241
7	37	Fib	A	93.23076
7	37	Fib	A	103.1778
7	37	Fib	A	34.9686
7	37	Fib	A	63.88949
7	37	Fib	A	86.15969
7	37	Fib	A	60.57706
7	37	Fib	M	103.58
7	37	Fib	M	111.9751
7	37	Fib	M	128.9015
7	37	Fib	M	125.9603
7	37	Fib	M	175.4182
7	37	Fib	M	161.6906
7	37	Fib	M	154.1515
7	37	Fib	M	79.00433
7	37	Fib	M	229.1844

Table A12, cont.

Fetus	Dev_Age	Bone	Quad	Trab(nm)
6	38	Fib	P	112.9903
6	38	Fib	P	93.96283
6	38	Fib	P	106.4794
6	38	Fib	P	144.7994
6	38	Fib	P	67.36089
6	38	Fib	P	122.7962
6	38	Fib	P	81.17605
6	38	Fib	P	112.1423
6	38	Fib	P	105.3292
6	38	Fib	P	177.8188
7	37	Fib	L	28.4078
7	37	Fib	L	73.66466
7	37	Fib	L	52.84223
7	37	Fib	L	90.44408
7	37	Fib	L	64.07255
7	37	Fib	L	121.9827
7	37	Fib	L	84.23502
7	37	Fib	L	96.9204
7	37	Fib	L	167.4974
7	37	Fib	L	119.2295
7	37	Fib	L	107.3613
7	37	Fib	L	88.67857
7	37	Fib	L	80.0061
7	37	Fib	L	69.67714
7	37	Fib	L	104.7326
7	37	Fib	L	111.5559
7	37	Fib	L	110.6069
7	37	Fib	L	68.86553
7	37	Fib	L	78.11724
7	37	Fib	L	118.8014
7	37	Fib	L	131.5992
7	37	Fib	L	83.24896

Fetus	Dev_Age	Bone	Quad	Trab(nm)
7	37	Fib	M	185.8733
7	37	Fib	M	107.1374
7	37	Fib	M	143.4993
7	37	Fib	M	131.9681
7	37	Fib	M	147.1861
7	37	Fib	M	276.1289
7	37	Fib	M	85.10651
7	37	Fib	M	88.08886
7	37	Fib	M	191.4728
7	37	Fib	M	126.6419
7	37	Fib	M	163.8815
7	37	Fib	M	135.0431
7	37	Fib	P	164.8329
7	37	Fib	P	95.318
7	37	Fib	P	116.4816
7	37	Fib	P	37.31805
7	37	Fib	P	79.83023
7	37	Fib	P	85.55946
7	37	Fib	P	80.44409
7	37	Fib	P	113.3216
7	37	Fib	P	55.6597
7	37	Fib	P	162.1391
7	37	Fib	P	100.1536
7	37	Fib	L	25.17252
7	37	Fib	L	88.29471
7	37	Fib	L	71.34654

Vita

Courtney D. Eleazer was born February 25th, 1983 in Tallahassee, Florida. She was raised in Florence, South Carolina and graduated from West Florence High School in 2001. She attended Florida State University and graduated summa cum laude with her Bachelor of Science degree in anthropology in 2004. She was accepted to the University of Tennessee-Knoxville anthropology program in August 2004 and earned her Master of Arts in physical anthropology in August 2007. She is currently enrolled as a PhD student in physical anthropology at the University of Tennessee-Knoxville.